Using Multiple Conceptual Models to Understand Transboundary Groundwater Flows in Red Cliff Reservation, WI

By

Yang Li

A Thesis submitted in partial fulfillment of

the requirements for the degree of

MASTER OF SCIENCE

(Geological Engineering)

at the

UNIVERSITY OF WISCONSIN-MADISON

2015

Abstract

Interactions between surface water and groundwater play a crucial role in water resources management. Understanding recharge dynamics in the vicinity of surface water bodies has important implications for stream ecology. A comprehensive approach is required to quantify recharge, defined as the entry of water into the saturated zone. The objective of this study is to investigate the transboundbary water impacts on groundwater-fed streams in Red Cliff reservation in northern Wisconsin under different recharge scenarios.

A modified Thornthwaite-Mather Soil-Water-Balance code (USGS, 2010) which takes spatially variable factors including climate, land cover and topography into consideration to estimate the spatially- variable recharge rate, is used in this study. The main objective of this study is to understand the probable extent of groundwater recharge areas that contribute to the streams of the Red Cliff Reservation. Stream baseflows and the water configuration can be estimated using the groundwater flow model developed using MODFLOW (Harbaugh, 2005; Harbaugh et al., 2000). Three groundwater models, forced by three conceptual models representing different assumptions about estimated recharge and aquifer hydrological properties, are calibrated through PEST (Doherty, 2010a, b) to obtain a plausible model with the best match between simulated observations (heads and stream flows) and corresponding field observations. Capture zones are then delineated by using backward transport of particles through numerical flow modeling with MODPATH (Pollock, 1994). Different conceptual models give similar range of recharge rate throughout the peninsula, while SWB-based recharge show a better estimation. The recharge at this site appears to be predominantly controlled by soil types and land cover.

Acknowledgement

The UW-Madison Geological Engineering Department has helped me on my path to discovery in my Master's studies. The wonderful professors and graduate students of Geological Engineering have taught me critical thinking skills, writing techniques, and presentation proficiency. The geological engineering department has been both extremely challenging and supportive.

First and foremost, I need to thank my advisor, Professor Michael Cardiff, who taught me about creative thinking in research and always being supportive and patient. This thesis would not exist without him. I would also like to thank Professor Jean Bahr for teaching me knowledge needed to be a professional hydrogeologists and providing advices for both career and life to me. Thank you to Professor Bill Likos for sharing his unique insights on my research topic. Many thanks are also due to Dr. Michael Fienen, Dr. Daniel Feinstein and Stephen Westenbroek for their time and expertise to provide help and suggestions in the project. Financial support for this study (September. 2013 to August. 2014) was from the University of Wisconsin – Madison. This support is gratefully acknowledged.

Thank you also to my friends and family for their positive affirmations and motivation. I would like to extend a special thank you to the whole hydro group, Yaoquan Zhou, David Lim, Stephen Sellwood and Megan Haserodt, who helped me prepare for research presentations, solve problems, and generate ideas that helped me on my research path. Much of this work also could not have been accomplished without the assistance of Aaron Pruitt, who helped me solve problems when building SWB models at the beginning and Jie Chen in ECE Department, who helped me with the MATLAB codes.

Thanks to the whole Geological Engineering family, particularly Missy Setz, Idil Akin, and Faith Zangl. Endless thanks are extended to my parents, Changshan Li and Yongjuan Yang, for all the support and encouragement. Finally, I dedicate the thesis to Eric Parfitt for his company and love.

TABLE OF CONTENTS

Chapter 1 – Introduction

Interactions between surface water and groundwater play a crucial role in the functioning of ecosystems, prominently in the dynamics of gaining and losing streams (Kalbus et al., 2006). The direction of the water exchange between surface water and groundwater depends on the hydraulic gradient. In gaining conditions, the outflow from a groundwater reservoir becomes a portion of stream flow as baseflow. During periods of low precipitation, baseflow may contribute most of the discharge in some streams (Brunke and Gonser, 1997; Sophocleous, 2002). Baseflow in perennial streams is continuous, keeping them flowing and sustaining biological populations throughout the year (Gordon et al., 2004). The recharge to groundwater represents the source water that perennial streams are dependent upon for regularity of baseflow (Brunke and Gonser, 1997). Thus, understanding recharge dynamics in the vicinity of surface water bodies has important implications for stream ecology and ecosystem stability.

A comprehensive approach is required to quantify recharge, defined as the entry of water into the saturated zone. Such an approach reduces uncertainties and increases confidence in the estimates (Scanlon and Cook, 2002). Taking both space and time scales into consideration when developing models of recharge will increase the accuracy of groundwater flow modeling as well as contaminant transport modeling. Some studies focus on quantifying recharge for water resource assessment (Kearns, 1998), while other researchers have concentrated on locating local areas of minimal recharge for radioactive and hazardous-waste disposal sites (Taylor and Howard, 2000). In terms of water-resources management, the time scales studied can range from days to hundreds of years

or tens of thousands years for radioactive waste research, which is also an important factor. Seasonal variations also alter recharge, the elevation of the water table, and stream stages.

Techniques used to quantify groundwater recharge vary depending on space/time scales and reliability of the estimates (Scanlon et al., 2002). Water-balance methods can be used to quantify recharge, since recharge represents one of the components in the balance. The inaccuracies in the water balance determination are dependent on the errors associated with measurements of other components of the water balance (De Vries and Simmers, 2002).Furthermore, even when a reasonable estimate of total recharge is obtained by a water-balance method, such methods do not typically quantify the spatial distribution of recharge (Stone et al., 2001). Another approach to estimating recharge is by incorporating effects from climate, hydrology, geomorphology, and geology to describe location, timing and mechanisms of recharge through coupled numerical simulation (Scanlon and Cook, 2002).

Understanding the spatial distribution of natural groundwater recharge is important to predictions of impacts of land cover change (Taylor and Howard, 1996; Zhang et al., 1999) and climate change (Gleick, 1989) on water resources, which give decision makers a more reliable basis for understanding impacts of potential urban, industrial, and agricultural development (Scanlon and Cook, 2002; De Vries and Simmers, 2002).

The main objective of this study is to understand the probable extent of groundwater recharge areas that contribute to the streams of the Red Cliff Reservation, located on the Bayfield Peninsula of northern Wisconsin. It is likely that the recharge areas for these streams occur on Wisconsin state land, meaning that the movement of recharged water

represents an important “trans-boundary” flow. In Chapter 2, I describe the site under study in further detail. In this study, we use a modified Thornthwaite-Mather Soil-Water-Balance (SWB) code (Westenbroek, 2010), based on the initial research of Dripps (2003), which takes spatially variable factors including climate, land cover and topography into consideration to estimate the spatially- variable recharge rate. After developing recharge scenarios using the SWB model, stream baseflows and the water table configuration can be estimated through a groundwater flow model developed in MODFLOW (Harbaugh, 2005). Chapter 3 discusses the conceptual underpinnings of both the SWB model and MODFLOW model. Chapter 4 discusses the application of both the SWB and MODFLOW models to the site study area of the Red Cliff Reservation. Because of the limited characterization information available for the aquifer materials, each realization of the groundwater model (i.e., the groundwater model under each recharge scenario) is calibrated through PEST (Doherty, 2010a, b) to obtain a plausible model with the best match between simulated observations (heads and stream flows) and corresponding field observations.

The data available for constraining the spatial distribution of recharge throughout the study site are sparse and incomplete, and many assumptions and algorithms are required to develop spatially-distributed recharge estimates. Thus, the groundwater flow models of the Bayfield peninsula is forced by three different conceptual models representing different assumptions about estimated spatial distributions of recharge. Capture zones are then delineated by simulating backward transport of particles through numerical flow modeling with MODPATH, an extension of the MODFLOW groundwater flow numerical model. Chapter 5 discusses the process of model calibration and the comparison between different conceptual models of recharge on the Bayfield Peninsula. Chapter 6 summarizes the

findings from the numerical modeling of the peninsula, including the probable extent of recharge areas on the peninsula and the predominant factors that control the recharge at the study site.

Chapter 2 – Field Site Description

2.1 Study Area

The Bayfield Peninsula, the northern point of which is home to the Red Cliff Band of the Lake Superior Chippewa and their reservation, is at the northernmost tip of Wisconsin, neighboring the Apostle Islands in Lake Superior. The study domain used in the SWB and MODFLOW models, shown in Figure 2.1, covers 1100 mi^2, 41.7% of which is covered by Lake Superior. The mean water level of Lake Superior is 602 feet above mean sea level (AMSL) based on NGVD-29, and the peninsula reaches a maximum elevation of 1400 feet AMSL (Fig.2.2).

The Bayfield Peninsula is a large part of the Lake Superior lowland, which occupies portions of Bayfield, Douglas and Ashland counties in the northwestern part of Wisconsin. The Lake Superior lowland originated as a down-dropped block of the Earth's crust bounded by normal faults. Subsequent erosion and deposition by the continental glacier modified the Lake Superior lowland as well as the escarpments that bound it (Martin, 1916). Deeply trenched by postglacial streams, the plain far from the lake is relatively hilly, with ravines about 40 to 100 feet deep. Erosion varies by surficial geology, with clayey areas more severely dissected than sandy areas.

2.2 Climate and Land Cover

Annual climate and land-cover, as well as topography and soil properties, result in a recharge rate to groundwater that varies spatially and temporally throughout the peninsula.

Due to the humid, continental type of climate, there are long and cold winters as well as short and warm summers in the Bayfield Peninsula. The average annual temperature is around 41 ˚F. The average period of the frost-free season is 116 days in the peninsula, normally from May 30th to September 23th. Lake Superior does not completely freeze. Annual mean snowfall varies from 50 to 75 inches along the Upper Bayfield Peninsula, covering about 140 days of a year. In terms of precipitation, the overall annual average is 28.0 inches of water, mostly falling from May 1st to October 1st, which is less than the state average. In contrast, during the growing season, the average amount of precipitation in the peninsula is higher than the state average. Prevailingly, winds are westerly from the early spring until early fall and are easterly during the remainder of the year. The climate on the peninsula is affected by Lake Superior and Chequamegon Bay. As a result, the period of frost-free days in winter, as well as the number of cooler days in summer, is longer along the lake. Therefore, the northern part of the peninsula, surrounded by Lake Superior, has more precipitation and a longer growing season compared to other areas. Each of these factors contributes to complex hydrogeology on the Bayfield peninsula, which is driven by snow accumulation and snow melt as well as climatic influences associated with Lake Superior.

Evapotranspiration, and thus, the water available to recharge to groundwater, is also likely impacted by the distribution of vegetation on the peninsula. Hardwoods and mixed conifers

are present on the sandy loams, clay loams and clays generally, which are located on the lake plain and the highlands of the south peninsula. The loamy sands and sands of the outwash plains are predominantly covered by jack pine and scrub oak.

2.3 Site Geology and Hydrostratigraphy

The Bayfield Peninsula is mostly underlain by Precambrian sandstone and igneous rocks. The Precambrian Bayfield Group underlying the peninsula consists of sandstone, siltstone, shale and conglomerate (Ojakangas and Morey, 2001). The estimated surface of the Precambrian bedrock is shown in Figure 2.3. Covering most of the Bayfield peninsula, glacial deposits, generally shallow lake basin deposits, reach 300 feet of thickness covering the bedrock in some parts.

Bedrock is overlain by sand and gravel Copper Falls Formation and clayey glacier deposits of the Miller Creek Formation. The Copper Falls Formation occurs largely in the Bayfield Highlands, while clayey glaciolacustrine deposits of the Miller Creek Formation can be found at lower altitudes towards Lake Superior (Fig. 2.4) (Goebel and others, 1983; Clayton and others, 1983).

Compared to the coarse-grained, homogenous Copper Falls Formation, the Miller Creek Formation is fined-grained and heterogeneous in character, with sandy pockets found in silt and clay. In terms of soils, clayey soils and sandy soils over clay are located around the fringe of the Bayfield Peninsula, containing the major agricultural areas. Sandy soils are

mostly found in the inland areas of the Bayfield Ridge, whereas loamy soils are dominant in the southern part (Fig. 2.5).

There is a large portion of recharge to the groundwater originating from the precipitation in the Bayfield Peninsula. Lateral groundwater in flow from outside of the watershed and the surface water also contributes to the groundwater flow. Groundwater, including from glacial deposits and bedrock, serves as the water supply source in most areas of the Bayfield Peninsula. In terms of domestic wells in the region, most of the wells in glacial drift draw from Copper Falls sand and gravel deposits. Relatively high yields are also found in some areas in the sandstone along the eastern part of the peninsula. The quality of groundwater is good and pollution from human activities is not a serious problem. The mineral composition, as well as the surface area of the particles of soil and rock through which the water moves and the duration of the water being in contact with these soils leads to the differences in groundwater quality. Higher concentrations of dissolved solids and greater hardness are found in the bedrock aquifers, especially sandstone. Objectionable quantities of iron and manganese can be found in water from some of the aquifers in the region.

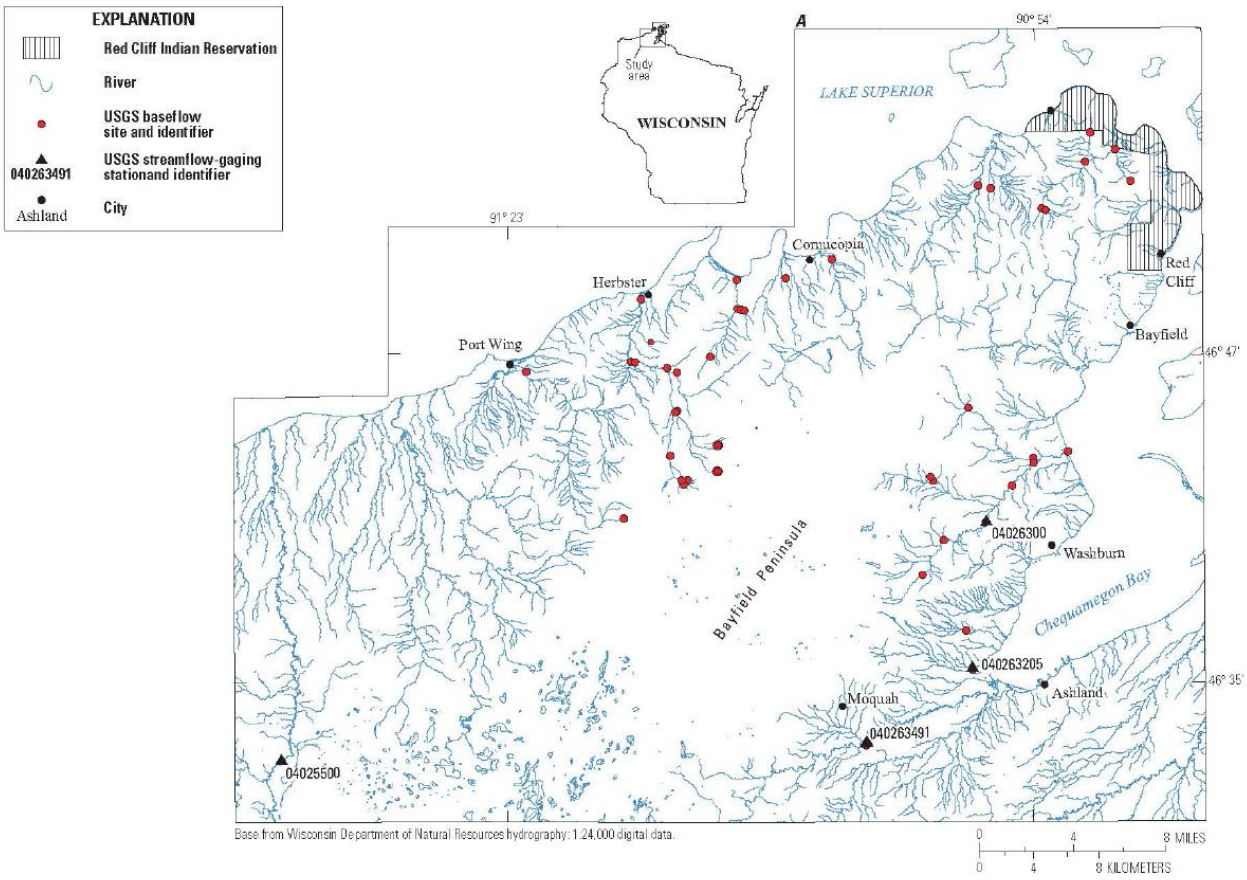

Figure 2.1: Study area, Bayfield Peninsula, WI (USGS, 2015)

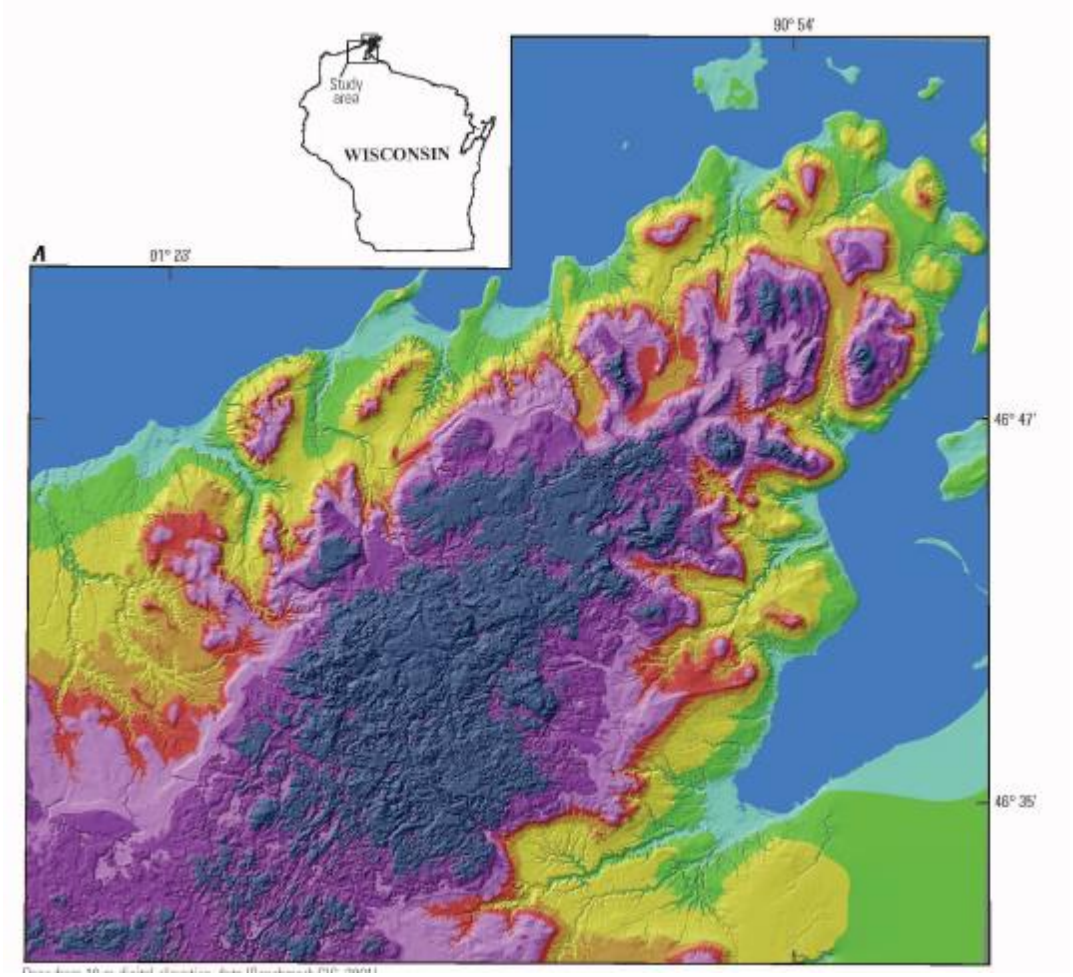

Figure 2.2: Topographic surface of the Bayfield Peninsula, WI (USGS, 2015)

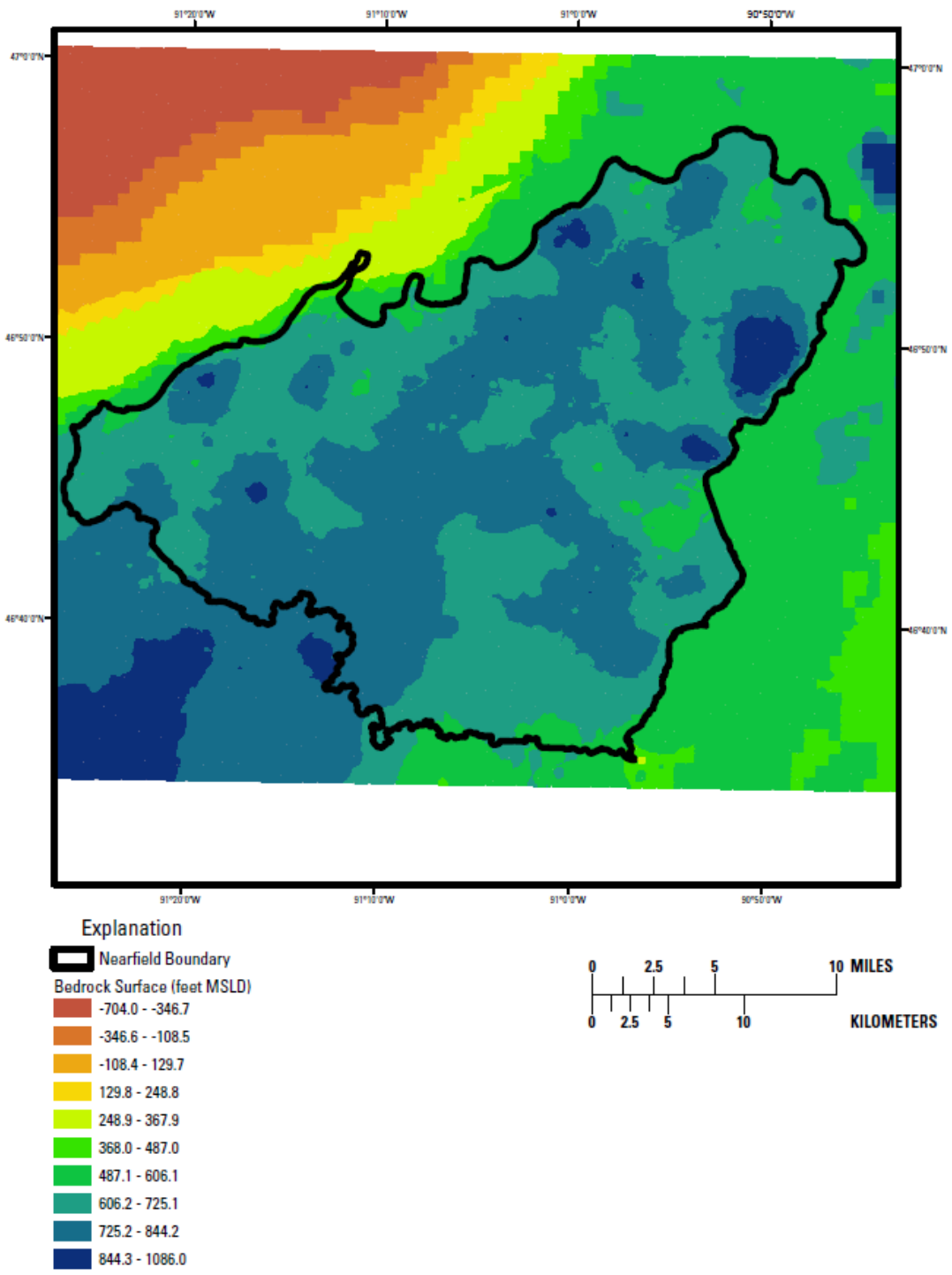

Figure 2.3: Bedrock surface altitude of the Bayfield Peninsula, WI (USGS, 2015)

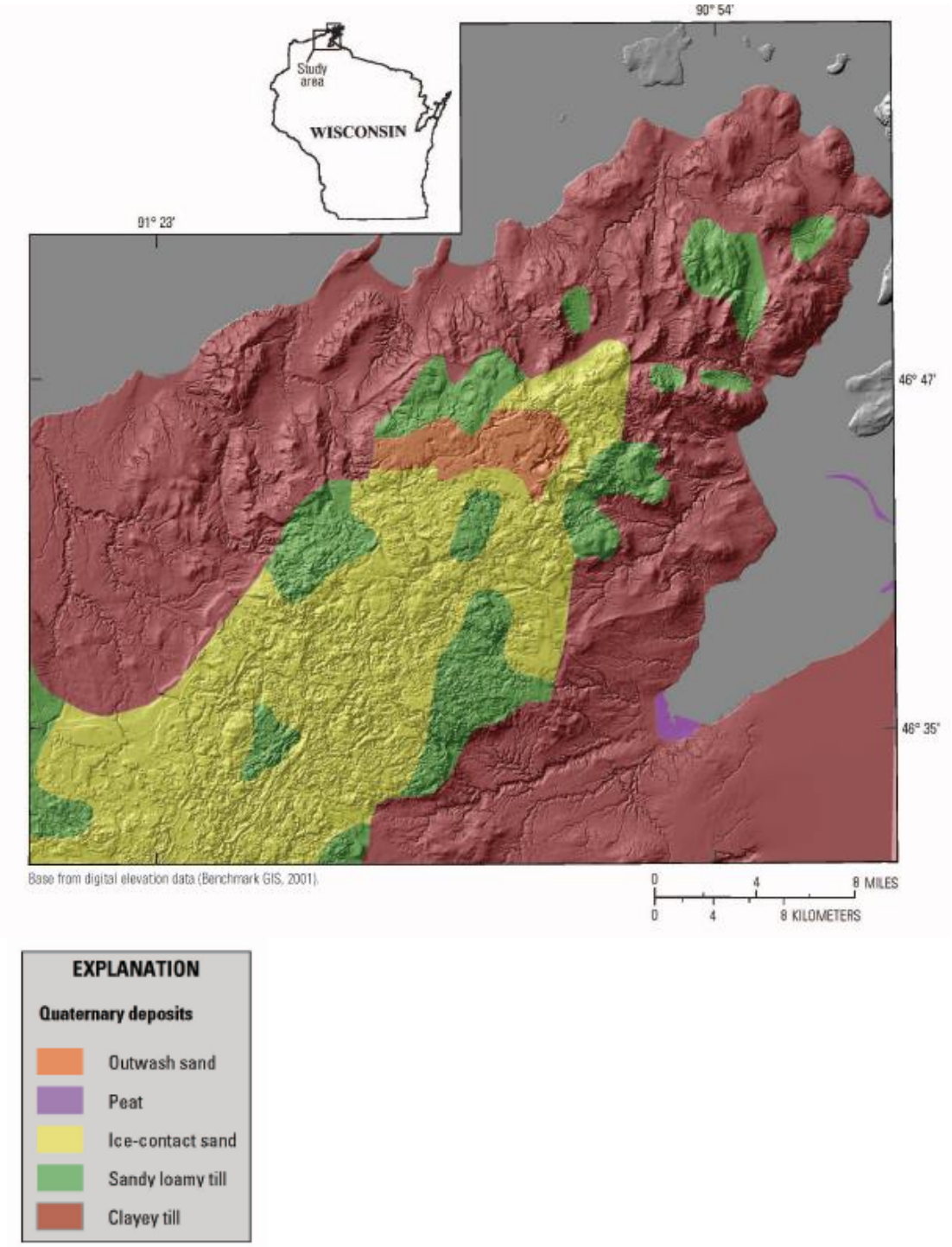

Figure 2.4: Quaternary geologic deposits of the Bayfield Peninsula, WI (USGS, 2015)

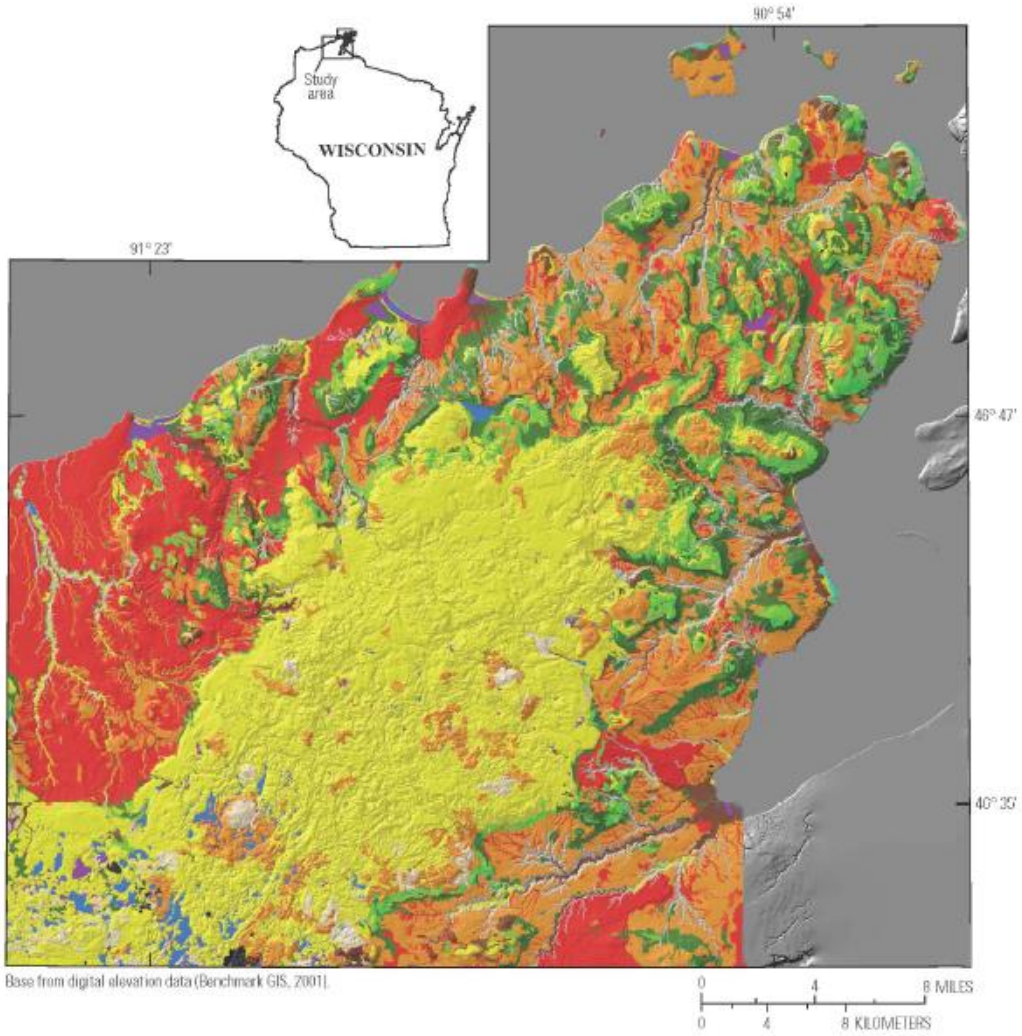

Figure 2.5: Soils of the Bayfield Peninsula, WI (USGS, 2015)

Chapter 3 – Numerical Modeling Approach

3.1 Introduction

A groundwater flow model of the Bayfield Peninsula, consistent with the subsurface hydrostratigraphy, is used to simulate groundwater flow and discharge to streams. The numerical models are forced by recharge scenarios, generated using a physically-based soil-water balance model (see Appendix B). The Soil Water Balance (SWB) code (Westenbroek, 2010) provides a spatially distributed recharge rate throughout the peninsula by taking climate, land cover, soil and topography variables into consideration. In this study, climate represents the most uncertain input to the SWB model. Thus, different climate scenarios are applied within SWB to yield the different corresponding recharge scenarios throughout the groundwater flow model. The different climate scenarios are the results of applying different interpolation schemes for temperature and precipitation throughout the peninsula. In terms of the numerical groundwater flow model, it is developed using the Groundwater Vistas interface for the USGS code, MODFLOW (Harbaugh, 2005; Harbaugh et al., 2000). Since groundwater flow parameters within the modeled domain (i.e., hydraulic conductivity) also have high uncertainty, under each climate scenario, parameter estimation is performed on the MODFLOW model by using groundwater heads and stream baseflows as targets. Parameters estimated within the MODFLOW model include hydraulic conductivities within each geologic unit and a "recharge multiplier" which modifies the recharge rate to the saturated flow system. The groundwater model is calibrated through PEST under each climate scenario (Doherty,

2010a, b) by updating the initial estimates of parameters to obtain the optimized match between simulated head and baseflow values and corresponding observed values.

3.2 MODFLOW model

MODFLOW-2005 is a modular ground-water numerical model using a block-centered finite-difference approach (Harbaugh, 2005). The model consists of a main program and subroutines called "packages" to simulate different elements of the hydrologic system.

Packages utilized in the Red Cliff MODFLOW model include the basic package (BAS6), solver package (DE4), well package (WEL), recharge package (RCH), streamflow-routing package (SFR2) and the general head boundary package (GHB) to facilitate the geometry of the numerical model including grids and layers, boundary conditions, subsurface characteristics, recharge and solver parameters. Lake Superior is implemented as a third-type boundary condition through the GHB package, such that flux to the lake varies as a function of stage and lakebed leakance. A stage of 600 feet for Lake Superior was assigned based on the mean elevation over the past 150 years. The lakebed leakance is defined as the ratio of the vertical hydraulic conductivity to the thickness of the lakebed. As a result of preliminary simulations to meet the groundwater flux targets, a 5- ft thickness and a 0.0001ft/d vertical hydraulic conductivity are assigned to the model. The input for the recharge package (RCH) is generated based on the soil-water balance (SWB) model results, which will be discussed in Chapter 4. Surface water flows are simulated through the SFR2 package. The data required for streamflow routing include the hydraulic conductivity and thickness (or leakance) of the streambed, the top elevation of the streambed and the

downstream order of the reaches. Stream stage and exchange with the groundwater are the outputs of this package.

3.3 SWB model

The Soil-Water-Balance (SWB) computer code is designed to calculate the spatial distribution of groundwater recharge over time using a modified Thornthwaite-Mather soil-water balance method (Thornthwaite and Mather, 1957). Recharge is estimated within each grid cell based on climate and land cover characteristics (eq. 1, Westenbroek, S.M. et al., 2010), with climate information provided in daily time steps. The fundamental conceptual model used to calculate recharge within SWB is shown in formula (1).

Recharge = (rain precipitation + snowmelt + inflow) – (interception + outflow + Evapotranspiration) - Δ soil moisture (1)

Temperatures are used to determine the form of precipitation (rain or snow), and also whether snow accumulation or snow melting processes occur. Snow accumulation is calculated according to the following rule: precipitation that falls "on a day when the mean temperature minus one-third the difference between the daily high and low temperatures is less than or equal to the freezing point of water is considered to fall as snow" (Dripps and Bradbury, 2005). Similarly, snowmelt is calculated based on the index method – it is assumed that 1.5 mm (0.059in.) of snow melts per day per average degree Celsius that the daily maximum temperature is above the freezing point (Dripps and Bradbury, 2005).

Frozen ground is also tracked by applying CFGI, known as continuous frozen-ground index (Molnau and Bissel, 1983).

Precipitation is sometimes captured on the surfaces of vegetation before it reaches the land surface, the process of which is called interception. The value of interception is dependent on land cover types and growing seasons (Anderson, 1976; Dripps, 2003), and is calculated using a land-use lookup table.

Water that is not intercepted is assumed to reach the land surface, and may then become either infiltrated water or runoff. The distribution of water between outflow (i.e., runoff) and infiltration is calculated based on the curve number rainfall-runoff relation (Cronshey et.al, 1986), which is based on soil type, land use, surface condition, and antecedent runoff condition. Outflow (runoff) from surrounding cells can lead to inflow in a down-slope cell. Inflow is calculated by use of a flow direction grid to determine the routes of overland flow between cells. The D8 algorithm (O' Callaghan and Mark, 1984) is applied to assign a specific flow direction to each grid cell by finding the steepest slope between the central cell and its eight neighboring cells. In simulating runoff and infiltration processes, the curve number method, widely used for estimating runoff from precipitation on ungauged basins, is applied to the SWB model. According to an extension of the US Soil Conservation Service curve number procedure (Morel- Seytoux & Verdin, 1981), direct runoff is computed to assign the antecedent soil moisture, shown as equation 2 (Woodward et al., 2002):

$$R = \frac{(P-0.2Smax)^2}{(P+0.8Smax)} \quad P > 0.2Smax \qquad (2)$$

where R is runoff, P is daily precipitation, S_{max} is the maximum soil-moisture holding capacity.

S_{max} is related to curve number as equation (3):

$$S_{max} = \left(\frac{1000}{CN}\right) - 10 \quad (3)$$

where CN is curve number.

The rate of infiltration at the soil surface, affected by the rainfall intensity, as well as the amount of water storage available in the soil profile leads to a smaller S_{max} value (Rallison, 1980).

The classification of the antecedent soil moisture condition (AMC) is obtained based on the total 5-day seasonal rainfall limits (Table 3.1).

Condition II represents an average rainfall- runoff condition for soil- moisture conditions between dry and near saturation. Curve numbers of condition I and III can be calculated using the curve number of condition II (Mishra and Singh, 2003). Considering a useful range of curve number from 30- 98, the range of maximum storage term (S_{max}) would be from 0.2 in. to 23 in. (eq. 3). Therefore, the initial abstraction ($I_a = 0.02\ S_{max}$) varies from 0.04 in. to 4.6 in. Under saturated condition, as in antecedent runoff condition III, higher values of runoff occur when rainfall falls on the soil (Mishra and Singh, 2003). When soils are in dry conditions, as in antecedent runoff condition I, the infiltration rates to soil would increase (Mishra and Singh, 2003).

After considering interception, snowmelt, inflow and runoff, the "effective precipitation" (P) is used as the input for calculating soil moisture changes and recharge to groundwater. To track the changes in soil moisture, which is defined as the amount of water held in soil storage, several values are necessary to be calculated, including the difference between precipitation and potential evapotranspiration (P –PE), accumulated potential water loss (APWL), actual evapotranspiration, soil-moisture surplus, and soil-moisture deficit. Negative values of P-PE represent a potential deficiency of water, while positive values represent a potential surplus of water.

Hydrologically, evaporation refers to the quantity of water lost from soils, rivers, and lakes. Evaporation by plants is called transpiration, whereas evapotranspiration is the combination of the process of evaporation and transpiration. Potential evapotranspiration is the amount of water that would evaporate if sufficient water is available in the soil to meet the demand. The potential evapotranspiration is calculated based on temperature data and other factors.

When P-PE is negative, accumulated potential water loss (APWL) is calculated. As the APWL grows, soil moisture is less readily given up (Westenbroek, S.M. et al., 2010). When P-PE is positive, the new soil-moisture value would be set equal to the preceding soil-moisture value plus (P-PE). If the new soil-moisture value is below the maximum water-holding capacity, a new accumulated potential water-loss value would be back-calculated according to the Thornthwaite-Mather soil-moisture tables (Figure 3.1). Conversely, if the new soil-moisture value exceeds the maximum water-holding capacity, the excess moisture

would become recharge to groundwater, and at the same time the accumulated potential water loss term is reset to zero.

When P-PE is positive, actual evapotranspiration should be equal to the value of potential evapotranspiration. Consequently, the excess value of precipitation over the potential evapotranspiration would be added to soil storage. If, in this manner, the water entering soil moisture exceeds the water-holding capacity, excess water becomes recharge to groundwater. When P-PE is negative, actual evapotranspiration is equal to the sum of precipitation and available water from the soil storage box, up to the amount equal to the potential evapotranspiration.

In short, SWB simplifies the hydrologic cycle by including only the unsaturated soil, snow-cover and groundwater as water storage boxes, and empirical relationships are used to describe fluxes between these storage locations. A conceptual picture of all water transfer processes and water storage locations modeled by SWB is shown in Figure 3.2. The SWB model should yield better results than can be obtained by assuming that a fraction of precipitation converts to recharge; conversely, the SWB model is much simpler and less time-intensive to apply than a fully coupled groundwater and surface-water model based on rigorous physical models (Markstrom and others, 2008; Jyrkama and others, 2002). Also SWB model is simpler than other estimates of potential evapotranspiration based on more complex energy budgets including wind speed, relative humidity, etc.

3.3 Data sources and uncertainties

Data are required to drive many aspects of the current modeling. Broadly, I use three sources of data that contribute to the modeling effort in different ways. Here I discuss briefly the different types of data that contribute to the modeling effort, how they are used, and their associated reliability.

Firstly, surface data include climate information (temperature and precipitation), land elevation / slope, available water capacity, hydrologic soil groups, and land cover. The DEM map used in this study was retrieved from the USGS National Geospatial Program (http://cdiac.ornl.gov/epubs/ndp/ushcn/access.html), providing information on land elevations and slopes. Climate data used was available from the United States Historical Climatology Network, at the Ashland Experimental Farm station (#WI470349). The Department of Natural Resources of Wisconsin provides precise local land cover information (http://dnr.wi.gov/maps/gis/datalandcover.html#data). Soil properties data were retrieved from the Natural Resources Conservation Service (NRCS) (http://soildatamart.nrcs.usda.gov/). These data are used as inputs to drive the Soil Water Balance (SWB) model, which estimates recharge to the hydrogeologic system based on the above described simplified soil water/ surface water routing routine. Uncertainties in the data sets have complex spatial as well as temporal dependencies. Additional data uncertainties may be present due to limited spatial coverage, numbers of samples and biases in the measurements. In particular, climate information is only reported at a single location on the peninsula, and extrapolation of climatic conditions across the peninsula represents a major source of uncertainty.

Secondly, subsurface structural hydrologic data include the site hydrostratigraphy and the boundary conditions. The subsurface stratigraphy is relatively well constrained, as much of the stratigraphy on the peninsula consists of thick, uniform sand deposits which have been mapped extensively thorough drilling records. Uncertainties are due to limited values of hydrologic properties and the spatial variability of these properties. And also uncertainties are associated with the particular flow parameter values within each hydrostratigraphic unit (i.e., hydraulic conductivity) as well as with the assumptions of boundary conditions, which impact hydrogeologic processes.

Finally, "conditioning data" consist of river baseflow measurements and well water levels measured within the study area. Surface hydrologic data include information from river "seepage runs", performed by the USGS at several streams within the Bayfield Peninsula, which measure baseflow contributions to water in these streams. Mean annual baseflow values were measured in November 2002 and October 2011. The 2011 data reflect the dry period in Northern Wisconsin in the early 2000's, while the baseflow values from 2002 are used to avoid bias due to the dry conditions in 2011. Water level measurement data were from Well Construction Reports available from the Wisconsin Department of Natural Resources (WDNR) from 2000 or later. The baseflow data for the streams and the head data from wells are used as targets during modeling, and provide the information for validation and tuning of conceptual models. Data uncertainties may be present due to numbers of samples and biases in the measurements.

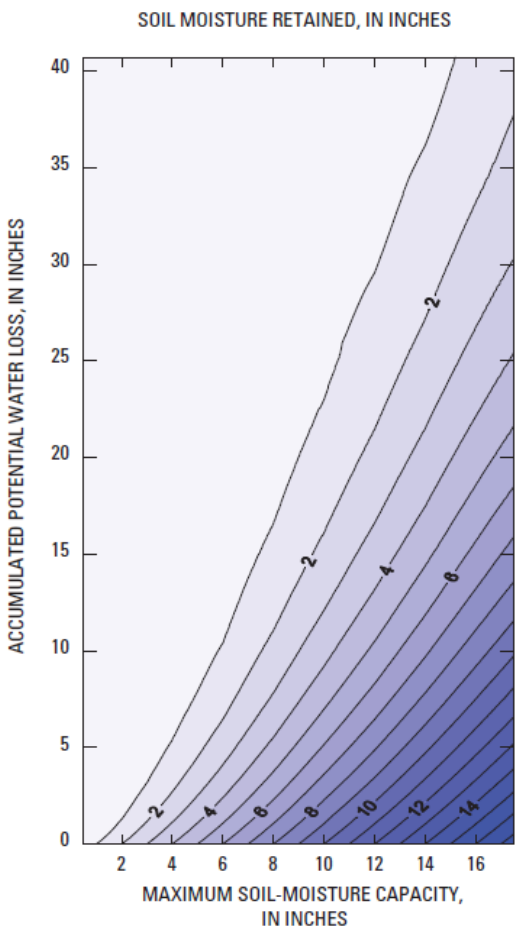

Figure 3.1: Soil-moisture-retention table (based on Thornthwaite and Mather, 1957)

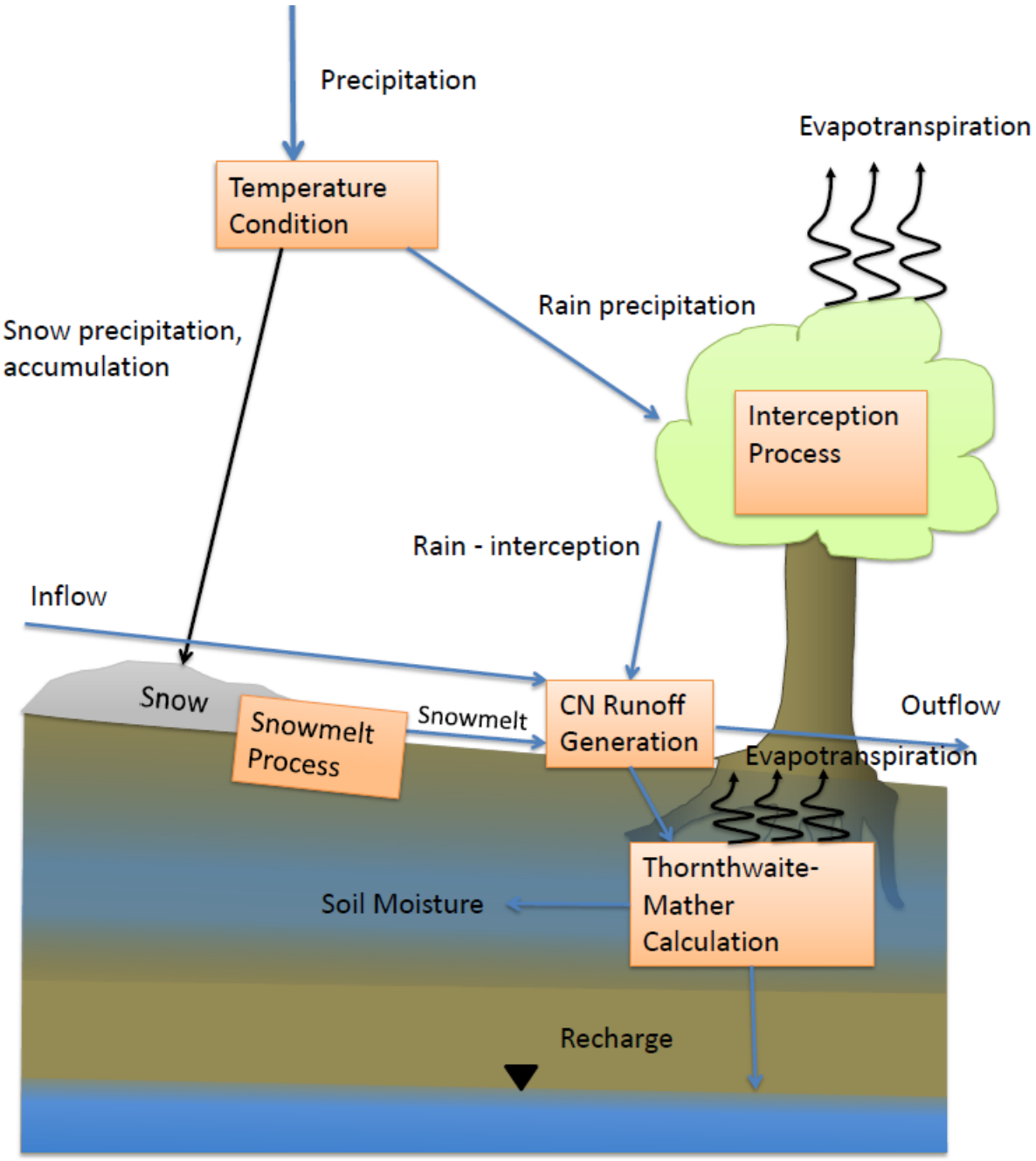

Figure 3.2: SWB concept model

Table 3.1: Definition of antecedent runoff conditions used in the SWB code (Precipitation in preceding 5 days, in inches) (Westenbroek et al., 2010)

Condition	Soil wetness	Dormant season	Growing season
I	Dry	< 0.05	< 1.4
II	Average	0.5–1.1	1.4 – 2.1
III	Near saturation	> 1.1	> 2.1

Chapter 4 – Site Conceptual Model

4.1 Groundwater flow model geometry

An existing model of the subsurface hydrogeology of the Bayfield Peninsula is developed, which is forced by conceptual models representing different assumptions about spatially-distributed recharge and hydrological properties. The groundwater flow model of the Bayfield Peninsula was built by the USGS through the MODFLOW Groundwater Vistas interface. The groundwater in the Bayfield Peninsula interacts with surface water features including Lake Superior located at the east and north sides, and with the inland stream network. Since temporal variations in water levels and streamflows are not available, the groundwater model is constructed as steady-state and the recharge estimates used represent mean daily recharge over a 24-year time period. The spacing of the grid is laterally uniform throughout the whole MODFLOW model, with each element square and 264 feet on a side. The numbers of rows and columns are 600 and 740 respectively. The model is divided into five layers vertically, with spatially-variable thicknesses. Conceptually, the top of layer 1 represents the land surface, and the bottom of layer 1 splits the unconsolidated unit into two parts of equal thickness. In the central peninsula, layer 1 and layer 2 represent the Copper Falls Formation, whereas on the fringes of Lake Superior, the Miller Creek Formation occupies layer 1 and layer 2. The bedrock surface is represented by the top of layer 3, with layers 4 and 5 all representing the deeper bedrock aquifers. The bottoms of layer 3 and layer 4 are 70 feet and 300 feet below the bedrock surface at every location in the model. The thickness of layer 5 is 630 feet, which is 1000 feet below the top of the bedrock (Fig. 4.1 & Fig. 4.2).

The Copper Falls Formation is treated as uniformly homogeneous in layer 1, while the Miller Creek Formation is relatively heterogeneous. Heterogeneity within the Miller Creek formation is interpolated based on descriptions of lithology from drilling logs. The basis function used for interpolation consists of lithological characteristics (coarse fraction), which is transformed to an estimated hydraulic conductivity and is interpolated over the map. A power law (Fig. 4.3) is used to convert between the coarse fraction values and hydraulic conductivity to be estimated. Layer 2 of the model uses the same homogeneous value for hydraulic conductivity as the Copper Falls value in layer 1. Miller Creek Formation is also regarded as homogeneous in layer 2. Layer 3, 4 and 5 all represent the sandstone bedrock aquifer. Layer 5 is treated as homogeneous throughout the entire study site.

4.2 Model forcing

Groundwater tends to move from the unconsolidated layers-- considered as the top two layers-- to the deep layers, due to recharge. The leakage to the bedrock aquifer, lateral flow within the sandstone and circulation to discharge areas can be quantified in the conceptual model. The surface water network includes all the inland perennial streams interacting with groundwater. The relationship between the simulated water table and stream stage mainly determine the exchange between groundwater and surface water. The effect of high-capacity pumping wells to the flow system in the domain can be neglected in the area of interest.

The groundwater model is forced primarily by recharge within the modeled domain. Three main conceptual models with different underlying assumptions are used to force the groundwater flow model. These models include zoned recharge, SWB-based recharge assuming spatially- constant climatological forcing based on a single climate station on the peninsula (which I refer to as "single station climate"), and spatially variable climate forcing based on a combination of the climate station data with a model describing spatial variability in climatological parameters (which I refer to as "gridded climate").

4.2.1 Zoned recharge conceptual model

In the zoned recharge conceptual model, the spatial variability of recharge throughout the same geologic formation is neglected. A single recharge value, of $1.0267*10^{-3}$ feet/day is assigned to the entire "fringe" area of the peninsula in which layer 1 of the model is the Miller Creek Formation, mainly covered by clay. The area of the model in which layer 1 is the Copper Falls Formation (the "central" peninsula) is considered to have a uniform recharge rate of $3.7871 *10^{-3}$ feet/day (Fig. 4.4). These recharge estimates were determined as part of the model calibration process based on existing data from the peninsula (USGS, 2014).

4.2.2 SWB-based conceptual models for estimating recharge

The Soil Water Balance (SWB) code takes spatially variable factors, including climate, land cover and topography into consideration (Westenbroek, 2010) and uses a semi-physical

model to provide a more physically- derived distributed recharge rate throughout the study site.

Tabular, gridded data as well as standard tables are required as input information to estimate the recharge rate based on the water budget in the SWB model. In terms of gridded input, all of the files should be gridded using the same reference locations and cell size as those of the model in MODFLOW. The coordinate (in Wisconsin State Plane) of the upper left corner of the grid is (47˚02'N, 91˚ 26'W) and the cell size is 264 feet by 264 feet. The numbers of cells of rows and columns are 600 and 740 respectively, matching the MODFLOW model grid.

The meteorological daily data required for SWB model include precipitation (inches), maximum temperature (°F), minimum temperature (°F), and average temperature (°F). Meteorological data can either be provided through a "single station" climate setup, where the same meteorological data is assumed to apply across the entire model domain, or through a "distributed climate" setup, where each of these parameters must be specified at all grid cells and across all days in the modeled period. In this study, we employed both a single-station (spatially constant) climate and a spatially variable climate.

4.2.2.1 Climatic data

Single station climate model

Daily climate data of a single station is from USHCN (United States Historical Climatology Network (M.J. Menne, C.N. Williams, Jr., and R.S. Vose, National Climatic Data Center,

National Oceanic and Atmospheric Administration; Karl et al., 1990). Daily data containing observations of maximum, minimum and average temperature as well as precipitation amount are required as inputs. The temperatures are used to determine the form (rain or snow) of the precipitation.

Based on the location of the study site, I choose the Ashland Experimental Farm station (#WI470349) as data source. The location of the station is 46°34'N, 90°58'W (shown in Fig. 4.5) and the elevation of which is 650 feet. Data from year 1981 to 2004 are used in this study (Fig. 4.6). There are missing data in the original dataset. Since daily records of precipitation data as well as temperature are required by the simulation, missing values were filled in using the average values in the previous three days.

Gridded climate model - PRISM model coupled with single station climate

While only a single climate station is available near the Bayfield Peninsula, it is likely that significant spatial differences in climate are associated with factors such as elevation, wind speed, and proximity to Lake Superior, among others. To represent this climate variability, I developed an interpolation of climatic parameters across the entire Bayfield region based on the PRISM spatially-distributed climate estimates. The PRISM model (Daly et al., 2002) describes the spatial patterns of climate and their relationship with geographic features to support the creation of high-resolution climate datasets. PRISM (parameter-elevation regressions on independent slopes model) is a dynamic knowledge-based framework that uses point data, a digital elevation model (DEM), and other spatial data sets to generate

estimates of annual, monthly and event-based climatic elements that are gridded and GIS-compatible (Daly et al., 2002).

PRISM is based on the assumption that elevation has the dominant influence on the distribution of temperature and precipitation for a localized region. The climate-elevation regression has the form:

$$Y = \beta_1 X + \beta_0 \qquad (4)$$

where Y is the predicted climate element, β_1 and β_0 are the regression slope and intercept, respectively, and X is the DEM elevation at the target grid cell (Daly et al., 2002).

Upon entering the regression function, each climate station is assigned a weight that is based on several factors. The combined weight (W) of a station is given by the following:

$$W = W_c \left[F_d W_d^2 + F_z W_z^2\right]^{1/2} W_p W_f W_l W_t W_e \qquad (5)$$

Where W_c , W_d , W_z, W_p, W_f, W_l, W_t and W_e are the cluster, distance, elevation, coastal proximity, topographic facet , vertical layer, topographic position, and effective terrain weights, respectively, and F_d and F_z are user-specified distance and elevation weighting importance scalars (Daly et al., 2002; Daly et al., 2007). In producing a spatially- distributed map of regional climate, these weights control the degree to which a given climate station influences the estimate of climate variables at an unmonitored location.

The 30-year normal PRISM dataset of precipitation, maximum temperature and minimum temperature are used as one part of the dataset for the gridded climate input to SWB. The products from the PRISM model are a baseline map describing average annual conditions over 1981-2004. The spatial resolution is 800m (2624.67 feet) in the original PRISM map,

which was downscaled using simple linear interpolation to the Red Cliff Region (Fig. 4.7, Fig. 4.8 & Fig. 4.9).

I developed a basic algorithm to combine PRISM datasets with single climate station data to obtain daily gridded climate inputs at the scale of the groundwater flow model grid cells throughout the years of 1981-2004, which represents the required gridded climate data for the SWB model. The sum of precipitation for each year is calculated using the single station data, from which the distributions of precipitation within years are calculated. The same algorithm is applied when calculating the distribution of precipitation within days in a single year (see Appendix A). The logic used to develop daily precipitation estimates is shown as follows:

$P(y) = \Sigma P(d)$ (in a year); $D\_p(y) = P(y)/\Sigma P(y)$ (year $1981 - 2004$);

P (i, j) = PRISM data (i, j) * years; P (i, j, y) = P (i, j) * D_p (y);

D_p (d) =P(d)/P(y) (in a year); P (i, j, d) = P (i, j, y)* D_p(d);

where P (y) is the precipitation of a year at a single station; P (d) is the precipitation of a day at a single station; D_p (y) is the percent of precipitation within years; P (i, j) is the gridded precipitation of all years; P (i, j, y) is the gridded precipitation of a year; D_p (d) is the percent of precipitation within days in a year; P (i, j, d) is the gridded precipitation of a day; and PRISM data (i, j) is the gridded average annual precipitation within years.

In terms of maximum temperature and minimum temperature, normalization is used to calculate the proportion for each day using the single station data, based on the assumption that the distribution of temperature is consistent with a Gaussian distribution. Coupling the

results with PRISM normal gridded data, the daily gridded climate data are produced for all years (see Appendix A). The logic for producing these estimates is shown as follows:

$D\_t\,(d) = \frac{T(d) - mu(d)}{sigma\,(d)}$ (within a year); T (i, j, d) = PRISM data (i, j) * sigma (d) + mu (d);

where D_t (d) is the distribution of temperature (maximum, minimum or mean) of a day at a single station, T (d) is the temperature (maximum, minimum or mean) of a day at a single station; mu (d) is the mean value of daily temperature (maximum, minimum or mean) in a year; sigma (d) is the standard deviation of daily temperature (maximum, minimum or mean) in a year; PRISM data (i, j) is the average daily temperature (maximum, minimum or mean) within the years and T (i, j, d) is the gridded daily temperature (maximum, minimum or mean). We assume the mean value (sigma) and standard deviation (mu) are the same throughout the years.

The ET method suitable for use with gridded precipitation data is the Hargreaves-Samani method, because all other methods require additional gridded data, such as relative humidity and wind speed, in order to properly apply them in a distributed fashion, and these data were not available for the investigated region. The 1985 Hargreaves method (eq. 6) is often used to provide ET_0 (potential evaporation) predictions for weekly or longer periods and is attractive due to its simplicity, reliability, minimum data requirements, ease of computation, and low impact by weather station aridity.

4.2.2.2 Soil and land uses

Land use/land cover

Land use/ land cover data is used to calculate surface runoff values. Along with the available soil-water capacity, maximum soil-moisture holding capacities can be determined. SWB model requires the land classification method following a modified Anderson Level II classification scheme (Anderson et al., 1976) of Dripps (2003). Curve-number, interception, maximum-recharge, and rooting-depth data for different land-use types are necessary in the land-use lookup table (Fig. 4.10), based on which runoff curve numbers and a maximum soil-moisture holding capacity are assigned for each grid.

We use the Wisconsin Land Cover (WLC) data as the land use information from the Department of Natural Resources of Wisconsin. The WISCLAND land cover data are derived primarily from satellite imagery. After processing, the data have a minimum mapping unit of five acres (217,800 square feet). The classified land cover types can be summarized to indicate how much of each land cover is present over the study area (Fig. 4.11).

Hydrologic soil group

According to the categorization conducted by the U.S. Department of Agriculture, Natural Resources Conservation Service (NRCS), there are four hydrologic soil groups (A-D) with a decreasing trend of infiltration capacity from A to D, consequently, with an increasing trend of overland flow potential (Table 4.1).

The data source used in my modeling is Soil Data Mart from Natural Resources Conservation Service of United States Department of Agriculture (Fig. 4.12).

Available water capacity

Available water capacity is the amount of water that a soil can store that is available for use by plants (USDA Natural Resources Conservation Service, 1998), which is affected by soil properties such as rock fragments, organic matter, and bulk density.

In the SWB model, to define a maximum soil moisture holding capacity (inches of water), the value of available water capacity (inches of water per foot of soil) assigned to each grid cell is multiplied by the depth of roots (feet) based on land cover categories (eq. 7).

maximum soil water capacity = available soil water capacity * root-zone depth (7)

(Westenbroek, S.M. et al., 2010)

Soil texture can be used as another reference if data for available water capacity are not available (Table 4.2).

The data source used to obtain soils data within the peninsula is Soil Data Mart from Natural Resources Conservation Service of United States Department of Agriculture (Fig. 4.13).

Matrix of soil-water retention for given accumulated potential water loss

Accumulated potential water loss as well as the maximum soil-moisture capacity is considered to determine the amount of soil moisture. Based on the original soil-moisture-retention table by Thornthwaite and Mather (1957), a modified table is incorporated in the SWB code to calculate the changes in soil moisture under the conditions with unsatisfied potential evapotranspiration. The modified table contains values of maximum soil-moisture capacities ranging from 0.5 to 17.5 inches, and the value of maximum accumulated potential water loss up to 40.7 inches.

The relationship between the accumulated potential water loss and soil moisture retained with respect to the maximum soil-moisture capacity is shown in Figure 4.14.

4.2.2.3 Flow direction

Water that is not infiltrated within a grid cell results in overland flow. The direction of overland flow is determined by the local slope of the land surface. The D8 flow-routing algorithm (O'Callaghan and Mark, 1984) is incorporated in the SWB model to assign a flow direction for each cell. Elevation in the area of interest is crucial to find the steepest slope between the central cell and its eight neighboring cells. Recharge to groundwater is accumulated when facing a closed depression, or when water infiltrated as soil moisture exceeds the soil moisture capacity of the soil.

I used the National Map Viewer and Download Platform to visualize the topographic base map (managed by the USGS National Geospatial Program). The elevation information (Fig.

4.15) is imported into ArcGIS (ESRI, 2013), and can be interpreted as flow direction using the D8 algorithm.

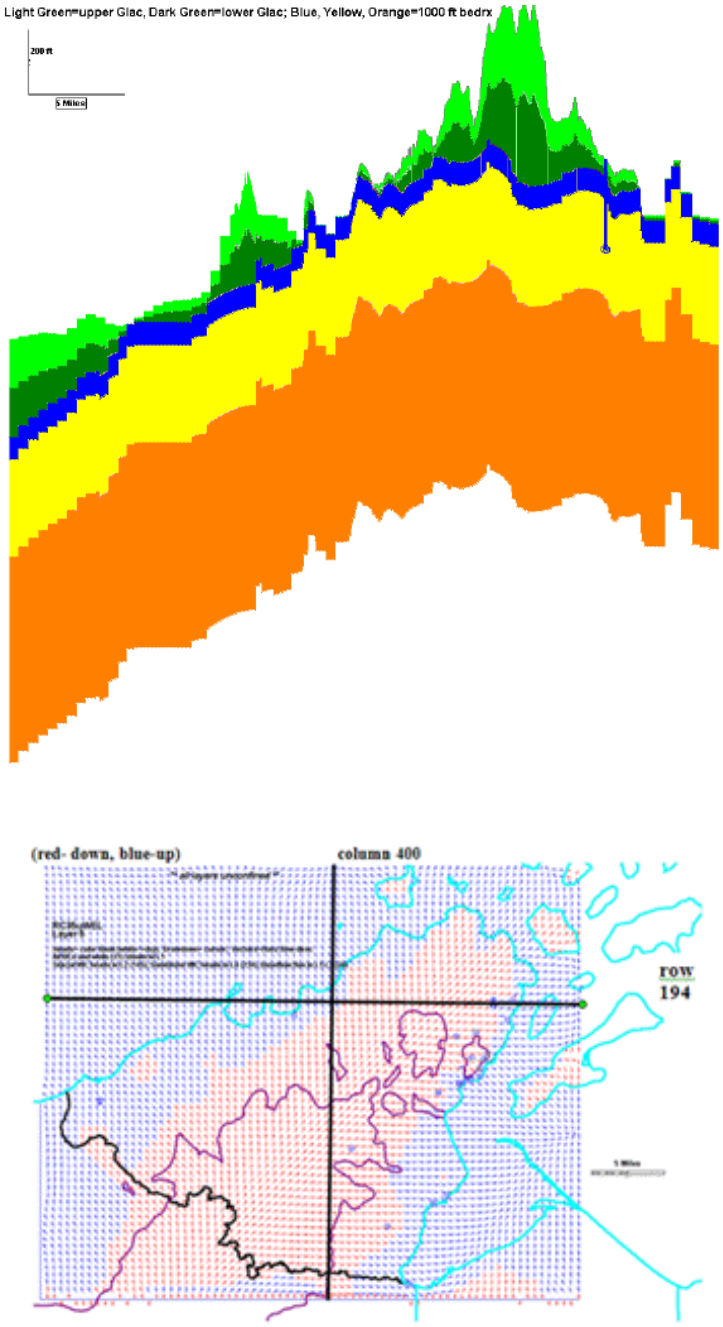

Light Green: Upper Glacier Deposits Dark Green: Lower Glacier Deposits

Blue, Yellow, Orange: Bedrock (1000 feet)

Figure 4.1: West to East cross section of model layering (Row 194), Bayfield Peninsula, WI (USGS, 2015)

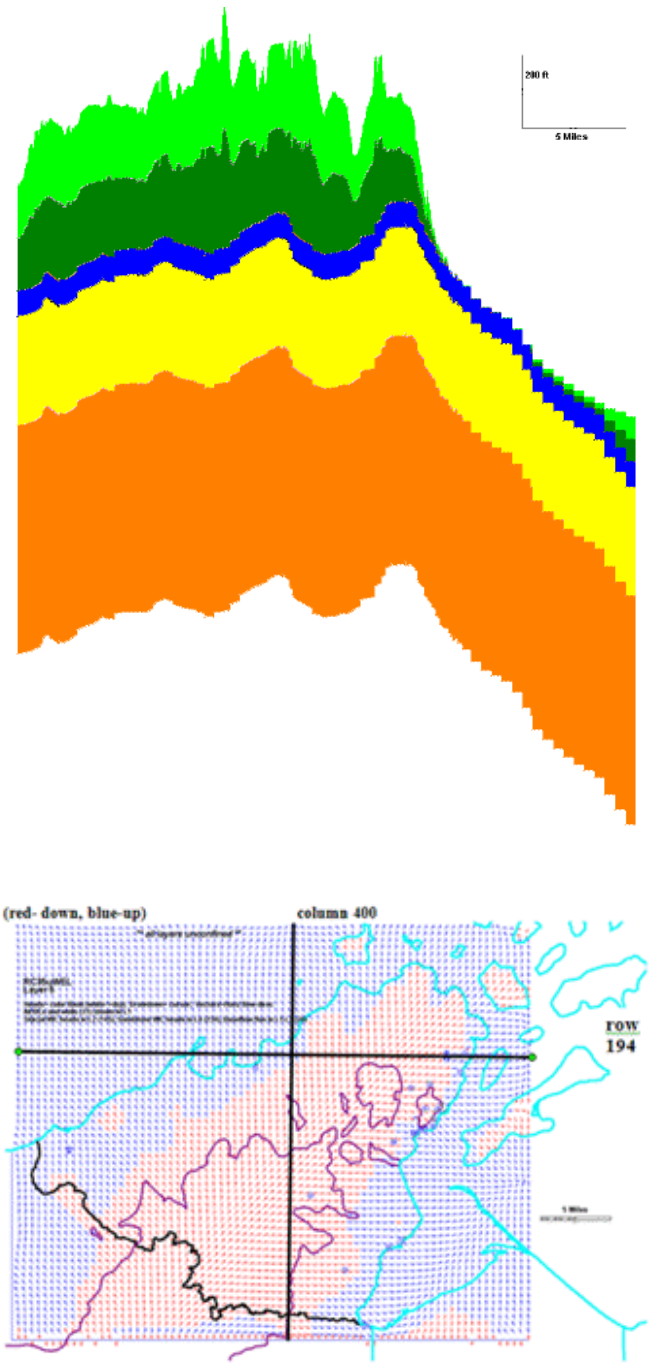

Light Green: Upper Glacier Deposits Dark Green: Lower Glacier Deposits

Blue, Yellow, Orange: Bedrock (1000 feet)

Figure 4.2: North to South cross section of model layering (Column 400), Bayfield Peninsula, WI (USGS, 2015)

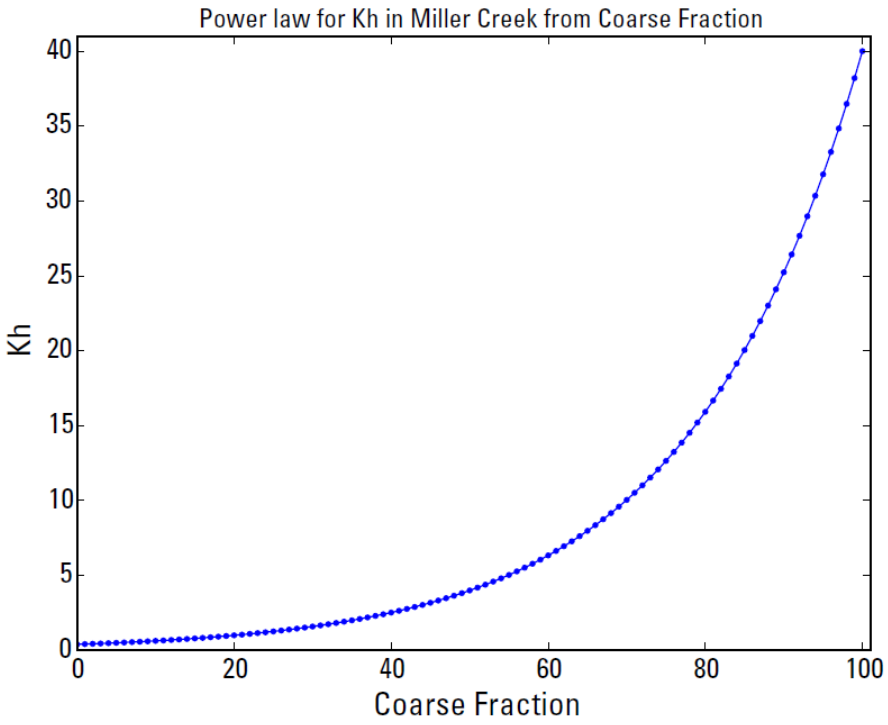

Figure 4.3: Power-law relationship between *PCTCoarse* and K_h for starting values of min_{kh} = 0.4 and K_{range} = 2.0, Bayfield Peninsula, WI (USGS, 2015)

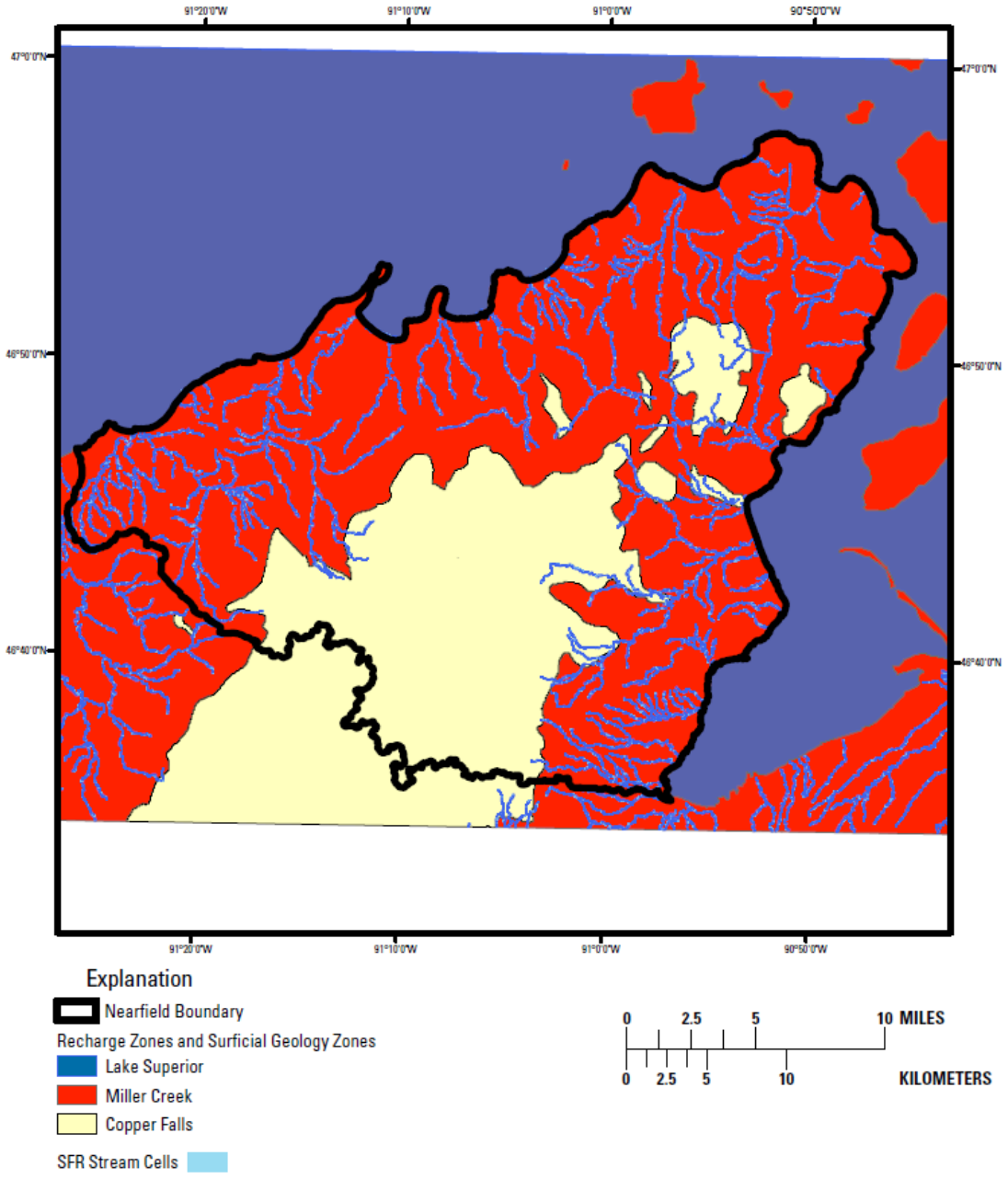

Figure 4.4: Recharge zones and stream flow routing cells of the Red Cliff model, Bayfield Peninsula, WI (USGS, 2015)

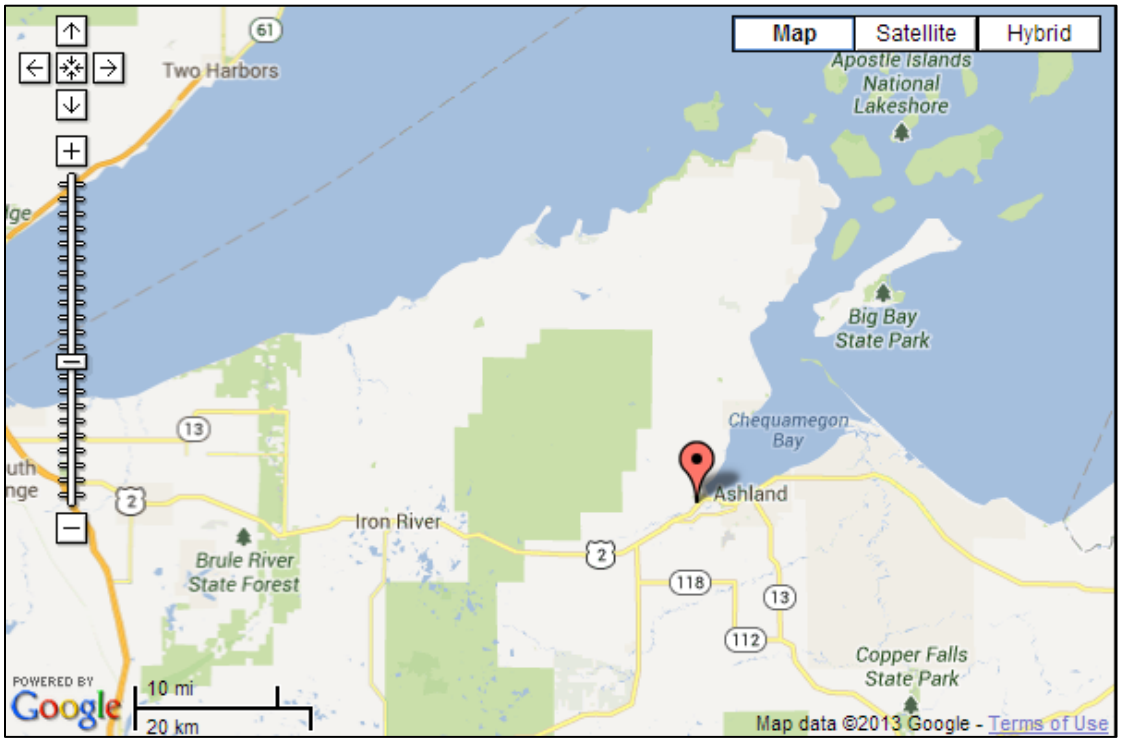

Figure 4.5: Location of the climate station (based on Google map)

Month	Day	Year	TAVG(F)	Precipitation(in)	Avg_Rel_Hum(%)	TMAX(F)	TMIN(F)	WINDVEL(m/sec)	Min_Rel_Hum(%)	Sunshine
1	1	1986	9.00	0.01	-99999.00	21.00	-3.00	-99999.00	-99999.00	-99999.00
1	2	1986	18.00	0.00	-99999.00	23.00	13.00	-99999.00	-99999.00	-99999.00
1	3	1986	13.00	0.00	-99999.00	24.00	2.00	-99999.00	-99999.00	-99999.00
1	4	1986	20.00	0.07	-99999.00	28.00	11.00	-99999.00	-99999.00	-99999.00
1	5	1986	12.00	0.00	-99999.00	20.00	4.00	-99999.00	-99999.00	-99999.00
1	6	1986	3.00	0.00	-99999.00	18.00	-12.00	-99999.00	-99999.00	-99999.00
1	7	1986	-11.00	0.00	-99999.00	0.00	-21.00	-99999.00	-99999.00	-99999.00
1	8	1986	4.00	0.00	-99999.00	20.00	-13.00	-99999.00	-99999.00	-99999.00
1	9	1986	33.00	0.00	-99999.00	46.00	20.00	-99999.00	-99999.00	-99999.00
1	10	1986	31.00	0.00	-99999.00	42.00	20.00	-99999.00	-99999.00	-99999.00
1	11	1986	37.00	0.00	-99999.00	46.00	28.00	-99999.00	-99999.00	-99999.00
1	12	1986	27.00	0.00	-99999.00	38.00	16.00	-99999.00	-99999.00	-99999.00
1	13	1986	9.00	0.00	-99999.00	18.00	-1.00	-99999.00	-99999.00	-99999.00
1	14	1986	16.00	0.00	-99999.00	23.00	8.00	-99999.00	-99999.00	-99999.00
1	15	1986	17.00	0.00	-99999.00	31.00	3.00	-99999.00	-99999.00	-99999.00
1	16	1986	22.00	0.00	-99999.00	40.00	4.00	-99999.00	-99999.00	-99999.00
1	17	1986	38.00	0.00	-99999.00	45.00	31.00	-99999.00	-99999.00	-99999.00
1	18	1986	30.00	0.02	-99999.00	41.00	18.00	-99999.00	-99999.00	-99999.00
1	19	1986	26.00	0.00	-99999.00	30.00	22.00	-99999.00	-99999.00	-99999.00
1	20	1986	24.00	0.00	-99999.00	27.00	20.00	-99999.00	-99999.00	-99999.00
1	21	1986	28.00	0.13	-99999.00	31.00	25.00	-99999.00	-99999.00	-99999.00
1	22	1986	19.00	0.20	-99999.00	30.00	7.00	-99999.00	-99999.00	-99999.00
1	23	1986	2.00	0.00	-99999.00	20.00	-16.00	-99999.00	-99999.00	-99999.00
1	24	1986	21.00	0.03	-99999.00	32.00	10.00	-99999.00	-99999.00	-99999.00
1	25	1986	25.00	0.04	-99999.00	34.00	15.00	-99999.00	-99999.00	-99999.00
1	26	1986	7.00	0.03	-99999.00	19.00	-5.00	-99999.00	-99999.00	-99999.00
1	27	1986	-7.00	0.01	-99999.00	8.00	-22.00	-99999.00	-99999.00	-99999.00
1	28	1986	8.00	0.00	-99999.00	15.00	0.00	-99999.00	-99999.00	-99999.00
1	29	1986	13.00	0.00	-99999.00	17.00	8.00	-99999.00	-99999.00	-99999.00
1	30	1986	11.00	0.00	-99999.00	21.00	1.00	-99999.00	-99999.00	-99999.00
1	31	1986	6.00	0.00	-99999.00	23.00	-12.00	-99999.00	-99999.00	-99999.00

Figure 4.6: Climate input file for “single station” climate run

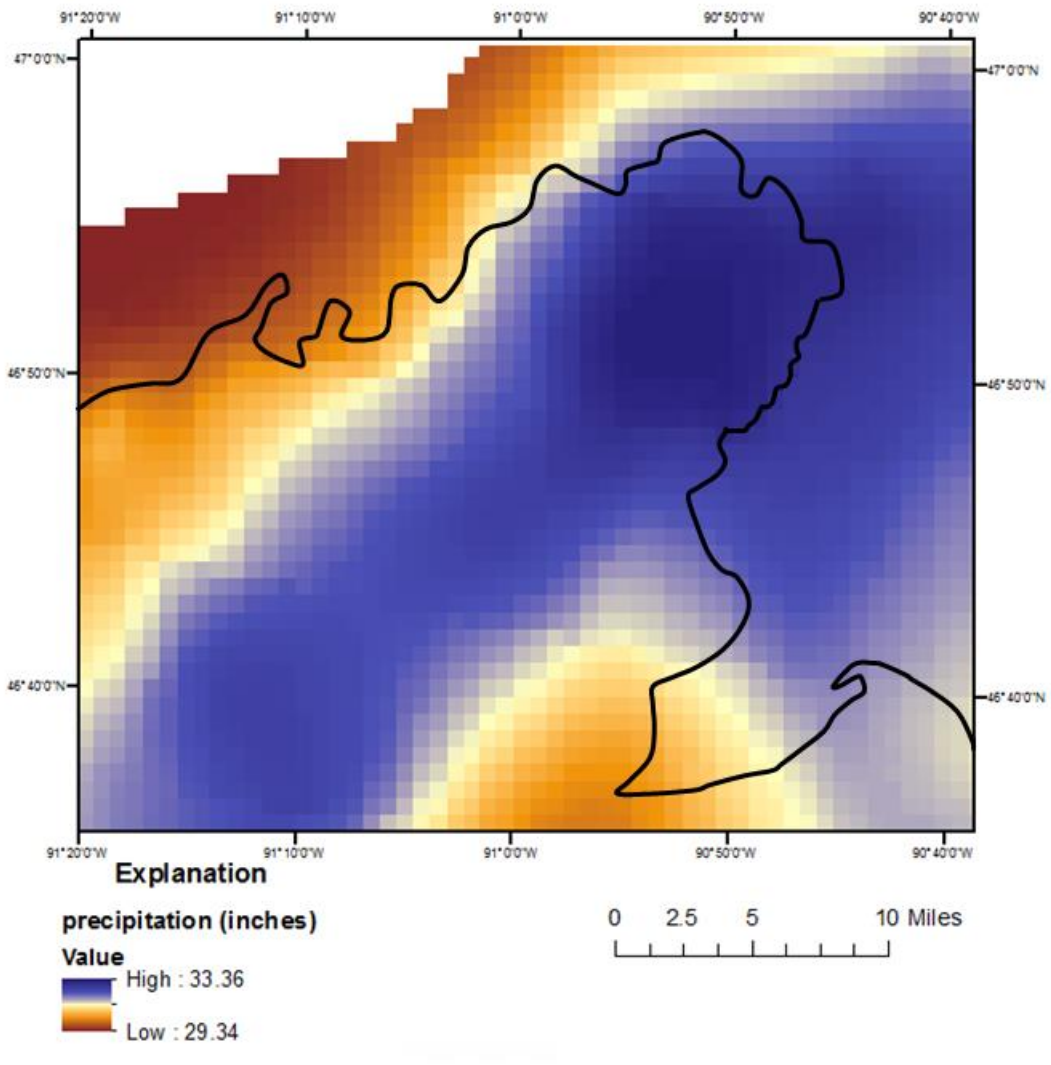

Figure 4.7: PRISM-estimated mean annual precipitation, for the years 1981- 2004, in the Red Cliff area, Bayfield Peninsula, WI

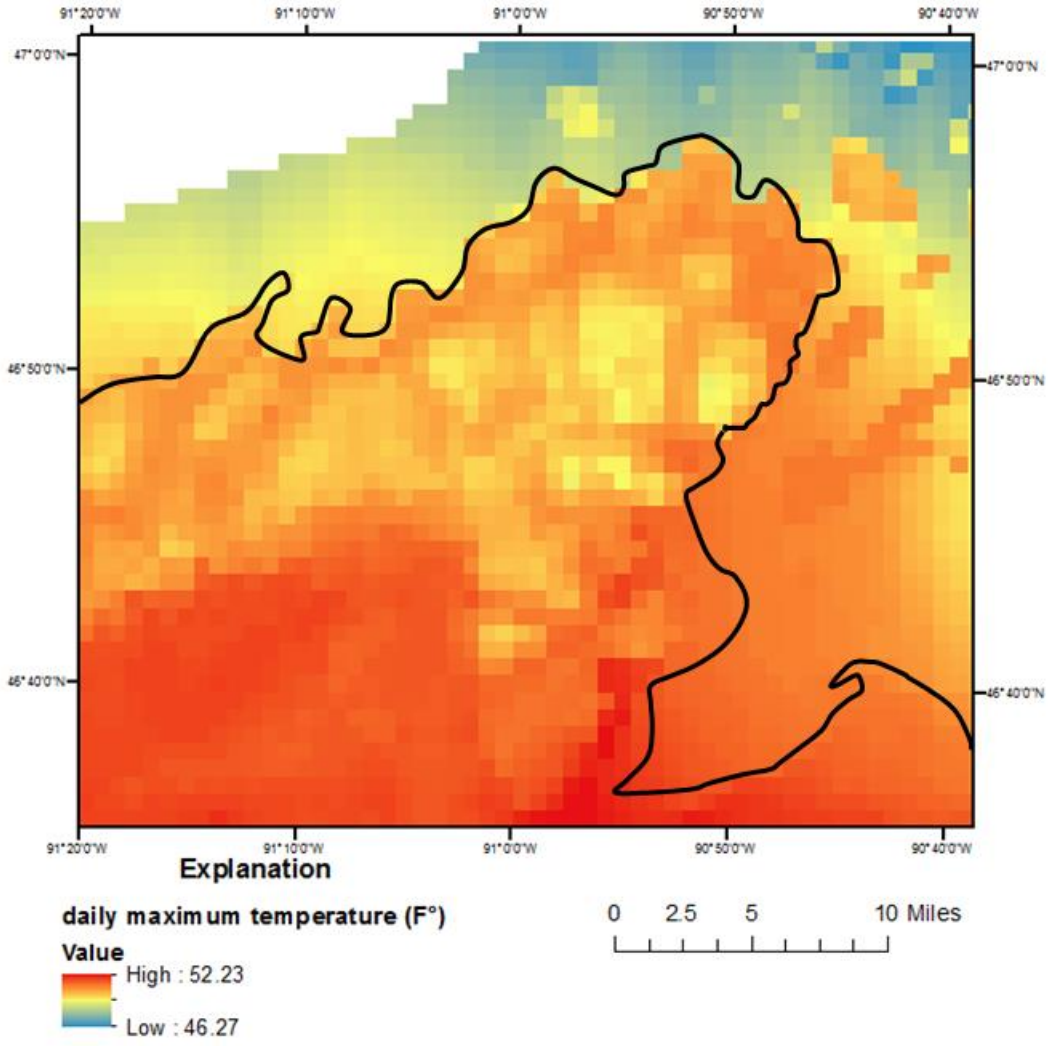

Figure 4.8: PRISM-estimated average daily maximum temperature, for the years 1981-2004, in the Red Cliff area, Bayfield Peninsula, WI

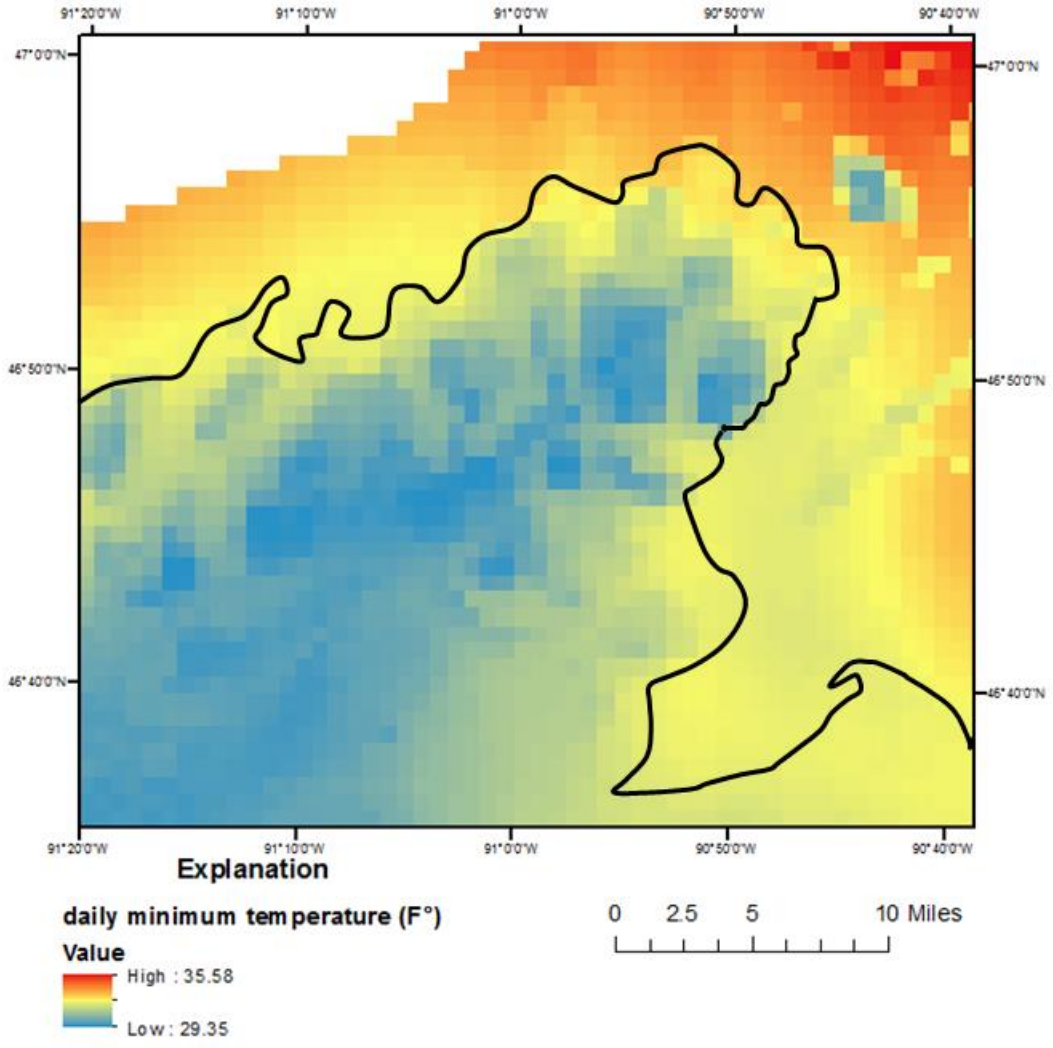

Figure 4.9: PRISM-Estimated average daily minimum temperature in the Red Cliff area, Bayfield Peninsula, WI

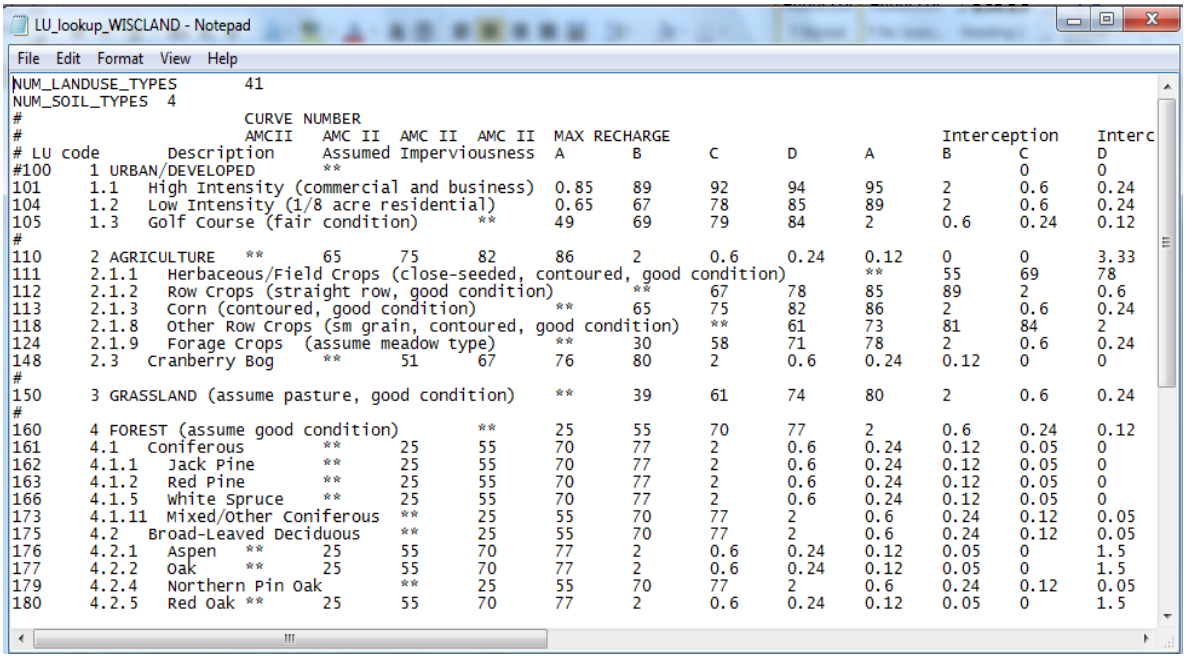

LU_lookup_WISCLAND - Notepad

File Edit Format View Help

```
NUM_LANDUSE_TYPES       41
NUM_SOIL_TYPES  4
#                       CURVE NUMBER                                                    Interception    Interc
# LU code       Description     Assumed Imperviousness  A       B       C       D       A       B       C       D
#100    1 URBAN/DEVELOPED       **                                                              0       0
101     1.1   High Intensity (commercial and business)  0.85    89      92      94      95      2       0.6     0.24
104     1.2   Low Intensity (1/8 acre residential)      0.65    67      78      85      89      2       0.6     0.24
105     1.3   Golf Course (fair condition)      **      49      69      79      84      2       0.6     0.24    0.12
#
110     2 AGRICULTURE   **      65      75      82      86      2       0.6     0.24    0.12    0       0       3.33
111     2.1.1   Herbaceous/Field Crops (close-seeded, contoured, good condition)                **      55      69      78
112     2.1.2   Row Crops (straight row, good condition)        **      67      78      85      89      2       0.6
113     2.1.3   Corn (contoured, good condition)        **      65      75      82      86      2       0.6     0.24
118     2.1.8   Other Row Crops (Sm grain, contoured, good condition)   **      61      73      81      84      2
124     2.1.9   Forage Crops  (assume meadow type)       **      30      58      71      78      2       0.6     0.24
148     2.3   Cranberry Bog     **      51      67      76      80      2       0.6     0.24    0.12    0       0
#
150     3 GRASSLAND (assume pasture, good condition)    **      39      61      74      80      2       0.6     0.24
#
160     4 FOREST (assume good condition)        **      25      55      70      77      2       0.6     0.24    0.12
161     4.1   Coniferous        **      25      55      70      77      2       0.6     0.24    0.12    0.05    0
162     4.1.1   Jack Pine       **      25      55      70      77      2       0.6     0.24    0.12    0.05    0
163     4.1.2   Red Pine        **      25      55      70      77      2       0.6     0.24    0.12    0.05    0
166     4.1.5   White Spruce    **      25      55      70      77      2       0.6     0.24    0.12    0.05    0
173     4.1.11  Mixed/Other Coniferous  **      25      55      70      77      2       0.6     0.24    0.12    0.05
175     4.2   Broad-Leaved Deciduous    **      25      55      70      77      2       0.6     0.24    0.12    0.05
176     4.2.1   Aspen   **      25      55      70      77      2       0.6     0.24    0.12    0.05    0       1.5
177     4.2.2   Oak     **      25      55      70      77      2       0.6     0.24    0.12    0.05    0       1.5
179     4.2.4   Northern Pin Oak        **      25      55      70      77      2       0.6     0.24    0.12    0.05
180     4.2.5   Red Oak **      25      55      70      77      2       0.6     0.24    0.12    0.05    0       1.5
```

Figure 4.10: Soil and land use properties lookup table

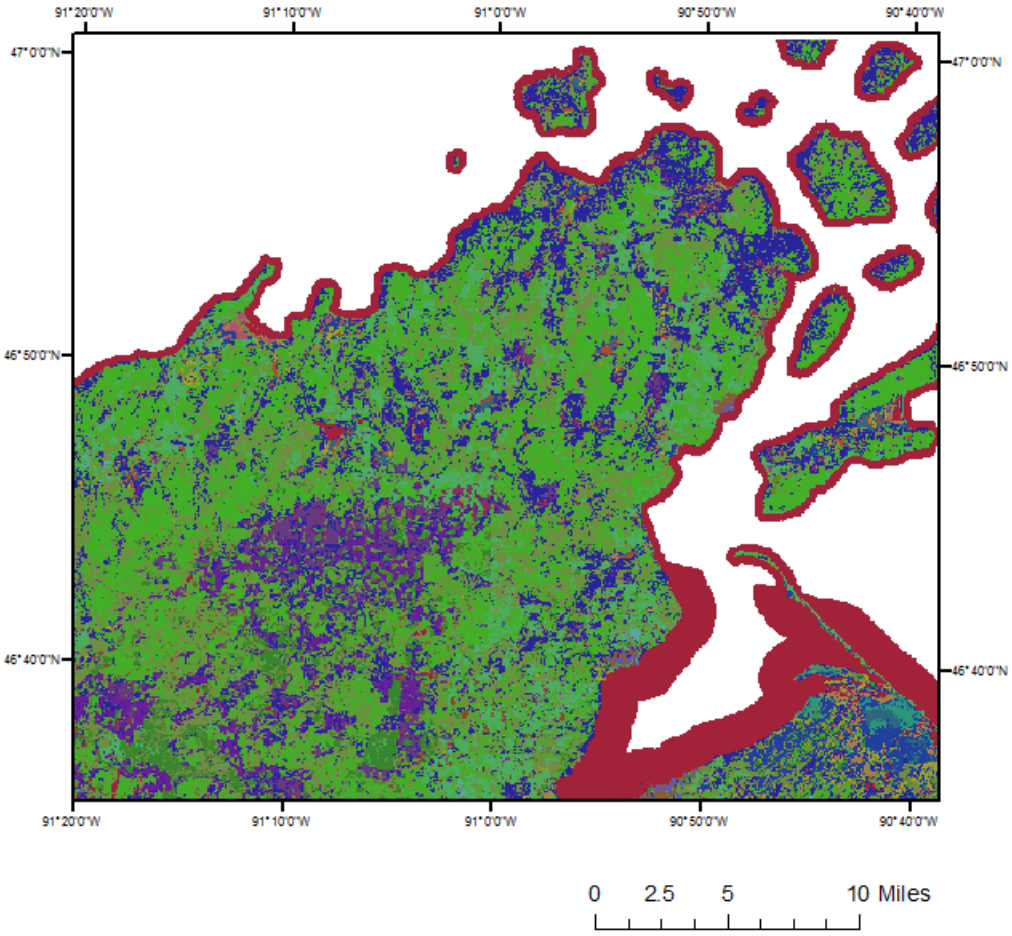

EXPLANATION

Land-cover classification

- Shrubland
- Barren
- Mixed Deciduous/Coniferous (Forested)
- Coniferous (Forested)
- Broad-leaved Deciduous (Forested)
- Broad-leaved Evergreen (Lowland Shrub)
- Broad-leaved Deciduous (Lowland Shrub)
- Lowland Shrub
- Emergent/Wet Meadow
- Open Water
- Mixed Deciduous/Coniferous
- Mixed/Other Broad-leaved Deciduous

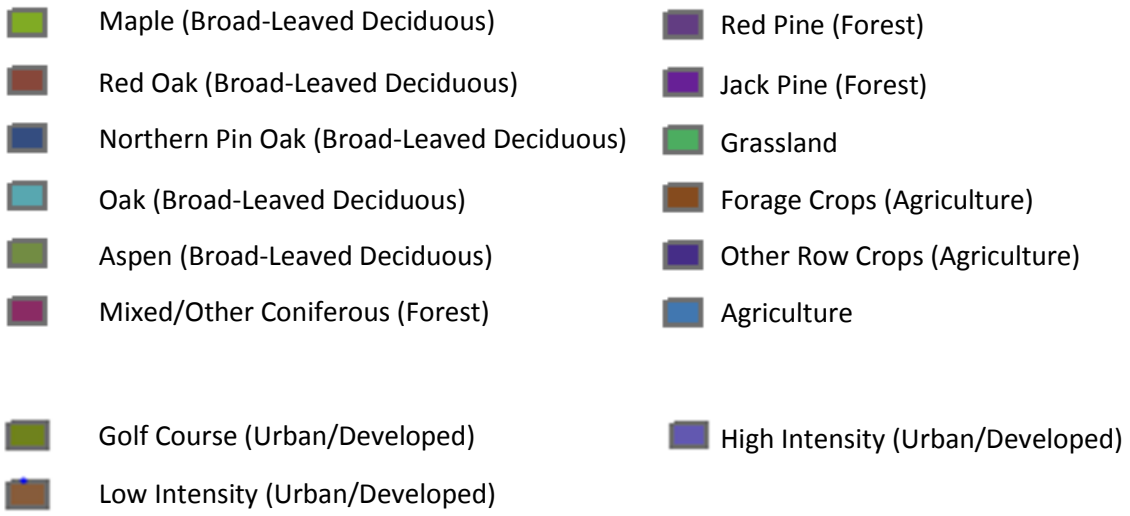

Figure 4.11: Land use/ land cover classification of the Red Cliff model, Bayfield Peninsula, WI

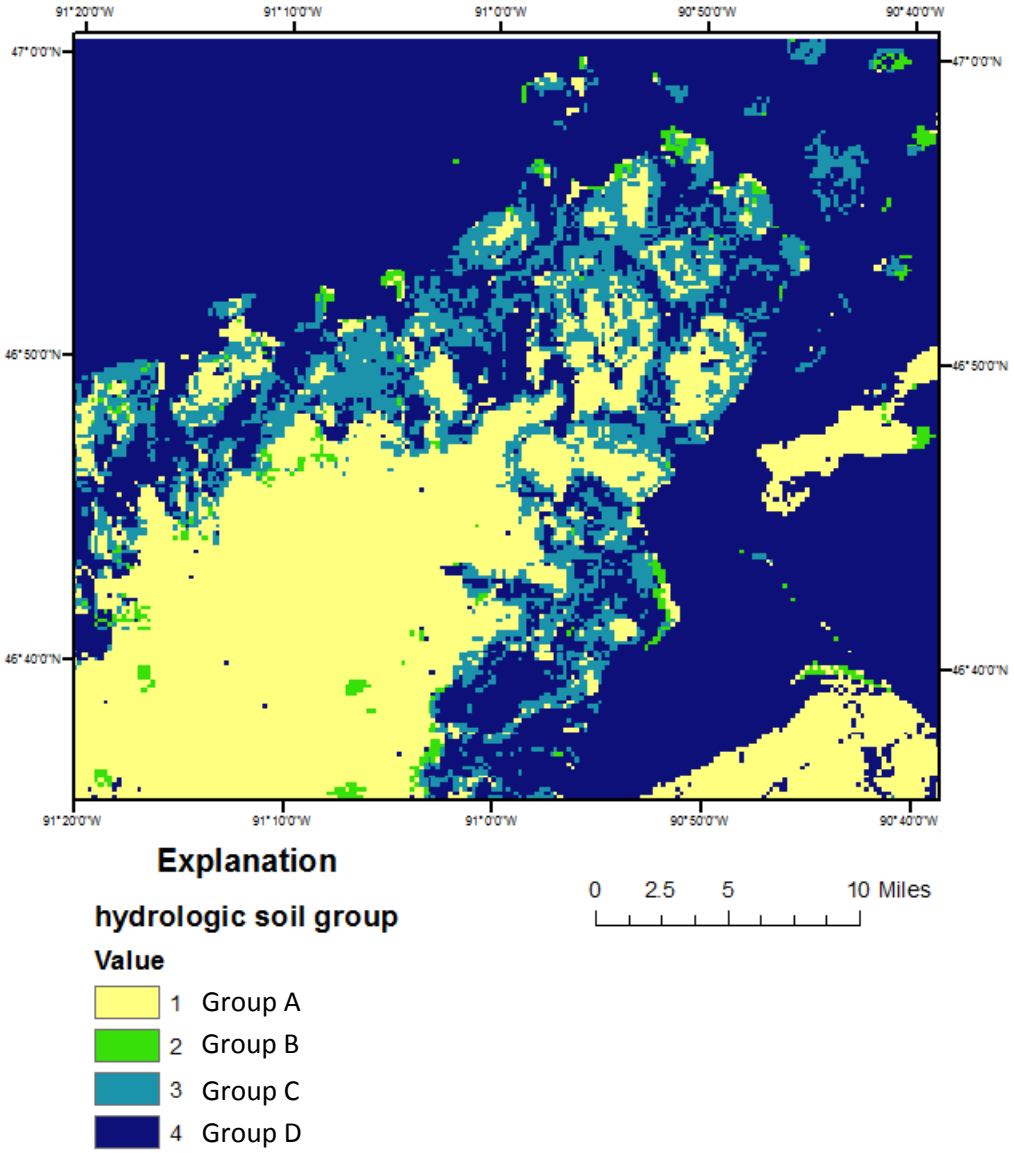

Figure 4.12: Hydrologic soil groups of the Red Cliff model, Bayfield Peninsula, WI

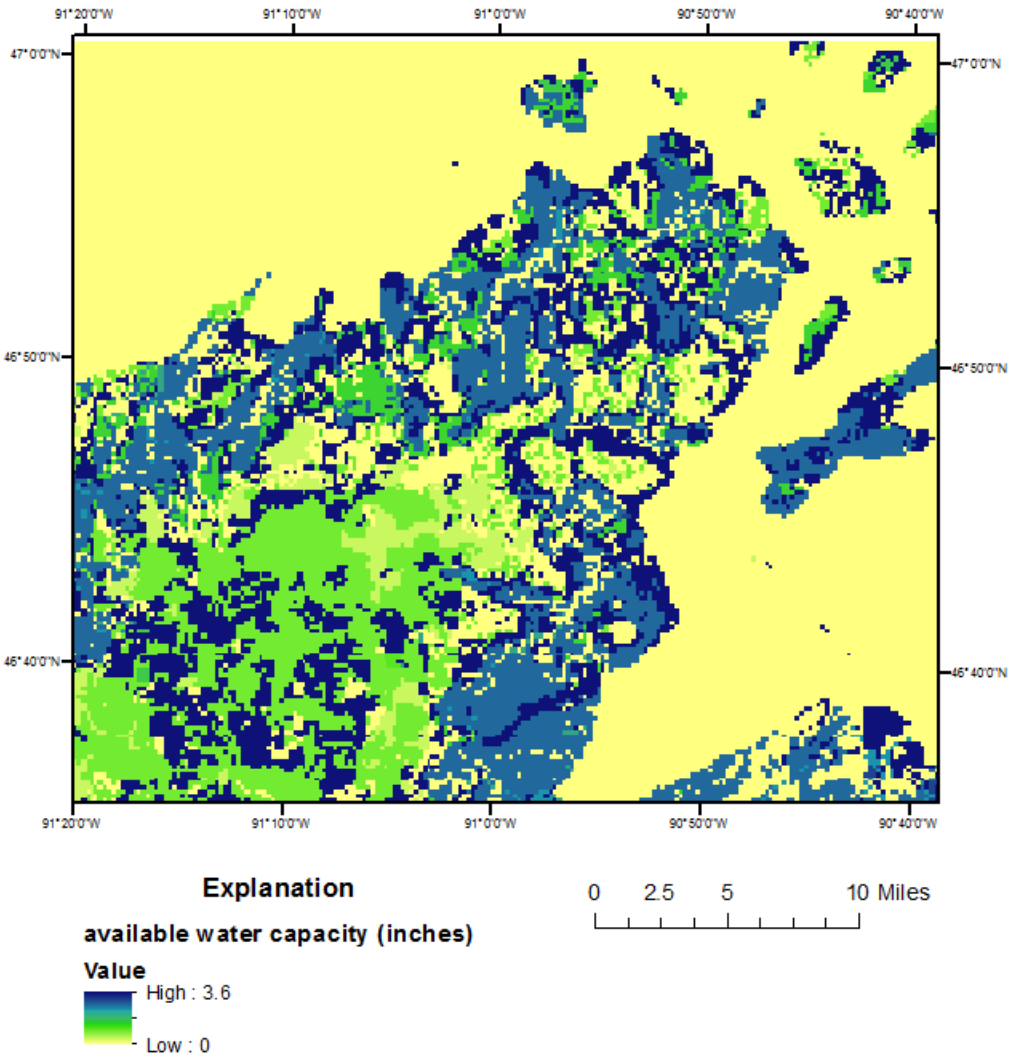

Figure 4.13: Available water capacity (AWC) for soils of the Red Cliff model, Bayfield Peninsula, WI

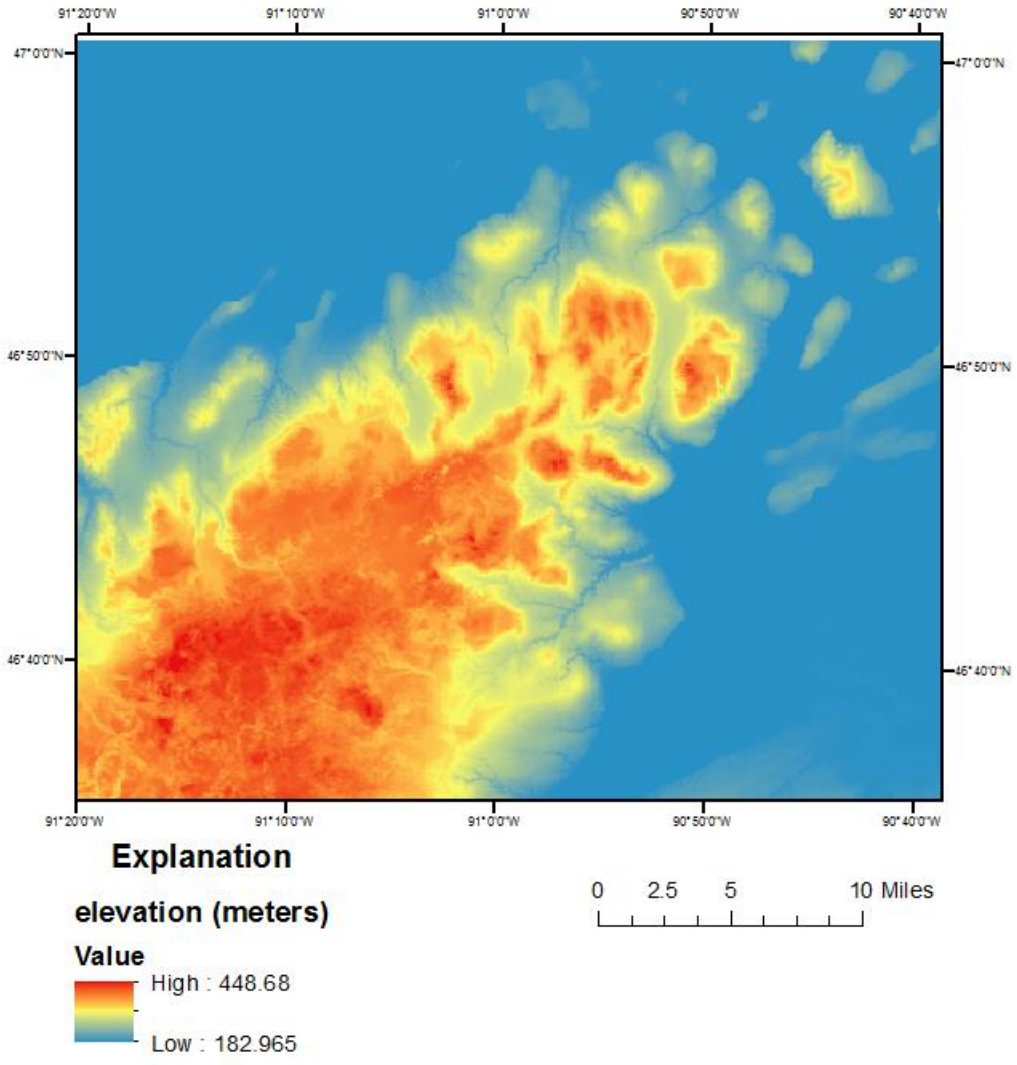

Figure 4.14: Topographic map of the Red Cliff model, Bayfield Peninsula, WI

Table 4.1: Infiltration rates for Natural Resources Conservation Service hydrologic soil groups (Cronshey and others, 1986)

Soil Group	Infiltration rate
A	> 0.3 inch per hour
B	0.15–0.3 inch per hour
C	0.05–0.15 inch per hour
D	< 0.05 inch per hour

Table 4.2: Estimated available water capacities for various soil-texture groups

(Dripps, 2003)

Soil texture	Available water capacity (inches per foot of thickness)
Sand	1.20
Loamy sand	1.40
Sandy loam	1.60
Fine sandy loam	1.80
Very fine sandy loam	2.00
Loam	2.20
Silt loam	2.40
Silt	2.55
Sandy clay loam	2.70
Silty clay loam	2.85
Clay loam	3.00
Sandy clay	3.20
Silty clay	3.40
Clay	3.60

Chapter 5 – Modeling Results and Capture Zone Delineation

5.1 Recharge scenarios

After collecting all required inputs and converting them to the required spatial and temporal format – i.e., daily data over the study region for grid cells 264 feet on a side – the SWB model is run to develop maps of total recharge over 24 years throughout the study area. This recharge was then averaged to obtain an average daily recharge to groundwater, which is used as the input for the steady-state groundwater flow model. Final gridded mean recharge scenarios over the entire simulation period are shown in Figure 5.1 and Figure 5.2.

The two different recharge scenarios using single station climate and gridded climate yield similar estimates, which are in the reasonable range of values based on the original zoned recharge estimations with higher recharge toward the center of the peninsula and lower recharge rates on the fringes.

5.2 Numerical model calibration

Several inputs required by the groundwater flow model MODFLOW are often not well-constrained, and must instead be estimated based on available data. In the case of this particular modeling effort, the hydraulic conductivity values within individual geologic units, and the parameters of the "scaling relationship" (which converts coarse fraction within the Miller Creek Formation to an absolute K value) represent the primary uncertain parameters. However previous modeling efforts coupling SWB to MODFLOW (Pruitt, 2012)

have noted that a "recharge multiplier"—which multiplies the SWB output by a set scalar value – is often necessary to obtain reasonable data fit within hydrogeologic models. The purpose of the calibration of the groundwater numerical model is to find a set of optimized parameters to match the simulated water table and streamflows with the corresponding observed values by updating the model parameters that are not well-constrained through other data sources. The targets include stream baseflow measurements and water levels in wells (Fig. 5.3).

In this study, the nonlinear regression method is used through PEST (Doherty, 2010a, b). The parameters estimated in the process of calibration are hydraulic conductivities in each of the geologic units of the model and a recharge multiplier, which scales SWB- generated recharge by a set constant. The hydraulic conductivities in the far-field and beneath Lake Superior are fixed values as homogeneous zones. Layer 5, the deep sandstone layer, is regarded as a homogeneous zone with fixed hydraulic conductivities, since relative shallow observations cannot present information at this depth. For unconsolidated sediments in other layers, hydraulic conductivity parameters Kh and Krange follow a power-law relationship with percent coarse sediments value, which can be calculated as

$$K_h = \min_{Kh} * 10^{(Krange * PCTcoarse/100)} \quad (8)$$

where K_h is horizontal hydraulic conductivity, min_{kh} is the minimum K_h value assumed if there is no coarse sediment, Krange is the range and PCTCoarse is the percent of coarse sediment (USGS, 2014). The coarseness values from boreholes are shown in Figure 5.4.

The calibration results are listed in Table 5.1. In the table, copfal_kh (feet/day) is horizontal hydraulic conductivity of Copper Falls Formation; submc_kh (feet/day) is horizontal

hydraulic conductivity of Miller Creek Formation; kxl3 and kxl4 (unitless) are multipliers from an initial guess of horizontal hydraulic conductivity of layer 3 and layer 4 respectively; kzl3 and kzl4 are multipliers of vertical hydraulic conductivity of layer 3 and layer 4 respectively; r1, r2 and r3 (feet/day) are zoned recharge rates in the zoned recharge model; and rm (unitless) is a recharge multiplier in SWB recharge models.

For each conceptual model of recharge, model parameters were adjusted until the best fit with well water levels and stream baseflow was obtained. The simulated water tables of the three calibrated conceptual models are shown in Figure 5.5, Figure 5.6 and Figure 5.7. Figure 5.8 ~Figure 5.13 represent the correlations between simulated values in three conceptual groundwater flow models and observed values (heads and streamflows), indicating the simulated values in groundwater flow model with SWB recharge (single station climate) are most correlated with observed values. In Figure 5.14 and Figure 5.15, the circles represent the differences between the errors in zoned recharge model and the other two SWB-based models at the observation locations. The error at each location is defined as the absolute value of the difference between simulated value and observed value divided by the observed value
($error = |simulated\ value - observed\ value|/observed\ value$). The larger the circles are, the larger differences between the errors indicated. If the difference between the errors is negative, it indicates the zoned recharge model has smaller error at the certain location, which is shown in red. If the difference between the errors is positive, it indicates the zoned recharge model has larger error at the certain location, which is shown in green. Comparing the conceptual models against each other, among the 379 observation spots, 272 simulated values have smaller errors in the SWB model with single station climate

scenario (Fig. 5.14). Although the parameters in the “far-land” from the Red Cliff Reservation, southwestern corner of the peninsula, are not calibrated, compared to zoned recharge model, the SWB model with gridded climate still gives a better realization in Red Cliff Reservation area (Fig. 5.15).

5.3 Correlation between recharge rates and SWB inputs

Since the groundwater flow model with SWB recharge (single station climate) gives the best realization among all the three conceptual models, the recharge rates of which were used to analysis the correlations between with it and each SWB inputs. Average recharge rates of same kind of land cover/ land use in a single grid were calculated. Fig. 5.16 shows the correlation between recharge rate and land cover/ land use. Areas covered by jack pine trees (# 162), red oak trees (# 180), golf course (# 105), red pine trees (# 163) and shrub lands (# 250) have higher recharge rates which are more than 0.002 feet/day. Areas covered by emergent/wet meadow (# 211), row crops (# 118), forage crops (# 124) and lowland shrub lands(# 217) have lower recharge rates which are less than 0.001 feet/day.

Similarly, average recharge rates of same hydrologic soil group and soil available water capacity in a single grid were calculated shown in Fig. 5.17 and Fig. 5.18. Fig. 5.17 indicates a strong correlation between recharge rate and hydrologic soil group, which is a decreasing trend of recharge rates from hydrologic soil group A to D.

Figure 5.19 and Figure 5.20 show relationships between recharge rate and surface water flow direction. A cell with the flow direction value that is not a power of 2 is considered as a

closed depression in the SWB code (Westenbroek, 2010). The average recharge rate of the grids that are closed depressions is higher than the grids that are not closed depressions.

5.4 Capture zone delineation

A capture zone is defined as a three- dimensional surface (Townley & Trefry, 2000) from which groundwater flows to a discharge area. In our study this is the area that contributes flow discharging to the streams in the Red Cliff reservation. Capture zones extending to the recharge area can be obtained by using backward transport simulations, which can be implemented using the particle-tracking program MODPATH (Pollock, 1994). Based on the water table as well as the flux outputs, particles are set and distributed throughout the aquifer along the plane of the Red Cliff Reservation and are tracked reversely to the points of recharge, the final locations of which are used to define the capture zone.

The travel time of the captured particles is related to hydraulic gradients, hydraulic conductivities and the effective porosity of the sandstone, which was estimated to be 0.2 for the steady-state model. The simulation results show the possible extents of groundwater recharge areas to the Red Cliff Reservation (Figure 5.21, Figure 5.22 and Figure 5.23). The flowpaths have travel times of around 164 years (60000 days) in all of the three models.

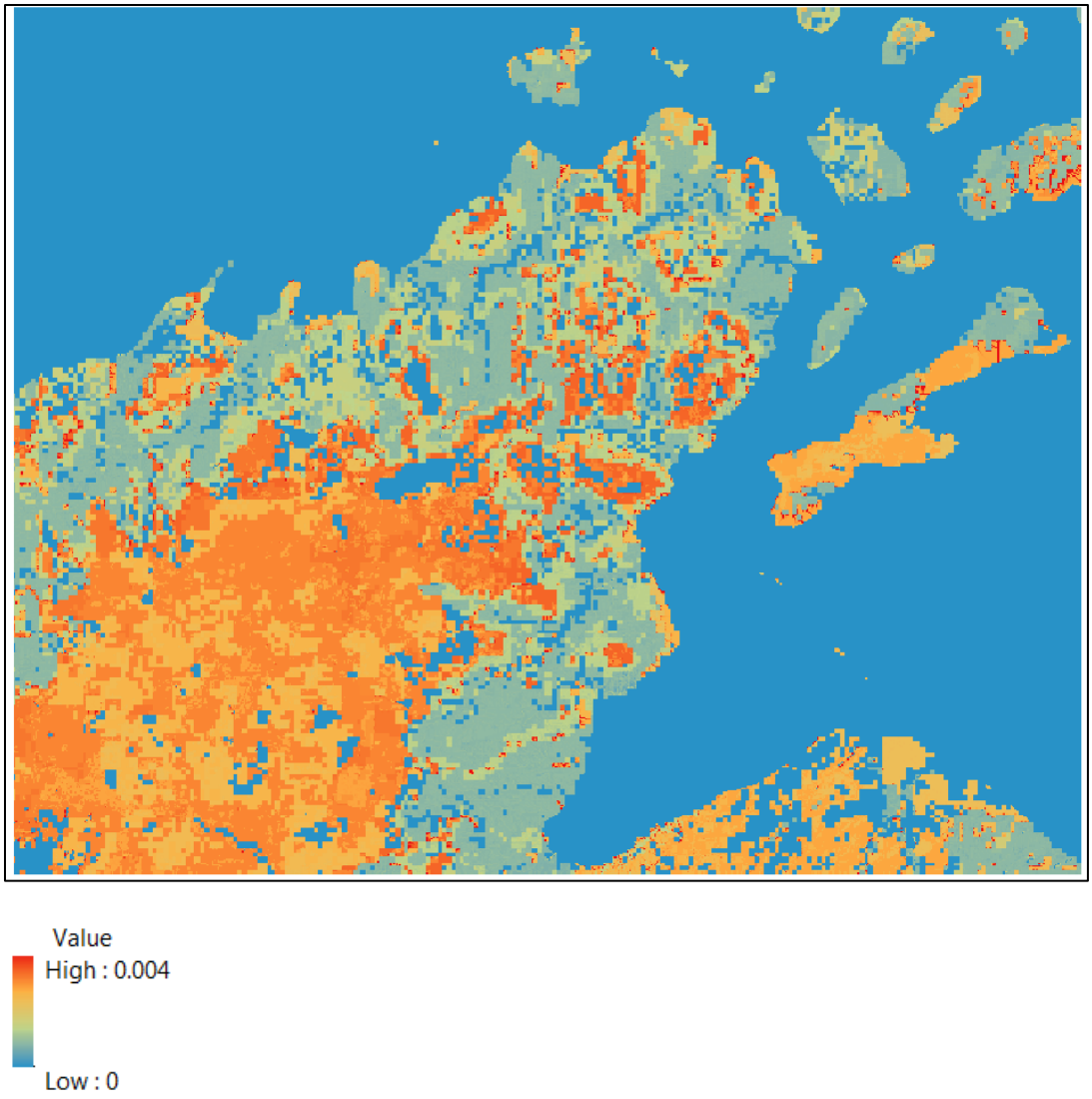

Figure 5.1: Estimated recharge rates (feet/day) using single station climate data from 1981- 2004 of the Red Cliff model, Bayfield Peninsula, WI

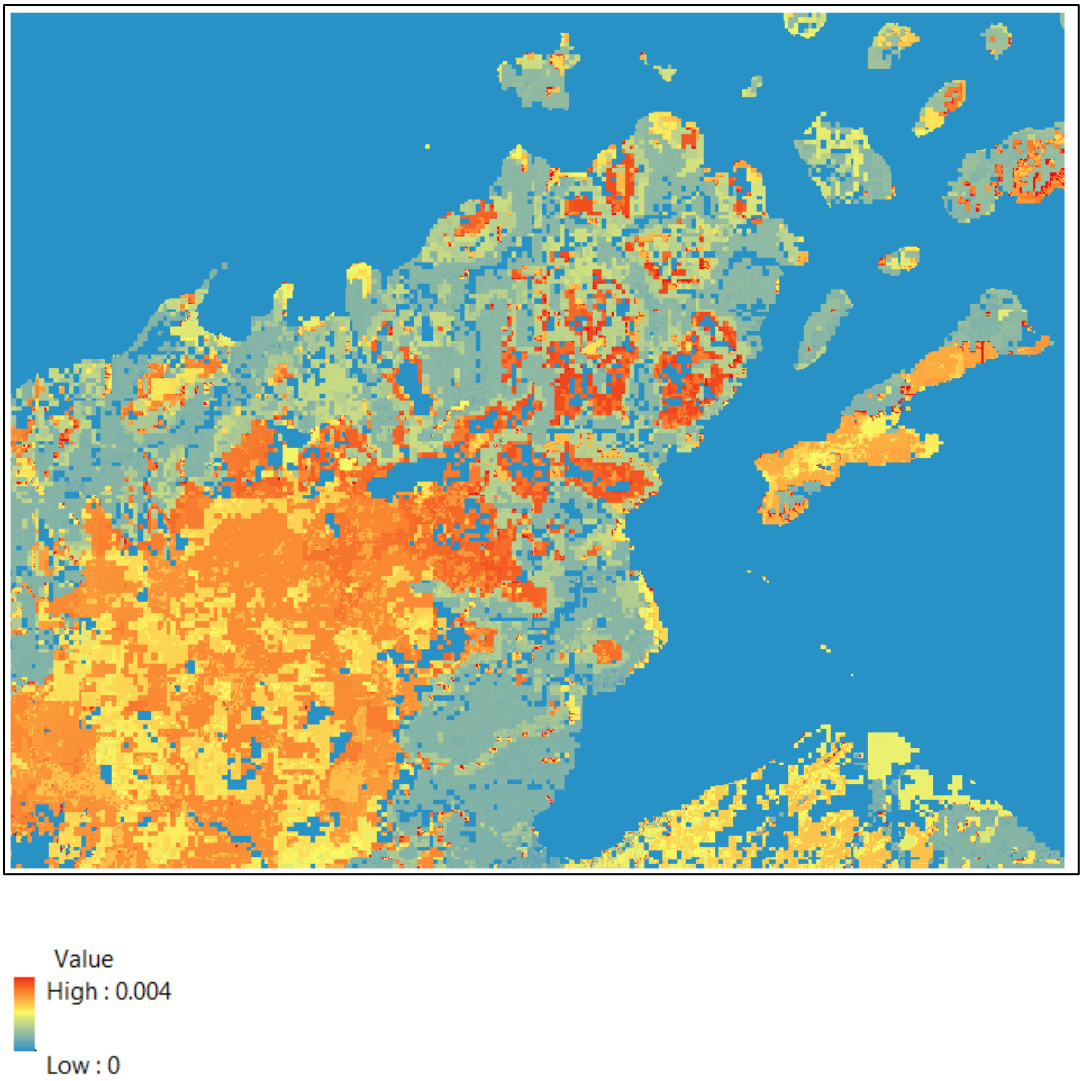

Figure 5.2: Estimated recharge rates (feet/day) using gridded climate data from 1981-2004 of the Red Cliff model, Bayfield Peninsula, WI

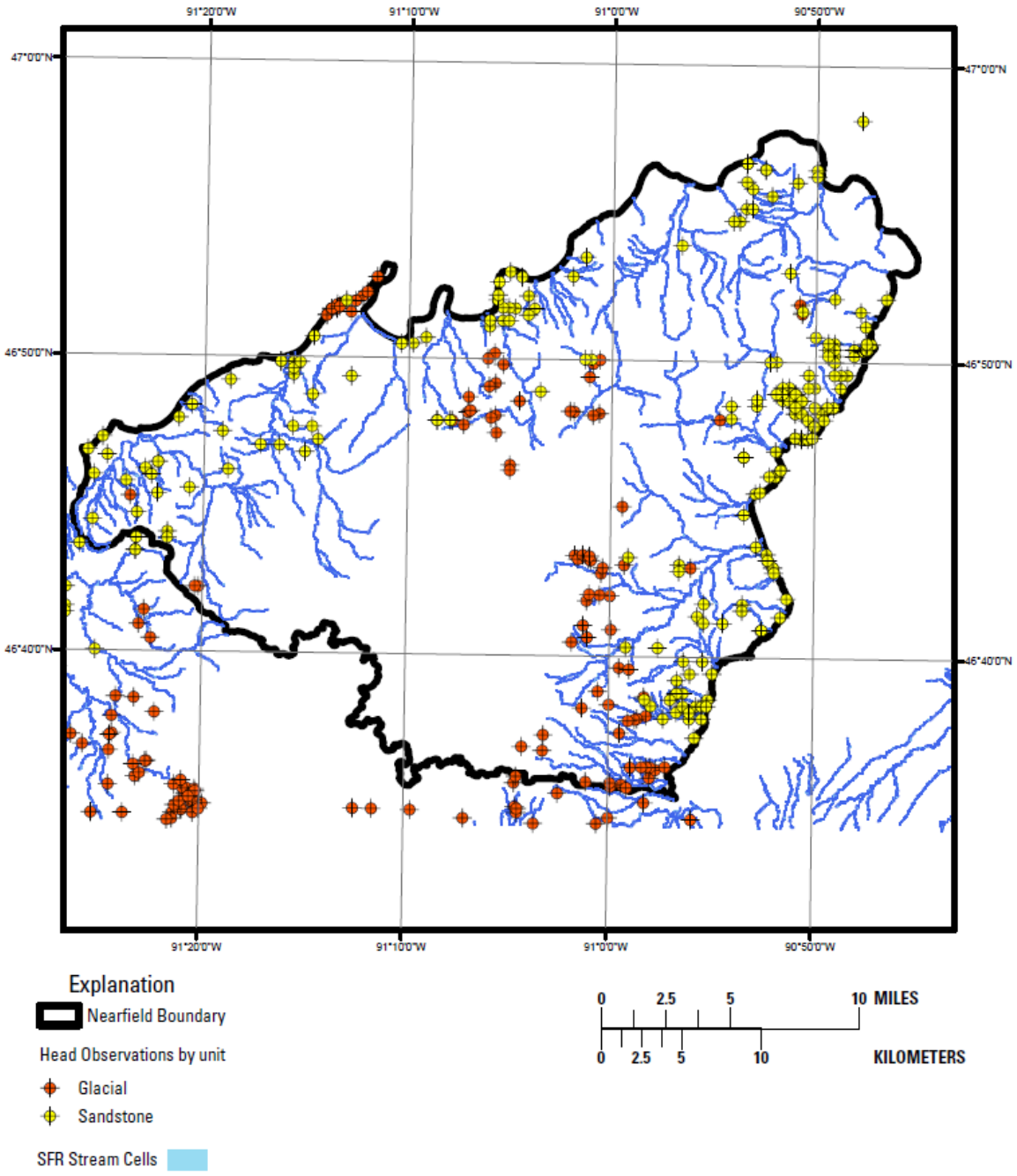

Figure 5.3: Locations of head observation wells (USGS, 2014)

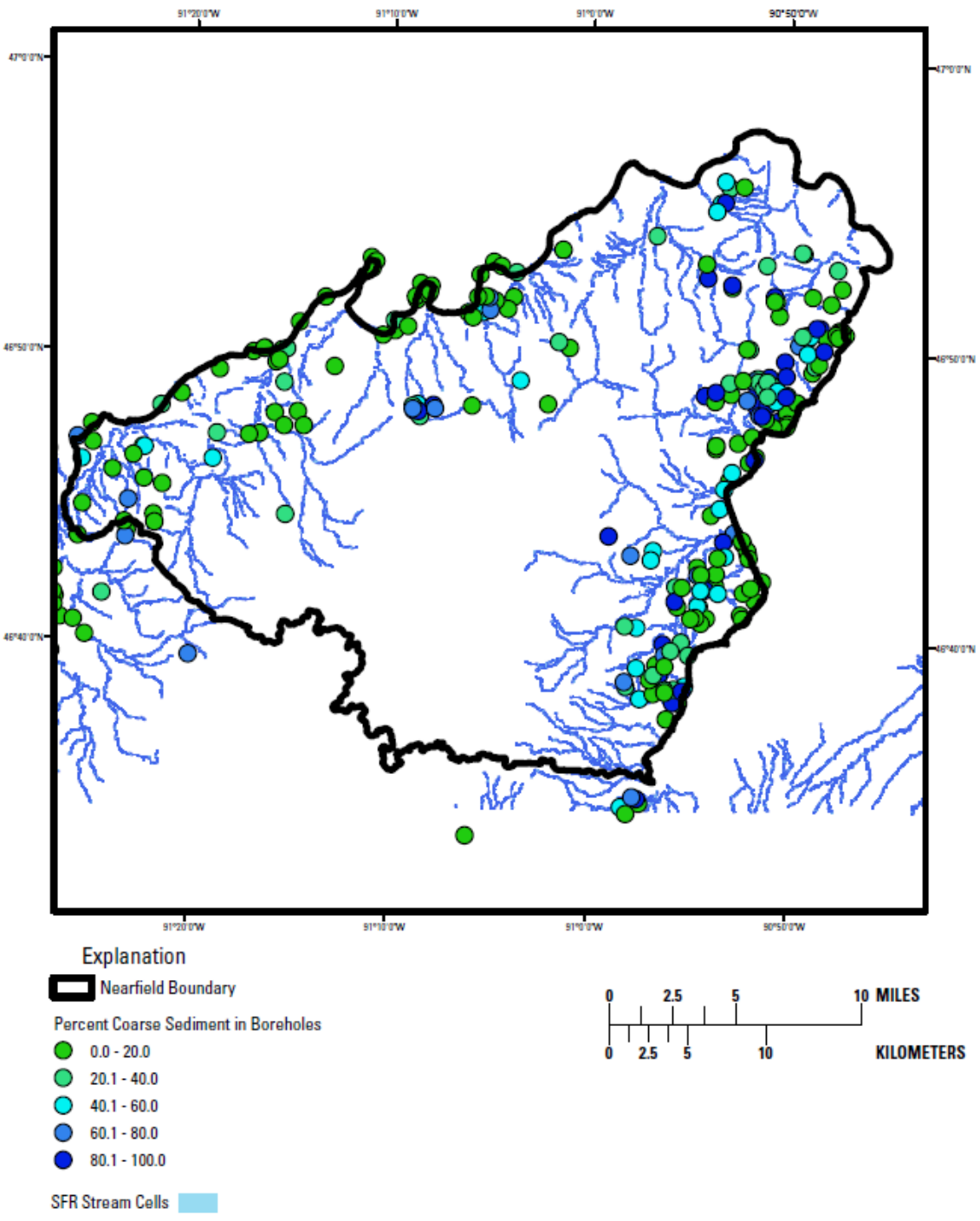

Figure 5.4: Well construction locations showing percent coarse (USGS, 2014)

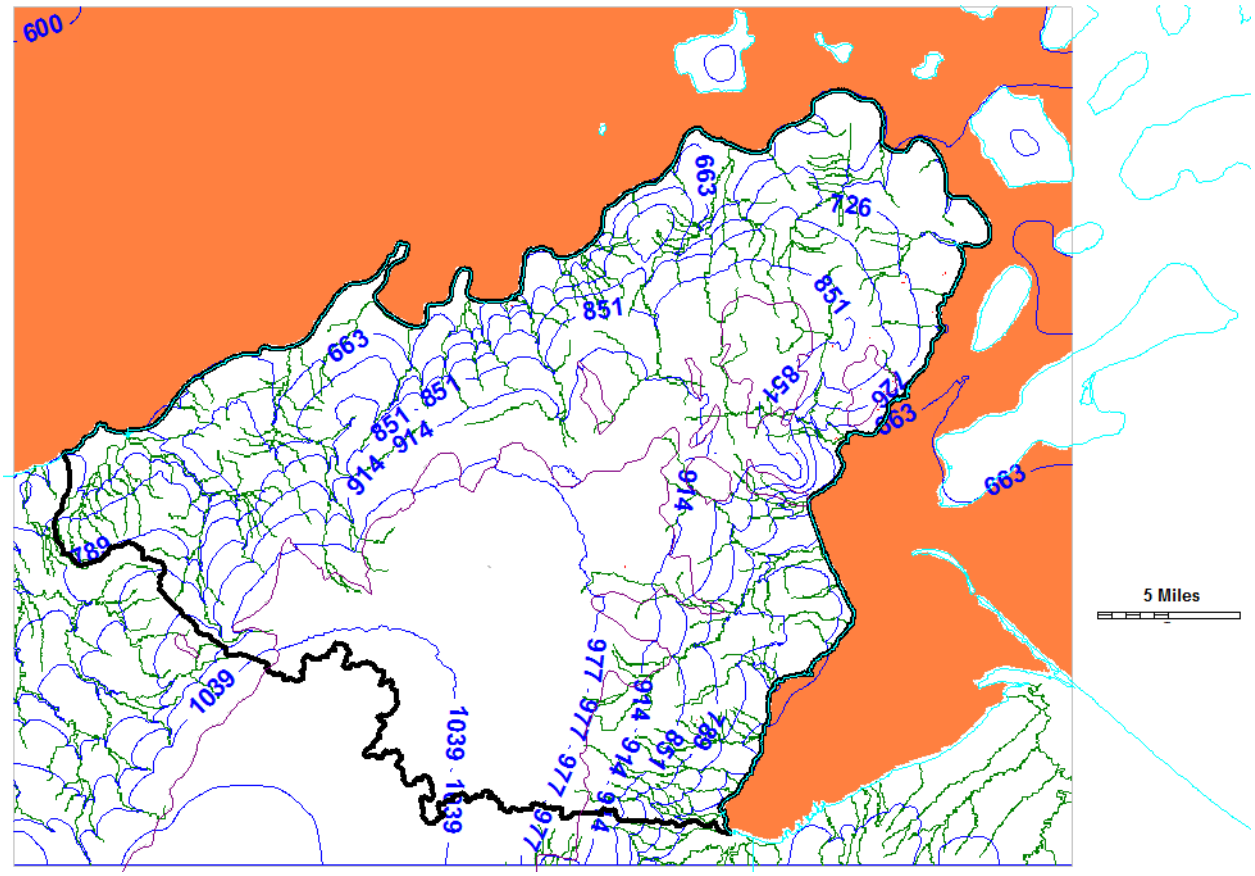

Figure 5.5: Simulated water table (feet) of calibrated zoned recharge model, Red Cliff, Bayfield Peninsula, WI

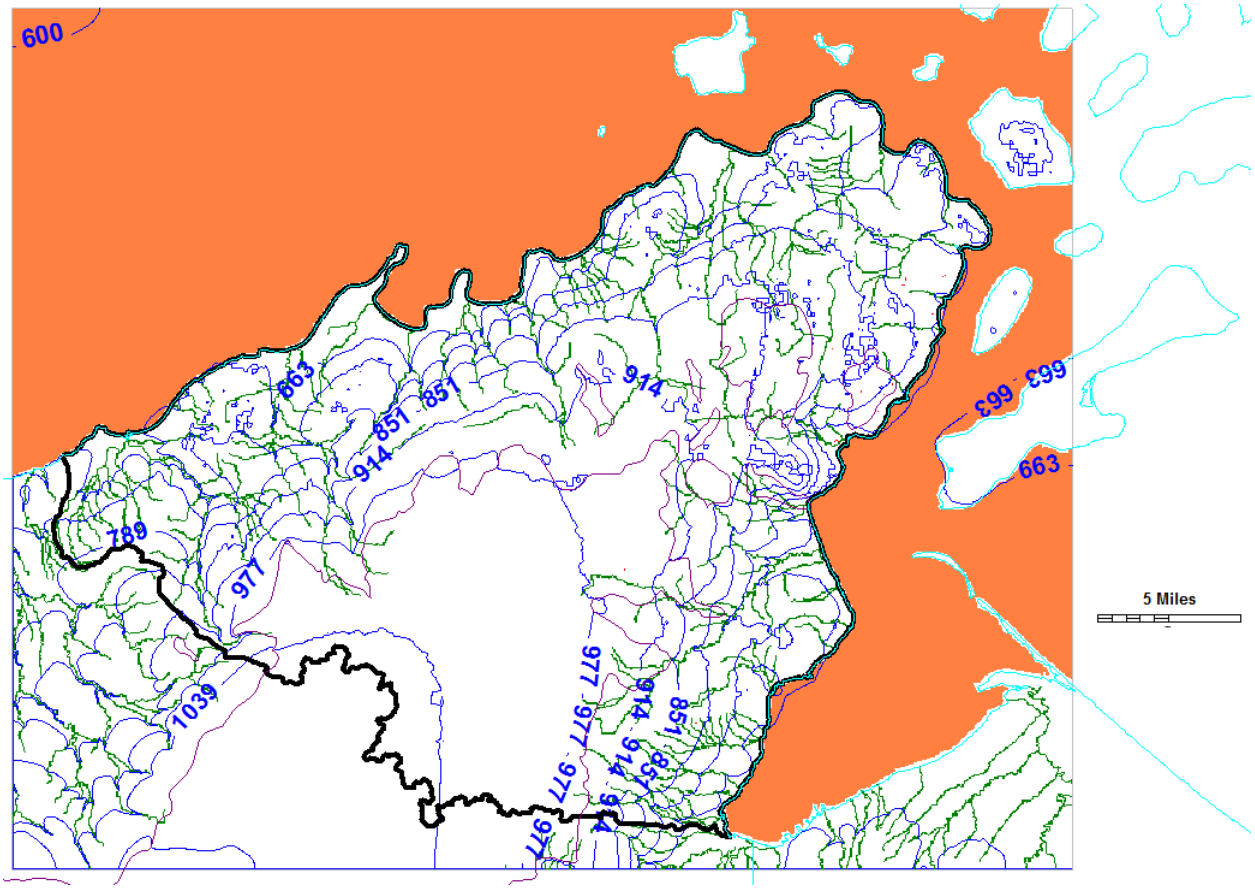

Figure 5.6: Simulated water table (feet) of calibrated SWB recharge model with single station climate, Red Cliff, Bayfield Peninsula, WI

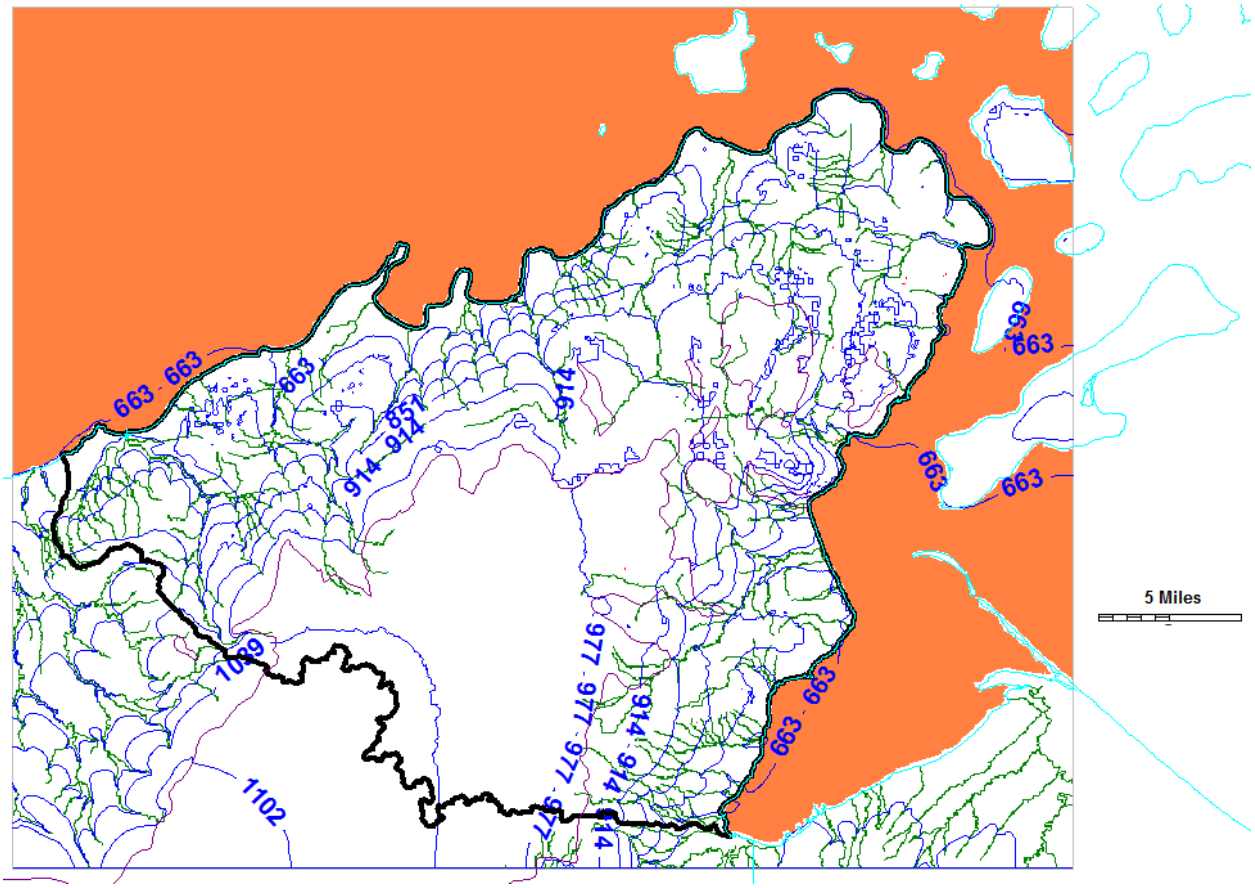

Figure 5.7: Simulated water table (feet) of calibrated SWB recharge model with gridded climate, Red Cliff, Bayfield Peninsula, WI

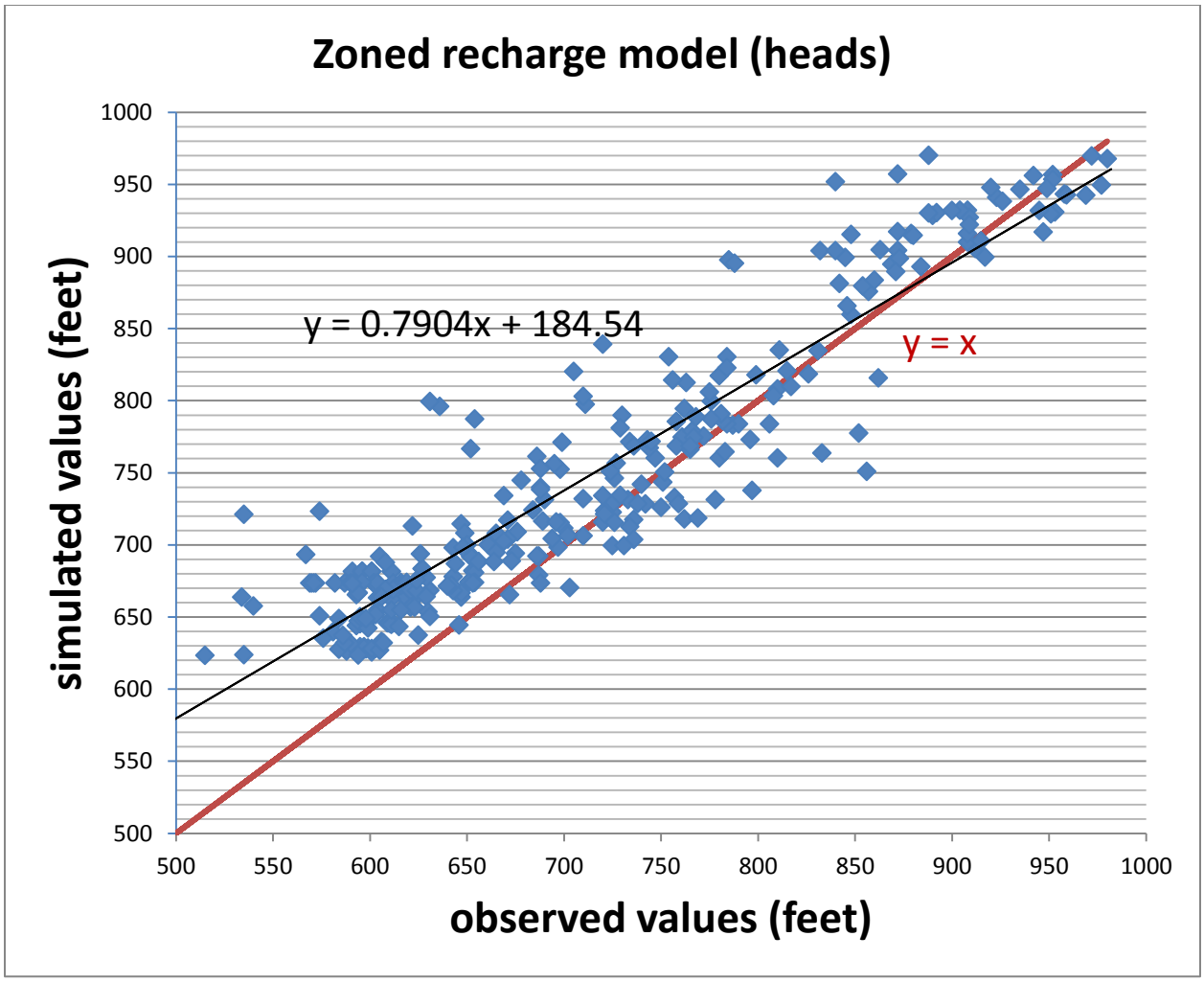

Figure 5.8: Comparison between simulated heads in zoned recharge groundwater flow model and observed heads

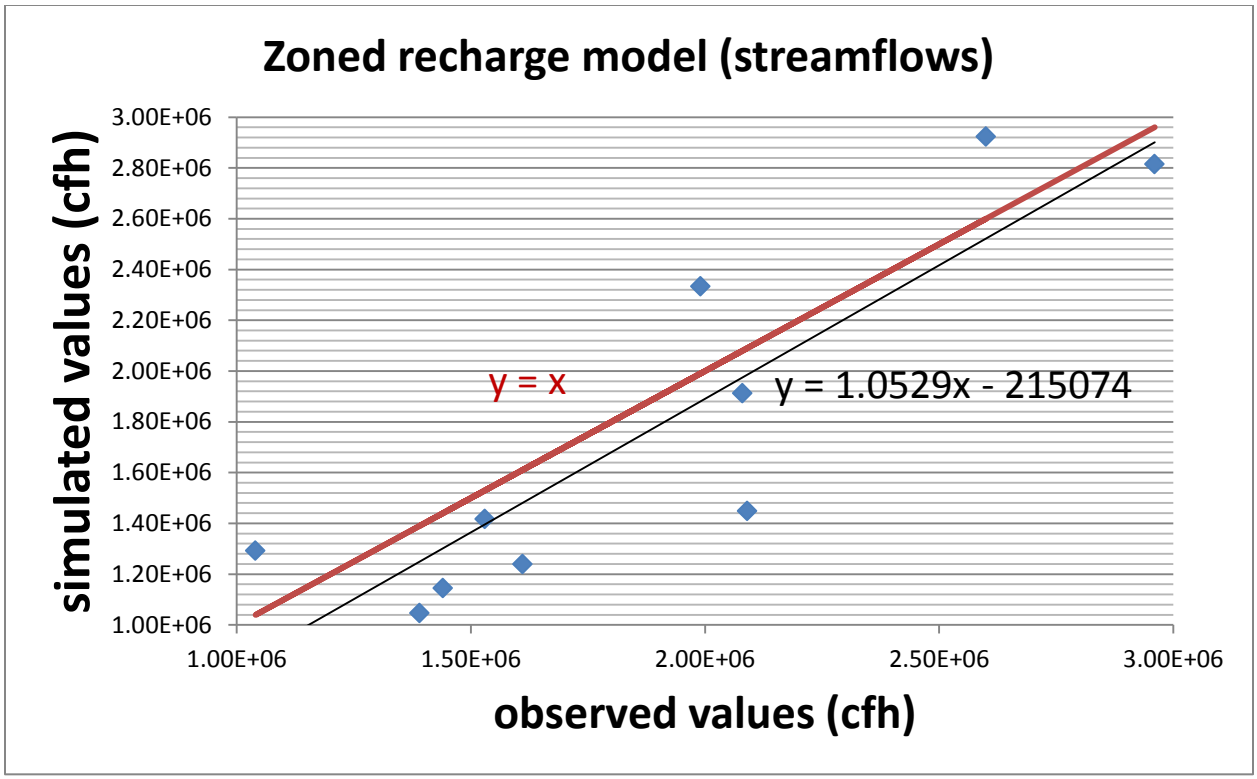

Figure 5.9: Comparison between simulated streamflows in zoned recharge groundwater flow model and observed streamflows

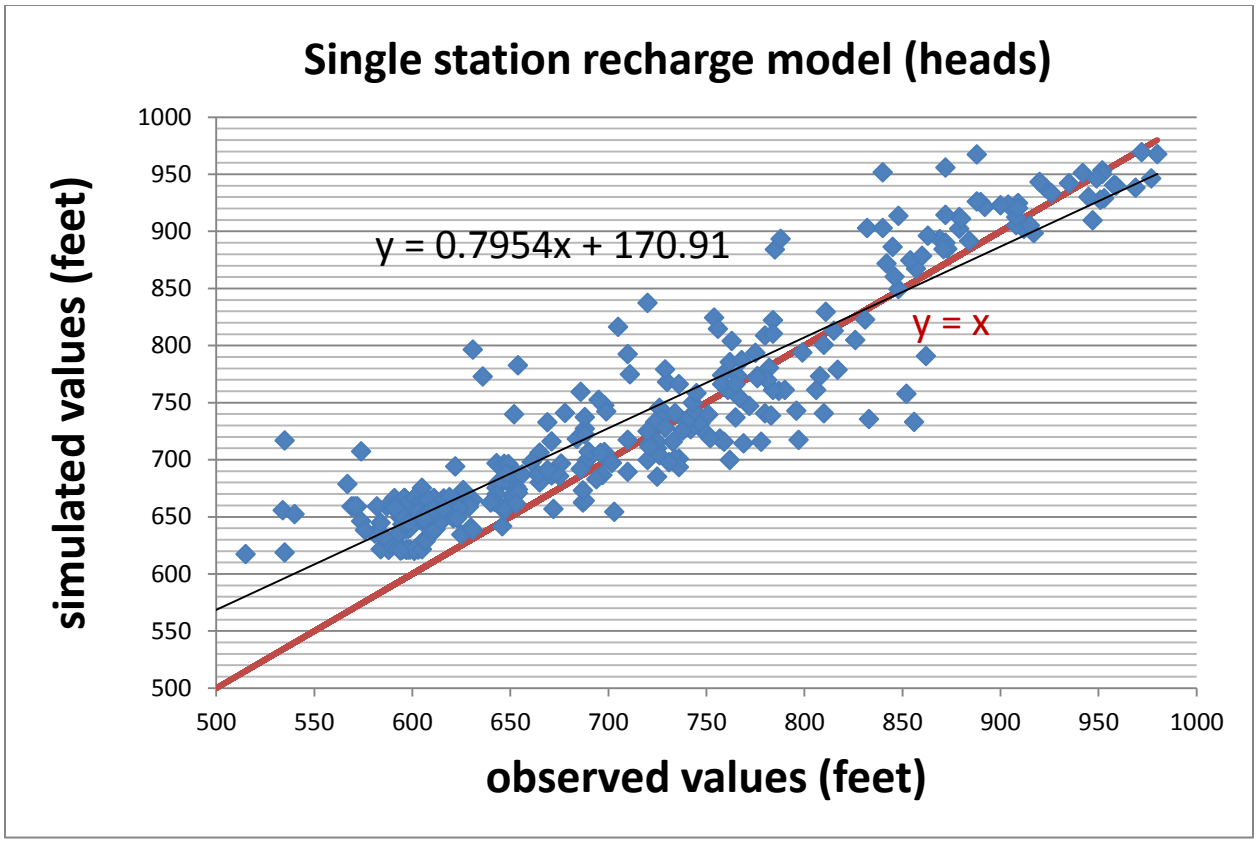

Figure 5.10: Comparison between simulated heads in groundwater flow model with SWB recharge (single station climate) and observed heads

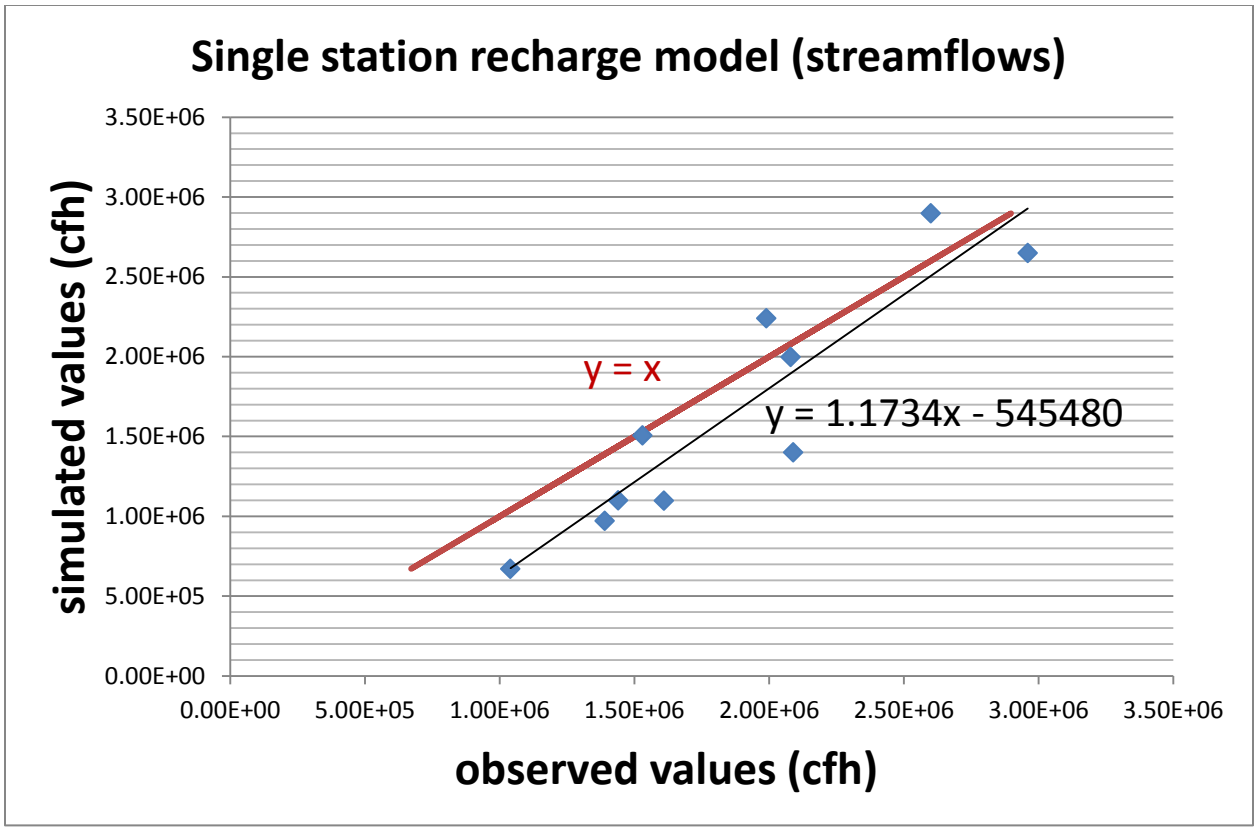

Figure 5.11: Comparison between simulated streamflows in groundwater flow model with SWB recharge (single station climate) and observed streamflows

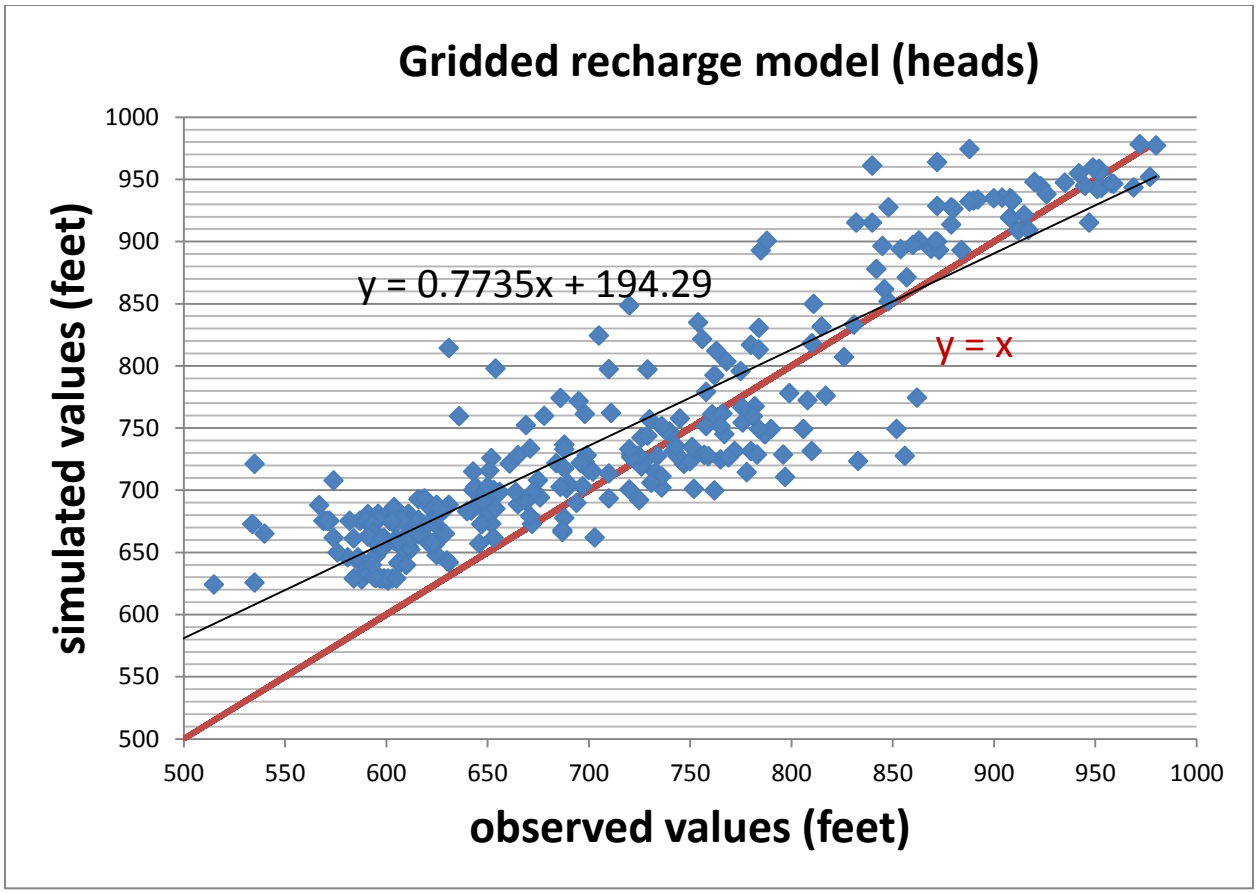

Figure 5.12: Comparison between simulated heads in groundwater flow model with SWB recharge (gridded climate) and observed heads

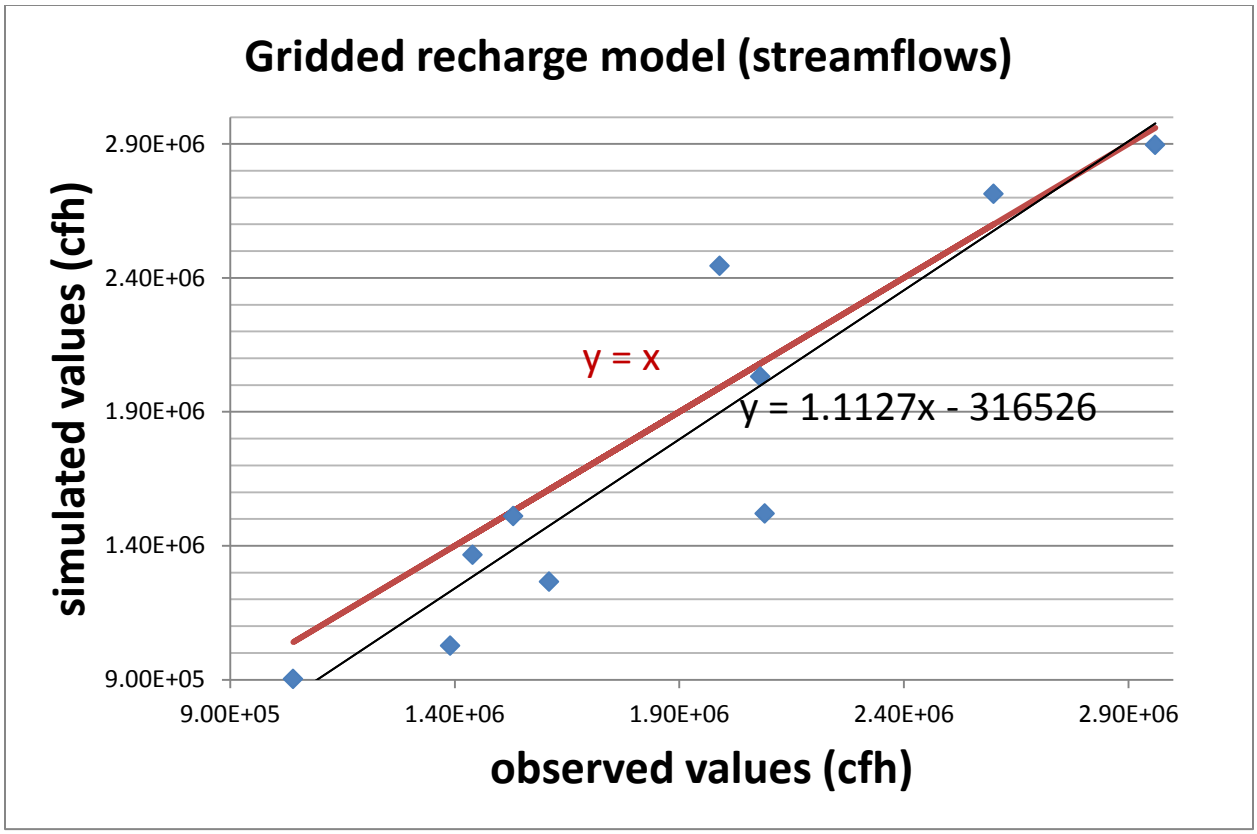

Figure 5.13: Comparison between simulated streamflows in groundwater flow model with SWB recharge (gridded climate) and observed streamflows

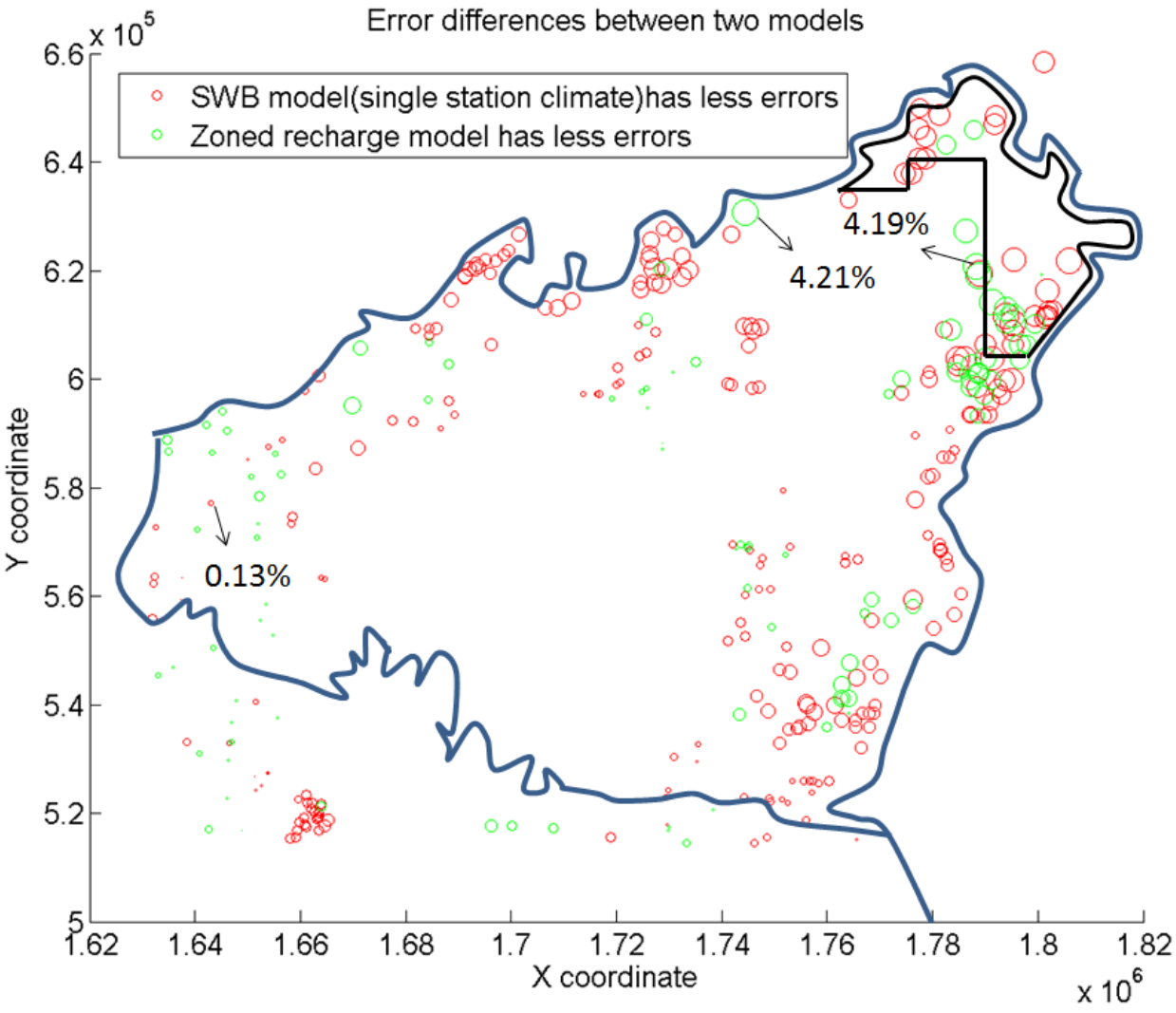

Figure 5.14: Error comparison between zoned recharge model and SWB recharge model with single station climate, Red Cliff, Bayfield Peninsula, WI

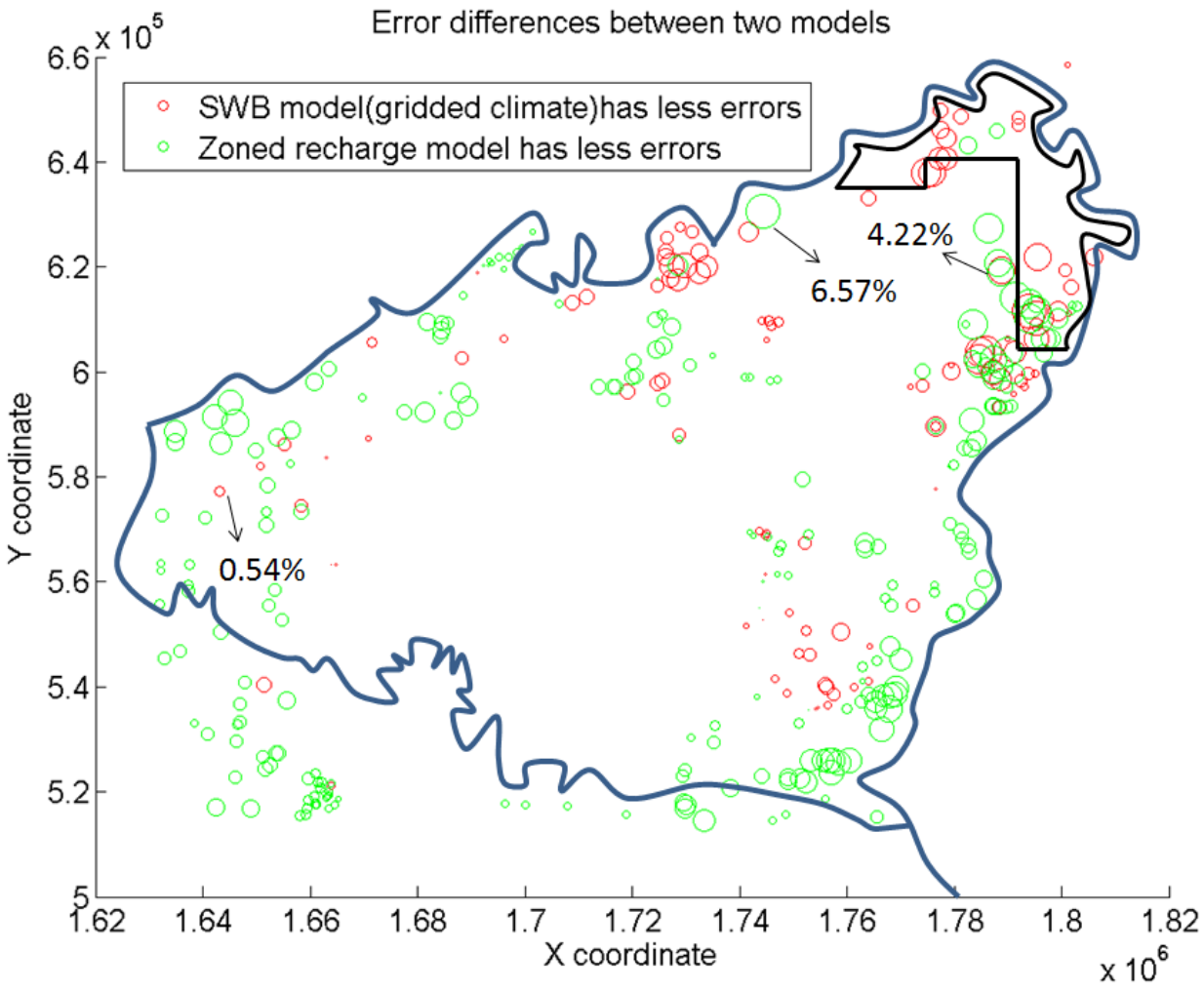

Figure 5.15: Error comparison between zoned recharge model and SWB recharge model with gridded climate, Red Cliff, Bayfield Peninsula, WI

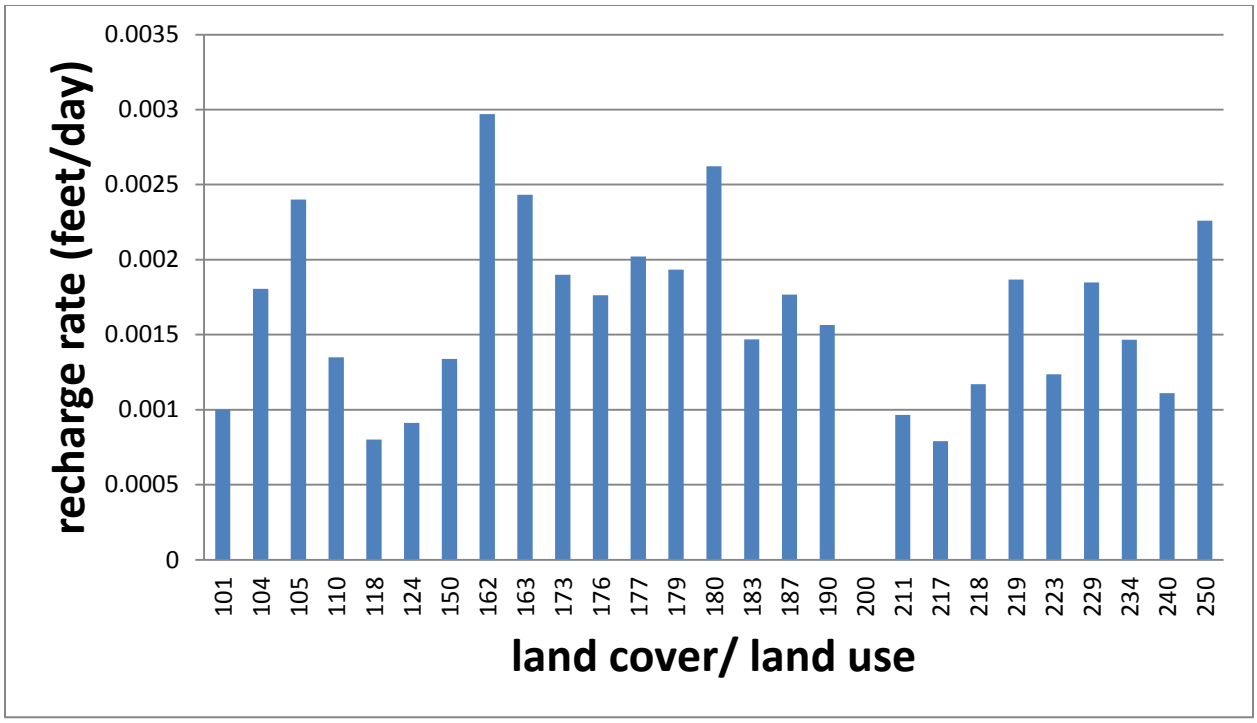

Figure 5.16: Average recharge rates of different land covers/ land uses at the study site

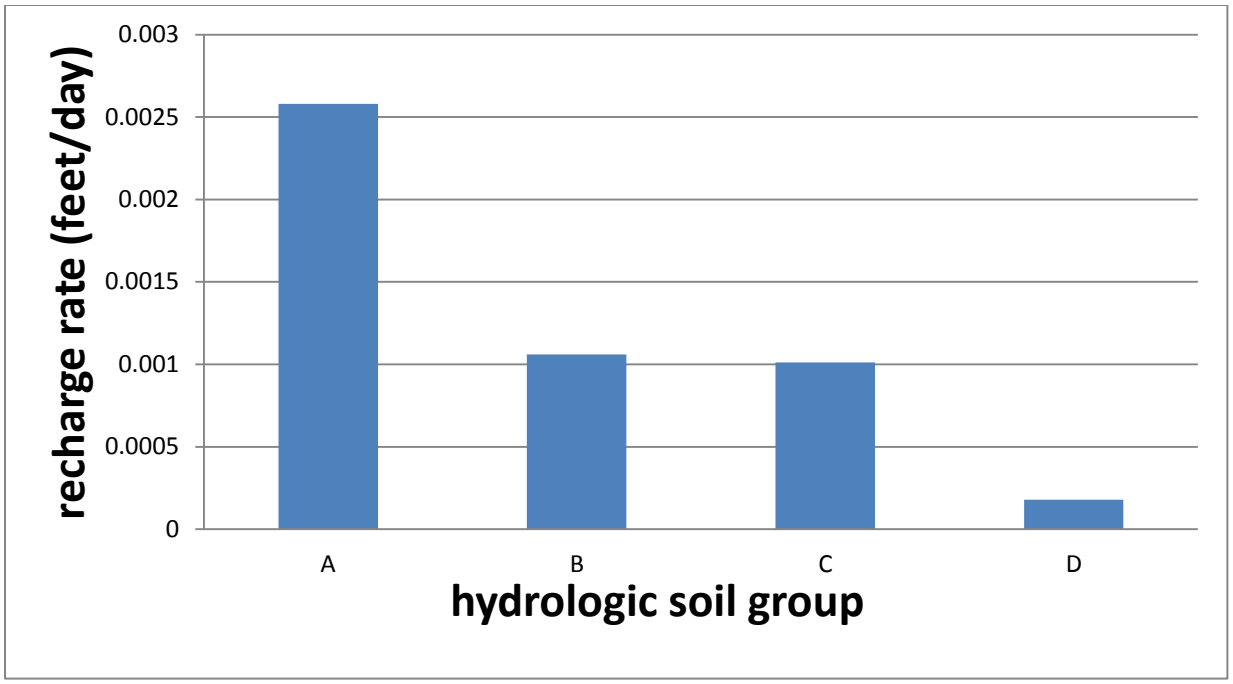

Figure 5.17: Average recharge rates of different hydrologic soil groups at the study site

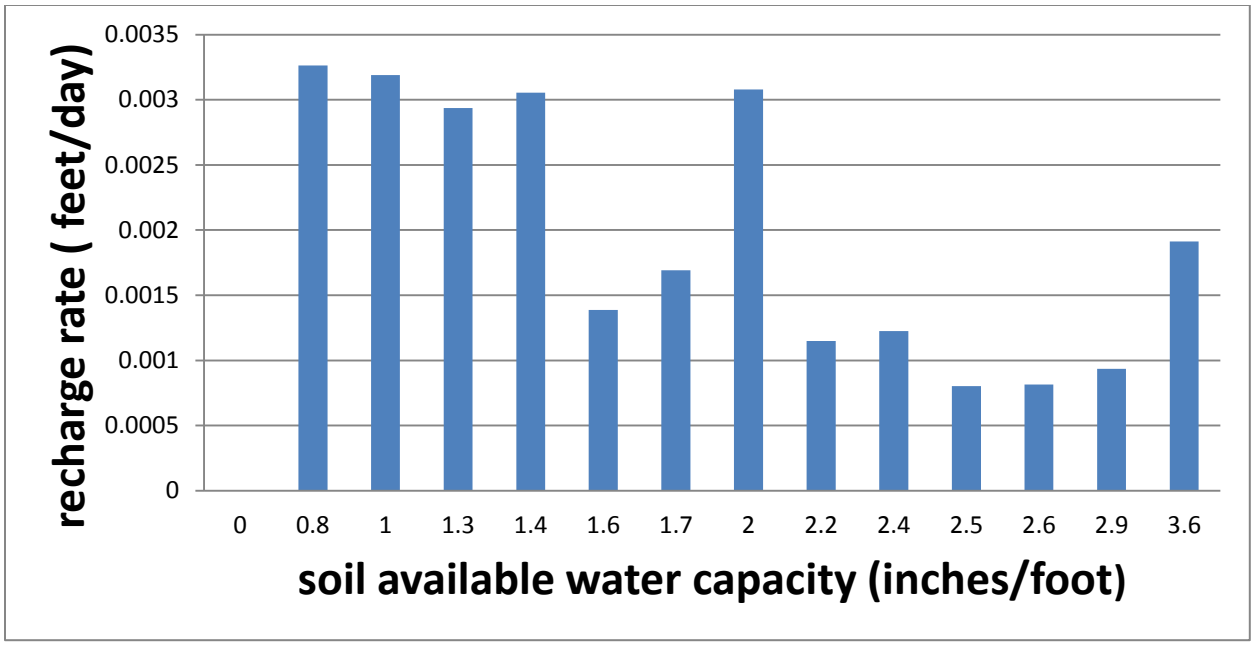

Figure 5.18: Average recharge rates of different soil available water capacities at the study site

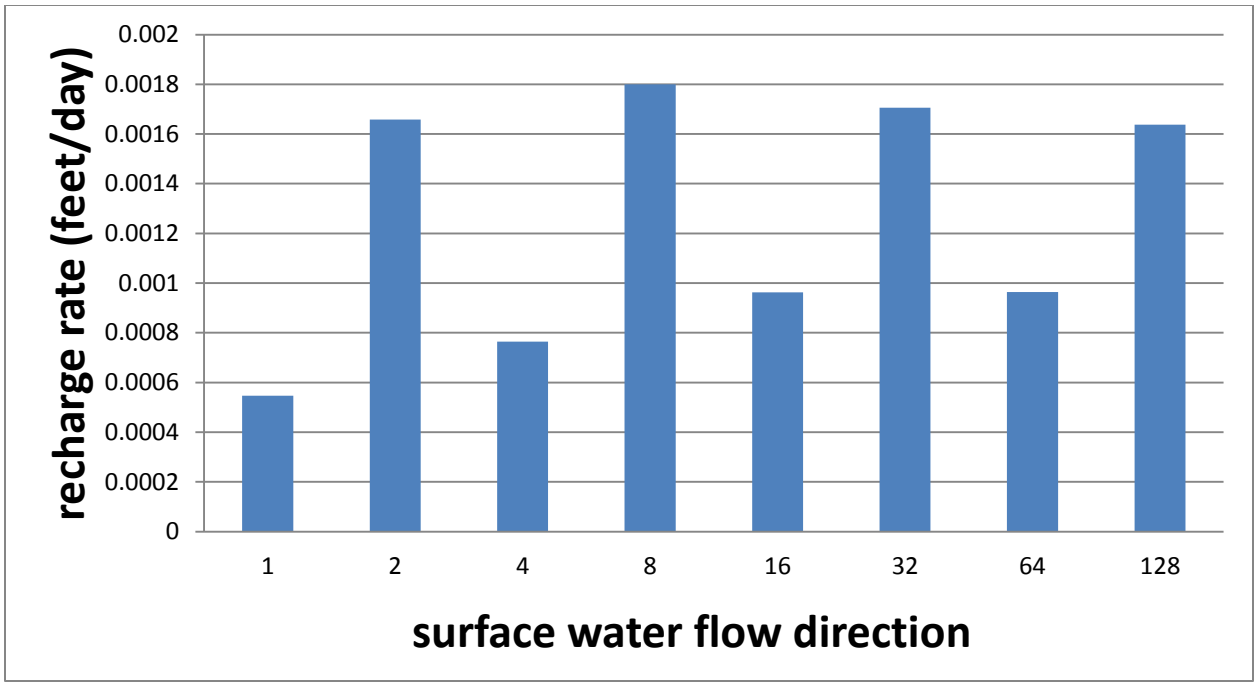

Figure 5.19: Average recharge rates of different surface water flow directions (the power of 2) at the study site

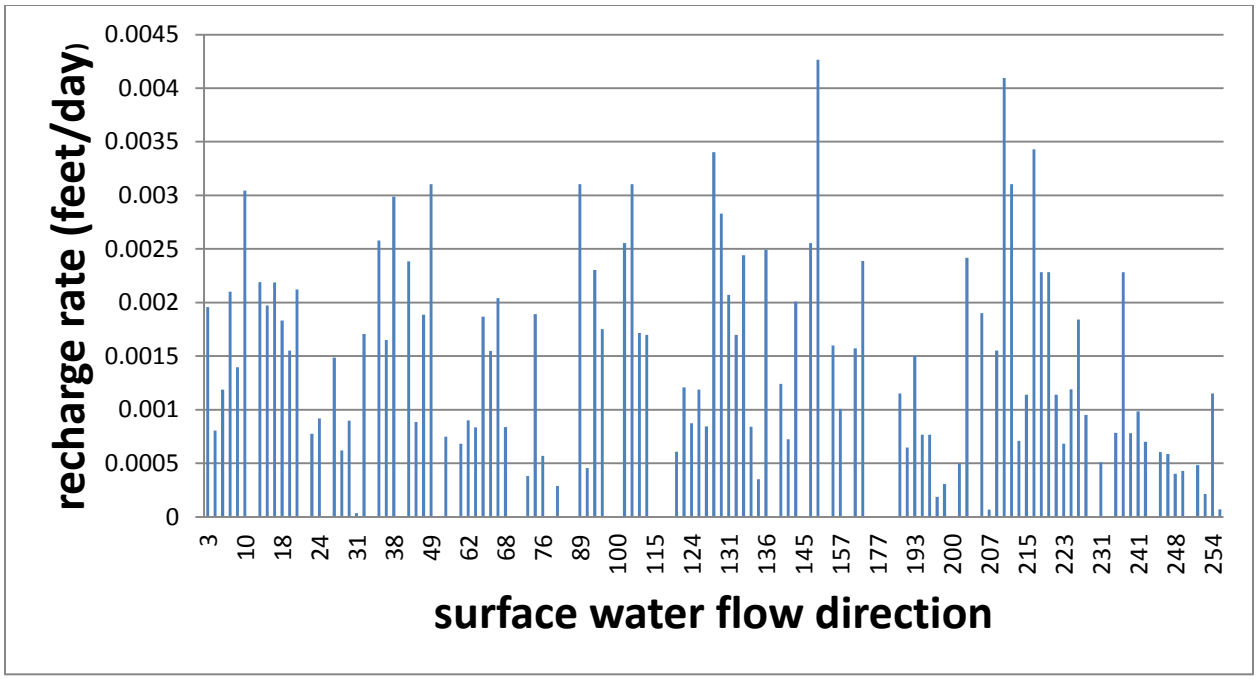

Figure 5.20: Average recharge rates of different surface water flow directions (not the power of 2) at the study site

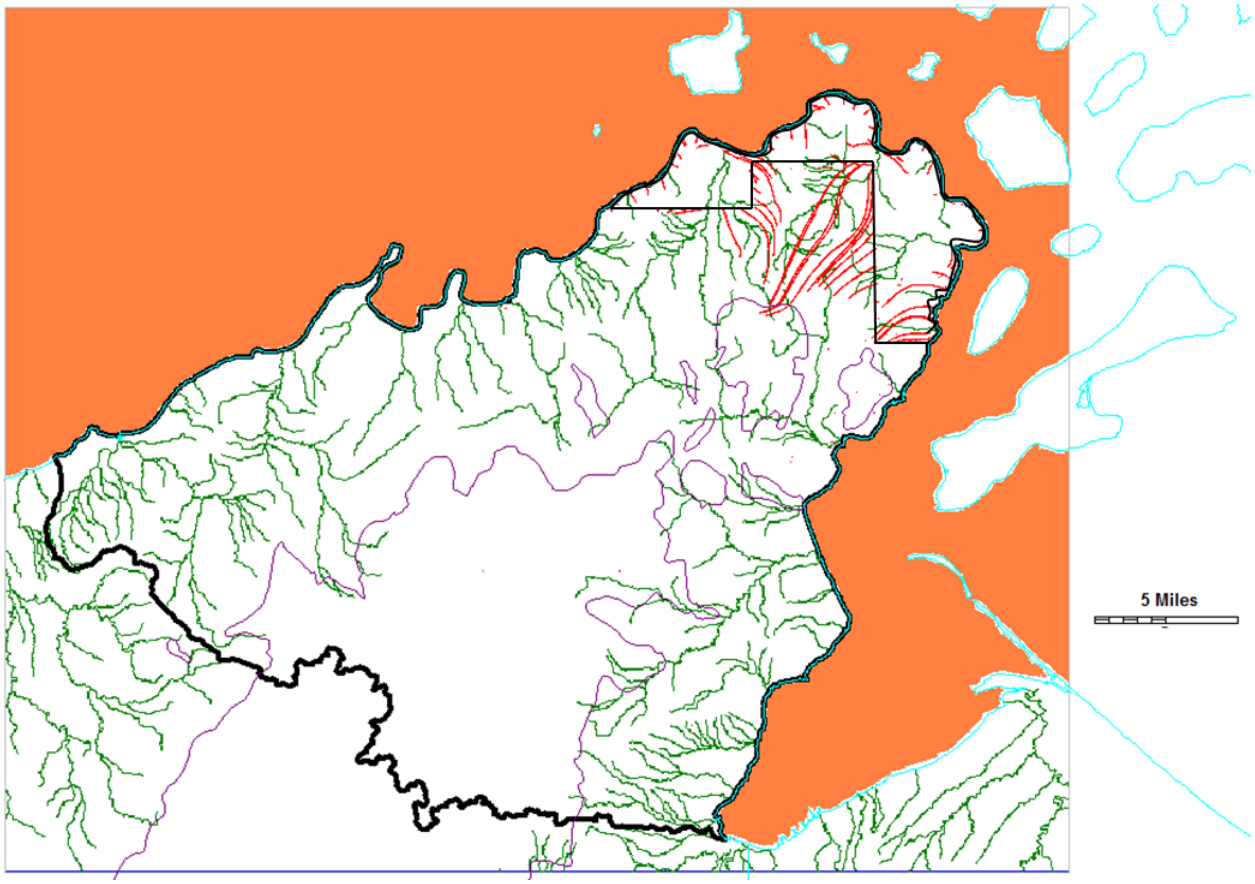

Figure 5.21: Flowpaths delineation of zoned recharge model

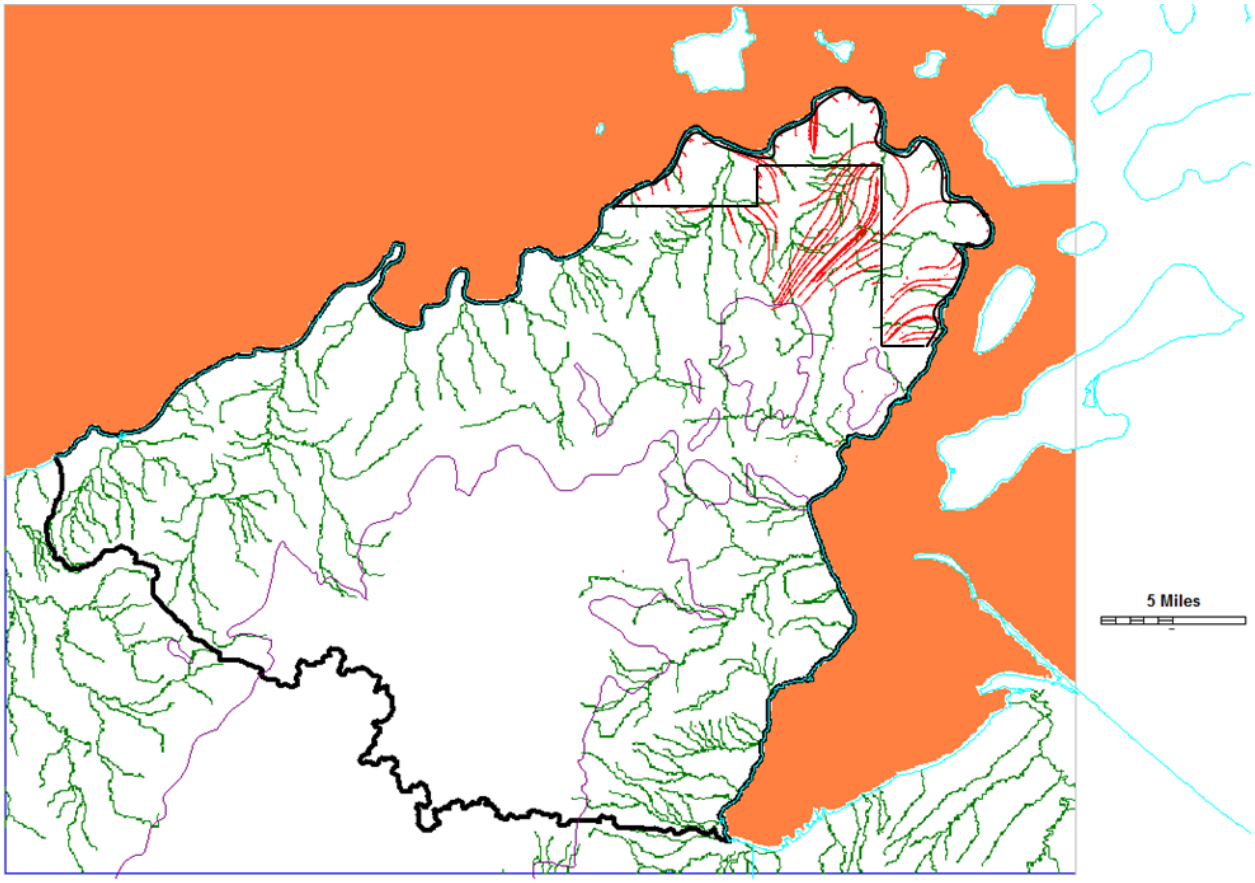

Figure 5.22: Flowpaths delineation of SWB recharge model with single station climate

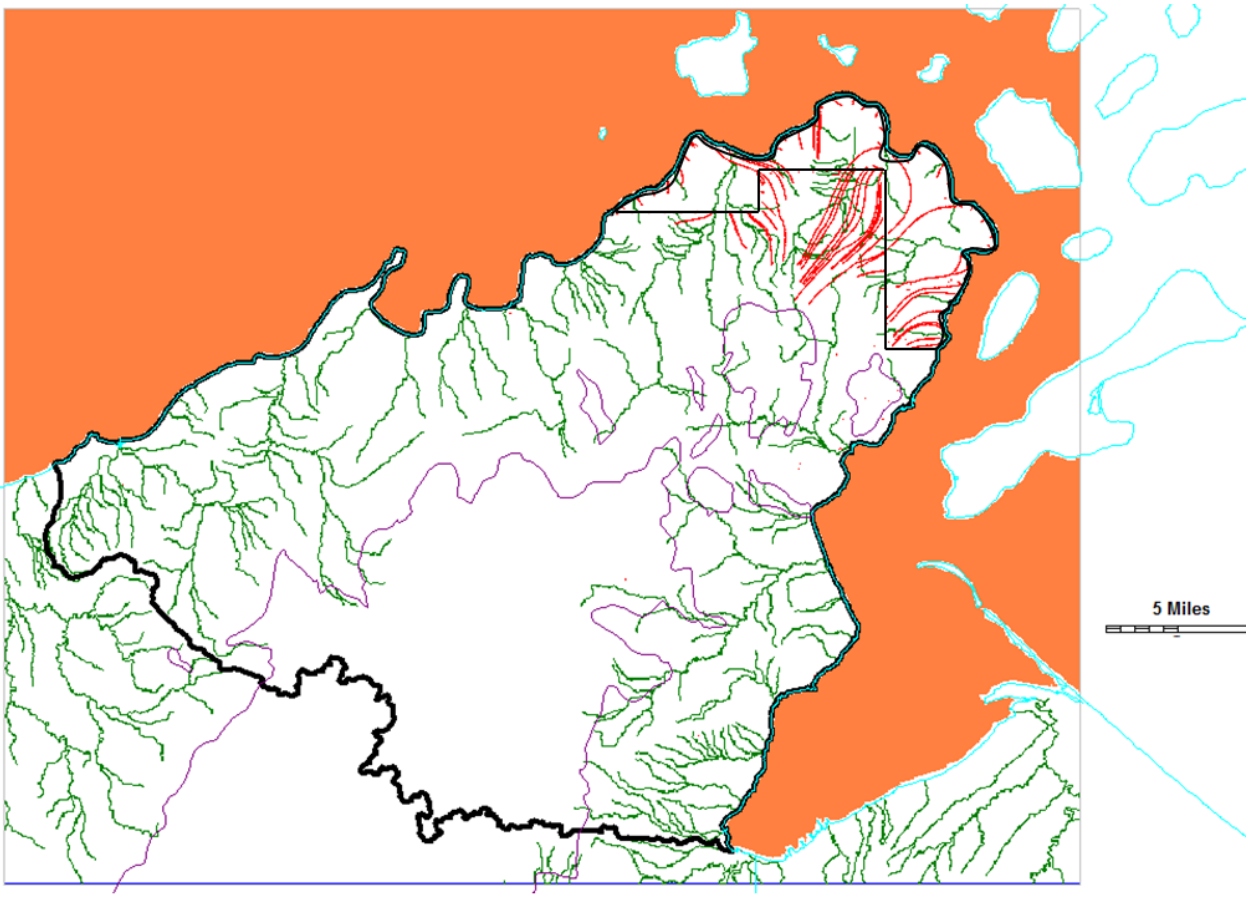

Figure 5.23: Flowpaths delineation of SWB recharge model with gridded climate

Table 5.1: Calibrated parameters in zoned recharge model

Parameters	Zoned recharge model	Parameters	SWB recharge model (single station climate)	SWB recharge model (gridded climate)
copfal_kh	62.85000	copfal_kh	91.03320	109.53600
submc_kh	30.26320	submc_kh	30.85095	23.67190
kxl3	1.16068	kxl3	1.17007	1.12611
kxl4	1.43470	kxl4	1.97906	4.91053
kzl3	0.98346	kzl3	1.14083	1.17949
kzl4	1.00176	kzl4	1.19111	1.22913
r1	0	rm	1.16364	1.42888
r2	0.002303			
r3	0.002596			

Chapter 6 – Conclusions and Future Work

6.1 Conclusions

Spatial distribution of groundwater recharge can be estimated on the basis of available data and a standardized set of parameters using SWB code (Dripps, 2003). One of the advantages of using the SWB model is that it is sensitive to snowmelt and accounts for the process of snowmelt translation into surface runoff, which is important for study areas that experience relatively high frequency of snowfall. One limitation of SWB model is the simulation of the interactions between surface-water and groundwater are not considered in the SWB code. This may lead to a problem especially between the bottom of the root zone and the top of the water table.

Different conceptual models give similar range of recharge rate throughout the peninsula, while from the comparisons of matching the observed values, SWB-based recharge show a better estimation than zoned recharge in the study site. The recharge at this site appears to be predominantly controlled by soil types and land cover. The simulated flowpaths of the groundwater provide where the recharge area that contributes flow to the streams in the Red Cliff reservation, which gives more reliable information for the water management in the area.

6.2 Future work

In this study, the conceptual model is driven by different climate scenarios. Other factors that affect recharge can also be considered in the future work. Land-cover is one of these.

An existing agent-based computer code (LTM, Pijanowski et al., 2002) is already built using satellite imagery showing the land cover changes over 20 years. The combination of land cover and climate information present more possible recharge scenarios, which can be used for a broader range of future steam baseflows.

In terms of the climate information itself, I used historical data from 1981-2004 as a long-term reference. For future predictions, Wisconsin Initiative on Climate Change Impacts (WICCI) provides different climate models to produce estimated future climate using downscaling algorithms (Department of Oceanic and Atmospheric Sciences, UW-Madison), which gives a more reliable dataset for future hydrologic prediction.

For the modeling, the conceptual models are developed through the Groundwater Vista for MODFLOW. HTCondor clusters (UW-Madison) provides a platform for high-throughput computing, which is time-saving.

Due to a lack of the available data subsurface, uncertainty evaluation has been put emphasis on. Model comparison is currently receiving a surge of attention in geology. Statistical methods are used to handle the uncertainty of conceptual models and derive predictive distributions of model output. Such density forecasts are necessary to help analyze which conceptual models are more reasonable, and which conceptual models are subject to considerable uncertainty. The Bayesian approach is a statistical process that weighs individual predictions based on their probabilistic likelihood measures, with the better performing predictions receiving higher weights than the worse performing ones (Duan et al., 2006). This study will provide stochastic evaluation as well as future prediction that would be valuable for decision makers in water resources community.

References

Brunke, M., & Gonser, T. O. M. (1997). The ecological significance of exchange processes between rivers and groundwater. Freshwater biology, 37(1), 1-33.

Clayton, L. (1983). Chronology of Lake Agassiz drainage to Lake Superior.Glacial Lake Agassiz, 26, 291-307.

Cronshey, R. (1986). Urban hydrology for small watersheds. US Dept. of Agriculture, Soil Conservation Service, Engineering Division.

Daly, C., Gibson, W. P., Taylor, G. H., Johnson, G. L., & Pasteris, P. (2002). A knowledge-based approach to the statistical mapping of climate. Climate research, 22(2), 99-113.

De Marsily, G. (1986). Quantitative hydrogeology. Paris School of Mines, Fontainebleau, 403-404.

De Vries, J. J., & Simmers, I. (2002). Groundwater recharge: an overview of processes and challenges. Hydrogeology Journal, 10(1), 5-17.

Doherty, J. E., & Hunt, R. J. (2010). Approaches to highly parameterized inversion: A guide to using PEST for groundwater-model calibration. US Department of the Interior, US Geological Survey.

Dripps, W. R., & Bradbury, K. R. (2007). A simple daily soil–water balance model for estimating the spatial and temporal distribution of groundwater recharge in temperate humid areas. Hydrogeology Journal, 15(3), 433-444.

Dripps W.R (2003). The spatial and temporal variability of groundwater recharge within the Trout Lake Basin of northern Wisconsin. Geology and Geophysics, UW-Madison.

Duan, Q., Ajami, N. K., Gao, X., & Sorooshian, S. (2007). Multi-model ensemble hydrologic prediction using Bayesian model averaging. Advances in Water Resources, 30(5), 1371-1386.

Fitzpatrick, F. A., Peppler, M. C., Saad, D. A., Pratt, D. M., & Lenz, B. N. (2015). Geomorphic, flood, and groundwater-flow characteristics of Bayfield Peninsula streams, Wisconsin, and implications for brook-trout habitat (No. 2014-5007). US Geological Survey.

Gleick, P. H. (1989). Climate change, hydrology, and water resources. Reviews of Geophysics, 27(3), 329-344.

Goebel, J. E., Mickelson, D. M., Farrand, W. R., Clayton, Lee, Knox, J. O, Cahow, Adam, Hobt, H. C., and Walton (1983). Quaternary geologic map of the Minneapolis 4° * 6° Quadrangle, United States: U.S. Geological Survey Miscellaneous Investigations Series Map 1-1420 (NL-15).

Gordon, N. D., McMahon, T. A., Finlayson, B. L., Gippel, C. J., & Nathan, R. J. (2004). Stream hydrology: an introduction for ecologists. John Wiley & Sons.

Harbaugh, A. W. (2005). MODFLOW-2005, the US Geological Survey modular ground-water model: The ground-water flow process (pp. 6-A16). Reston, VA, USA: US Department of the Interior, US Geological Survey.

Hijmans, R. J., Cameron, S. E., Parra, J. L., Jones, P. G., & Jarvis, A. (2005). Very high resolution interpolated climate surfaces for global land areas.International journal of climatology, 25(15), 1965-1978.

Jyrkama, M. I., Sykes, J. F., & Normani, S. D. (2002). Recharge estimation for transient ground water modeling. Groundwater, 40(6), 638-648.

Kearns, A. K. (1998). Temporal variability of diffuse groundwater recharge in New Mexico (Doctoral dissertation, New Mexico Institute of Mining and Technology).

Kalbus, E., Reinstorf, F., & Schirmer, M. (2006). Measuring methods for groundwater–surface water interactions: a review. Hydrology and Earth System Sciences, 10(6), 873-887.

Martin, L. (1965). The physical geography of Wisconsin (Vol. 36). Univ of Wisconsin Press.

Mishra, S. K., & Singh, V. P. (2003). Soil conservation service curve number (SCS-CN) methodology (Vol. 42). Springer.

Molnau, M., & Bissell, V. C. (1983). A continuous frozen ground index for flood forecasting. In Proceedings 51st Annual Meeting Western Snow Conference(pp. 109-119). Cambridge, Ont: Canadian Water Resources Assoc.

Morel-Seytoux, H. J., & Verdin, J. P. (1981). Extension of the Soil Conservation Service rainfall-runoff methodology for ungaged watersheds (No. FHWA/RD-81/060).

O'Callaghan, J. F., & Mark, D. M. (1984). The extraction of drainage networks from digital elevation data. Computer vision, graphics, and image processing,28(3), 323-344.

Ojakangas, R. W., Morey, G. B., & Green, J. C. (2001). The Mesoproterozoic midcontinent rift system, Lake Superior region, USA. Sedimentary Geology,141, 421-442.

Pijanowski, B. C., Brown, D. G., Shellito, B. A., & Manik, G. A. (2002). Using neural networks and GIS to forecast land use changes: a land transformation model. Computers, environment and urban systems, 26(6), 553-575.

Pollock, D. W. (1994). User's Guide for MODPATH/MODPATH-PLOT, Version 3: A Particle Tracking Post-processing Package for MODFLOW, the US: Geological Survey Finite-difference Ground-water Flow Model. US Department of Interior.

Rallison, R. E. (1980, July). Origin and evolution of the SCS runoff equation. InSymposium on Watershed Management 1980 (pp. 912-924). ASCE.

Scanlon, B. R., Healy, R. W., & Cook, P. G. (2002). Choosing appropriate techniques for quantifying groundwater recharge. Hydrogeology Journal, 10(1), 18-39.

Sophocleous, M. (2002). Interactions between groundwater and surface water: the state of the science. Hydrogeology journal, 10(1), 52-67.

Stone, D. B., Moomaw, C. L., & Davis, A. (2001). Estimating recharge distribution by incorporating runoff from mountainous areas in an alluvial basin in the Great Basin region of the southwestern United States. Groundwater, 39(6), 807-818.

Taylor, R., & Howard, K. (2000). A tectono-geomorphic model of the hydrogeology of deeply weathered crystalline rock: evidence from Uganda.Hydrogeology Journal, 8(3), 279-294.

Thornthwaite, C. W., & Mather, J. R. (1957). Instructions and tables for computing potential evapotranspiration and the water balance.

Westenbroek, S. M., Kelson, V. A., Dripps, W. R., Hunt, R. J., & Bradbury, K. R. (2010). SWB--a Modified Thornthwaite-Mather Soil-Water-Balance Code for Estimating Groundwater Recharge. US Department of the Interior, US Geological Survey, Ground Resources Program.

Zhang, L., Dawes, W. R., & Walker, G. R. (2001). Response of mean annual evapotranspiration to vegetation changes at catchment scale. Water resources research, 37(3), 701-708.

Appendix A

MATLAB CODE TO ACCOMPLISH DAILY GRIDDED CLIMATE DATA

Gridded Daily Precipitation

```
clear all; close all; clc;

% load single station climate data
load data_final.mat

% distribution for year
sum_24 = 0;
sum = zeros(24,1);
for year = 1981:1:2004
% Extract precipitation data from the climate table
rows = find(data_final(:,3)==year);
data_year = data_final(rows,:);
precip = data_year(:,5);

% Calculate the distribution of daily precipitation in each year
for i = 1:1:length(precip)

sum(year-1980) = sum(year-1980) + precip(i);
end

sum_24 = sum_24 + sum(year-1980);
end

precip_dist_year = sum/sum_24;


%   fileName = 'precip _annual' + int2str(year)+ '.txt';
% load PRISM climate data
fileName = 'prep_asc.txt';
fid = fopen(fileName, 'rt');

% Define the spatial size
maxX = 600;
maxY = 740;

% Define the format
format = '%f';
for i=1:maxY-1
format = strcat(format, '%f');
end

spatial_precip_input = textscan(fid, format, 'headerlines', 6);

precip_year_average = zeros(maxX, maxY, 24);
```

```
for i=1:maxX
for j=1:maxY
for y=1:24

% If there are missing data grids in the PRISM map, use
% the data from the climate table
if(abs(spatial_precip_input{j}(i) - (-9999)) < 1e-3)
precip_year_average(i, j, y) = sum(y);
continue;
end

% If there is no missing data in the grids
precip_year_average(i, j, y) = 24*spatial_precip_input{j}(i) *
precip_dist_year(y);

end
end
end


fclose(fid);

%% Analyze data year by year
for year = 1981:1:2004

%     % Create folders to store spatial-distributed precipitation data of
each year
%     if ~exist(int2str(year), 'dir')
%         mkdir(int2str(year));
%     end

%%
% Extract precipitation data from the climate table
rows = find(data_final(:,3)==year);
data_year = data_final(rows,:);
precip = data_year(:,5);

% Calculate the distribution of daily precipitation in each year
sum = 0;
for i = 1:1:length(precip)

sum = sum + precip(i);
end

precip_distribution = precip/sum;


%% Read the yearly spatial-distributed precipitation data
% Write files of new dialy spatial-distributed temperature data
write_format = '%3.2f';
for i = 1:maxY-1
write_format = strcat(write_format, ' %3.2f');
end
write_format = strcat(write_format, '\r\n');
```

```
headInfo = {'ncols         740'; ...
'nrows         600'; ...
'xllcorner     1632836.281442'; ...
'yllcorner     515650.417183'; ...
'cellsize      264'; ...
'NODATA_value  -9999'};

% Define the 3D precipitation matrix of space and time
time_space_precip = zeros(maxX, maxY, length(precip));

for i=1:maxX
i
for j=1:maxY
for k=1:length(precip)

% If there are missing data grids in the PRISM map, use
% the data from the climate table
if(abs(spatial_precip_input{j}(i) - (-9999)) < 1e-3)
time_space_precip(i, j, k) = precip(k);
continue;
end

% If there is no missing data in the grids
time_space_precip(i, j, k) = precip_year_average(i, j, year-1980) *
precip_distribution(k);
end
end
end


%% Save daily precipitation data in text files in standard format in SWB
model
for k = 1:length(precip)
fileName =
sprintf('C:/Users/yli352/Documents/SWB/climate/climate/precip/%s.asc',
strcat('precip_',datestr(datenum(year,1,0) + k, 'yyyy_mm_dd')));
fidSub = fopen(fileName,'w');

for i=1:length(headInfo)
fprintf(fidSub,'%s\r\n', headInfo{i});
end

data_part = time_space_precip(:,:,k);

fprintf(fidSub, write_format, data_part');
fclose(fidSub);
end


end
```

Gridded Daily Maximum Temperature

```
clear all; close all; clc;

% load single station climate data
load data_final.mat

% distribution for year
sum_24 = 0;
sum = zeros(24,1);
for year = 1981:1:2004
% Extract temp data from the climate table
rows = find(data_final(:,3)==year);
data_year = data_final(rows,:);
temperature = data_year(:,7);

% Calculate the distribution of daily temp in each year
for i = 1:1:length(temperature)

sum(year-1980) = sum(year-1980) + temperature(i);
end


end

temp_dist_year = zscore(sum);
temp_dist_year_sigma = std(sum);


% load PRISM climate data
fileName = 'tmax_asc.txt';
fid = fopen(fileName, 'rt');

% Define the spatial size
maxX = 600;
maxY = 740;

% Define the format
format = '%f';
for i=1:maxY-1
format = strcat(format, '%f');
end

spatial_temp_input = textscan(fid, format, 'headerlines', 6);

temp_year_average = zeros(maxX, maxY, 24);
for i=1:maxX
i
for j=1:maxY
for y=1:24

% If there are missing data grids in the PRISM map, use
% the data from the climate table
```

```
if(abs(spatial_temp_input{j}(i) - (-9999)) < 1e-3)
temp_year_average(i, j, y) = sum(y)/365;
continue;
end

% If there is no missing data in the grids
temp_year_average(i, j, y) = spatial_temp_input{j}(i) + (temp_dist_year(y) *
temp_dist_year_sigma)/365;

end
end
end

fclose(fid);


%% Analyze data year by year
for year = 1981:1:2004

%% Create folders to store spatial-distributed temperature data of each year
%     if ~exist(int2str(year), 'dir')
%         mkdir(int2str(year));
%     end
%
%%
% Extract temp data from the climate table
rows = find(data_final(:,3)==year);
data_year = data_final(rows,:);

%%%%%%%%%%%%%%%%%%%%%%%%%%%%%%%%%%%%%%%%%%%%%%%%%%%%%%%%%%%%%%%%%%%%%%%%%%%%
temp = data_year(:,7);



% Calculate the distribution of daily temperature using standard
% normalization. The standard score of a raw score x equals to (x-mu)/sigma,
% where mu is the mean of the population and sigma is the standard
% deviation of the population.
temp_distribution = zscore(temp);
temp_mu = mean(temp);
temp_sigma = std(temp);


%%%%%%%%%%%%%%%%%%%%%%%%%%%%%%%%%%%%%%%%%%%%%%%%%%%%%%%%%%%%%%%%%%%%%%%%%%%%


%% Read the yearly spatial-distributed temperature data
% Write files of new daily spatial-distributed temperature data
write_format = '%3.2f';
for i = 1:maxY-1
write_format = strcat(write_format, ' %3.2f');
end
write_format = strcat(write_format, '\r\n');
```

```
headInfo = {'ncols         740'; ...
'nrows         600'; ...
'xllcorner     1632836.281442'; ...
'yllcorner     515650.417183'; ...
'cellsize      264'; ...
'NODATA_value  -9999'};

% Define the 3D temperature matrix of space and time
time_space_temp = zeros(maxX, maxY, length(temp));

for i=1:maxX
i
for j=1:maxY
for k=1:length(temp)

% If there are missing data grids in the PRISM map, use the
% data from the climate table
if(abs(spatial_temp_input{j}(i) - (-9999)) < 1e-3)
time_space_temp(i, j, k) = temp(k);
continue;
end

% If there is no missing data in the grids
time_space_temp(i, j, k) = temp_distribution(k)* temp_sigma +
temp_year_average(i, j, year-1980);
end
end
end


%% Save daily temperature data in text files in standard format in SWB model
for k = 1:length(temp)
fileName =
sprintf('C:/Users/yli352/Documents/SWB/climate/climate/tmax/%s.asc',
strcat('tmax_',datestr(datenum(year,1,0) + k, 'yyyy_mm_dd')));
fidSub = fopen(fileName,'w');

for i=1:length(headInfo)
fprintf(fidSub,'%s\r\n', headInfo{i});
end

data_part = time_space_temp(:,:,k);

fprintf(fidSub, write_format, data_part');
fclose(fidSub);
end


end
```

Gridded Daily Minimum Temperature

```
clear all; close all; clc;

% load single station climate data
load data_final.mat

% distribution for year
sum_24 = 0;
sum = zeros(24,1);
for year = 1981:1:2004
% Extract temperature data from the climate table
rows = find(data_final(:,3)==year);
data_year = data_final(rows,:);
temperature = data_year(:,8);

% Calculate the distribution of daily temperature in each year
for i = 1:1:length(temperature)

sum(year-1980) = sum(year-1980) + temperature(i);
end

% sum_24 = sum_24 + sum(year-1980);
end

temp_dist_year = zscore(sum);
temp_dist_year_sigma = std(sum);


% load PRISM climate data
fileName = 'tmin_asc.txt';
fid = fopen(fileName, 'rt');

% Define the spatial size
maxX = 600;
maxY = 740;

% Define the format
format = '%f';
for i=1:maxY-1
format = strcat(format, '%f');
end

spatial_temp_input = textscan(fid, format, 'headerlines', 6);

temp_year_average = zeros(maxX, maxY, 24);
for i=1:maxX
i
for j=1:maxY
for y=1:24

% If there are missing data grids in the PRISM map, use
% the data from the climate table
```

```
if(abs(spatial_temp_input{j}(i) - (-9999)) < 1e-3)
temp_year_average(i, j, y) = sum(y)/365;
continue;
end

% If there is no missing data in the grids
temp_year_average(i, j, y) = spatial_temp_input{j}(i) + (temp_dist_year(y) *
temp_dist_year_sigma)/365;

end
end
end

fclose(fid);


%% Analyze data year by year
for year = 1981:1:2004

%% Create folders to store spatial-distributed temperature data of each year
%     if ~exist(int2str(year), 'dir')
%         mkdir(int2str(year));
%     end
%
%%
% Extract temperature data from the climate table
rows = find(data_final(:,3)==year);
data_year = data_final(rows,:);

%%%%%%%%%%%%%%%%%%%%%%%%%%%%%%%%%%%%%%%%%%%%%%%%%%%%%%%%%%%%%%%%%%%%%%%%%%%%
temp = data_year(:,8);



% Calculate the distribution of daily temperature using standard
% normalization. The standard score of a raw score x equals to (x-mu)/sigma,
% where mu is the mean of the population and sigma is the standard
% deviation of the population.
temp_distribution = zscore(temp);
temp_mu = mean(temp);
temp_sigma = std(temp);


%%%%%%%%%%%%%%%%%%%%%%%%%%%%%%%%%%%%%%%%%%%%%%%%%%%%%%%%%%%%%%%%%%%%%%%%%%%%


%% Read the yearly spatial-distributed temperature data
% Write files of new daily spatial-distributed temperature data
write_format = '%3.2f';
for i = 1:maxY-1
write_format = strcat(write_format, ' %3.2f');
end
write_format = strcat(write_format, '\r\n');
```

```
headInfo = {'ncols         740'; ...
'nrows         600'; ...
'xllcorner     1632836.281442'; ...
'yllcorner     515650.417183'; ...
'cellsize      264'; ...
'NODATA_value  -9999'};

% Define the 3D temperature matrix of space and time
time_space_temp = zeros(maxX, maxY, length(temp));

for i=1:maxX
i
for j=1:maxY
for k=1:length(temp)

% If there are missing data grids in the PRISM map, use the
% data from the climate table
if(abs(spatial_temp_input{j}(i) - (-9999)) < 1e-3)
time_space_temp(i, j, k) = temp(k);
continue;
end

% If there is no missing data in the grids
time_space_temp(i, j, k) = temp_distribution(k)* temp_sigma +
temp_year_average(i, j, year-1980);
end
end
end


%% Save daily temperature data in text files in standard format in SWB model
for k = 1:length(temp)
fileName =
sprintf('C:/Users/yli352/Documents/SWB/climate/climate/tmin/%s.asc',
strcat('tmin_',datestr(datenum(year,1,0) + k, 'yyyy_mm_dd')));
fidSub = fopen(fileName,'w');

for i=1:length(headInfo)
fprintf(fidSub,'%s\r\n', headInfo{i});
end

data_part = time_space_temp(:,:,k);

fprintf(fidSub, write_format, data_part');
fclose(fidSub);
end


end
```

Appendix B

MATLAB CODE TO TRANSFER SWB OUTPUT TO MODFLOW INPUT

Function SWB2RCH

```
function[] = SWB2RCH(fileName)

% This function is to change the unit of SWB output file from inch/year into
% ft/day and save it as the RCH file format in the input model

% C is the recharge unit change multiplier
C = 2.2816*10^(-4);

fid = fopen(fileName, 'rt');

format = '%f';
for i=1:739
format = strcat(format, '%f');
end

SWB_output = textscan(fid, format, 'headerlines', 6);

RCH = zeros(600, 740);

for i=1:740
RCH(:,i) = C * SWB_output{i};
end

fclose(fid)

fid_rch = fopen('MEAN_RECHARGE_1981_2004_single.asc', 'wt');

fprintf(fid_rch, '# MODFLOW2000 Recharge Package\nPARAMETER  0 \n         3
50\n         1         1\n        18   1.00000(10e13.4)                   -1
RECHARGE\n');


for i = 1:600
for j = 1:740
fprintf(fid_rch, stringFormat(RCH(i,j)));

if mod(j, 10)==0
fprintf(fid_rch, '\n');
end

end
end
```

```
fclose(fid_rch);

end
```

Function STRINGFORMAT

```
function [str] = stringFormat(originalStr)

str = sprintf('%13.4e', originalStr)

end
```